FH AACHEN
UNIVERSITY OF APPLIED SCIENCES

universiteit hasselt

2014 | Faculteit Industriële Ingenieurswetenschappen

DOCTORAATSPROEFSCHRIFT

# Novel strategies for evaluating the effectiveness of aseptic sterilisation processes by means of a multi-sensor set-up

Proefschrift voorgelegd tot het behalen van de graad van doctor
in de industriële ingenieurswetenschappen, te verdedigen door

**Steffen Reisert**

Promotor: Prof. dr. Patrick Wagner
Copromotor: Prof. dr.-ing. Michael J. Schöning

D/2014/2451/7

# Jury

| | |
|---|---|
| Chairman: | Prof. Dr. M. D'Olieslaeger<br>Hasselt University, Institute for Materials Research (IMO) |
| Promotor: | Prof. Dr. P. Wagner<br>Hasselt University, Institute for Materials Research (IMO) |
| Co-promotor: | Prof. Dr.-Ing. M. J. Schöning<br>FH Aachen, Institute of Nano- and Biotechnologies (INB) |
| Members of the jury: | Prof. Dr. H.-G. Boyen<br>Hasselt University, Institute for Materials Research (IMO) |
| | Dr. R. Thoelen<br>Hasselt University, Institute for Materials Research (IMO) |
| | Dr. W. Deferme<br>Hasselt University, Institute for Materials Research (IMO) |
| | Prof. Dr. A. Poghossian<br>FH Aachen, Institute of Nano- and Biotechnologies (INB) |
| | Prof. Dr.-Ing. H.-J. Ackermann<br>FH Aachen, Medical Engineering and Applied Mathematics |

# Acknowledgements

This thesis would not have been possible without the persistent help and guidance of many individuals, all of whom deserve my sincere gratitude:

First of all, I want to express my deepest appreciation to my supervisor and mentor Prof. Dr. Michael J. Schöning, who gave me the opportunity to explore my research interests at the Institute of Nano- and Biotechnologies (INB). Thank you for your trust in all these years, the vast amount of fruitful discussions, many hours of proof-reading (whether it be day, night or weekend), for keeping me motivated in less prosperous phases of my doctoral research and for all the non-scientific activities (ping-pong, pool and skittle matches) that have greatly contributed to my well-being at the INB. You have been extraordinarily tolerant and supportive. Even you kept "cool" after I had almost set the lab on fire!

In the same way, I would like to thank Prof. Dr. Patrick Wagner, who graciously agreed to be my promoter at Hasselt University. Thank you for the vast number of valuable remarks and all the last-minute corrections. Your boundless optimism and easy-going nature have never let me doubt to get this thesis written.

I am very grateful to my cooperation partners at SIG Combibloc, particularly to Dr. Gregor Pawlitzki, Dr. Werner Seiche, Rudolf Flörke, Hanno Geissler and Christian Weiler, not solely for the financial support that allowed me to work on such an exciting topic, but also for placing their trust and confidence in my abilities. Hanno, I have greatly benefited from all the discussions we had and I really appreciate your sometimes unconventional way of doing things. San Antonio has been a great experience for me! Christian, thank you for innumerous hours of counting bacterial colonies and for running the risk of getting your hair bleached during our "spore-killing sessions". I really enjoyed it!

Big thanks also to Dr. Niko Näther, who has introduced me into the topic and after all, paved the way for my PhD.

My gratitude is also extended to Dr. Jörg Berger and Dr. Peter Friedrich, who were instrumental in the development of the handheld sensor system and advised me with a lot of expert knowledge and some nuggets of wisdom.

Jozef Wiora, PhD, has significantly helped me planning experiments and analysing data. Also, he took away my "fear" of integrated circuits and microelectronics. Thank you Jozef!

Moreover, I want to thank Hans-Peter Bochem from the Peter Grünberg Institute (PGI-8) at Forschungszentrum Jülich for taking several SEM images and the whole clean-room team at PGI-8 for their excellent work and support.

Particularly, I am grateful for the assistance in XRD analysis given by Matthias van Gompel from Hasselt University (IMO).

A special thank goes out to Jörg Hennemann from Justus-Liebig-Universität Gießen for many immensely helpful discussions, for letting me be a co-author on one of his publications and for the nice evenings in Aachen and at various conferences.

Furthermore, I would like to thank Prof. Dr. Hans-Josef Ackermann for the troubleshooting in circuit design and several ping-pong matches and Heinrich-Gerd Römer for supplying me with some spare parts and fixing my hi-fi system.

My sincere thanks also go out to Dr. Bernd Kraus, whose negotiation skills contributed to the realisation of many projects that I have been involved in and benefited from. I also want to thank him for plotting all my posters during the last years.

I would like to show my greatest appreciation to all my colleagues at the INB, particularly to Prof. Dr. Arshak Poghossian, Dr. Torsten Wagner, Shoko Takenaga, PhD and our lab engineers David Rolka, Heiko Iken, Stefan Beging and Marcel Leinhos. I received generous support from all of you.

I am further deeply grateful to all former and present fellow PhD students at the INB. First and foremost to Dr. Patrick Kirchner, who was sharing an office with me for four years, tolerating my idiosyncrasies. You have always been a team player. In the same way, I want to thank Carl Frederik Benedikt Werner for his immense willingness to help me with whatever I needed from him and furthermore, for all those exciting and mind-freeing tea breaks, swimming sessions and dinners at "Pizza Inn". Big thanks also to Christina Huck for bonding several sensors for me and for so many delicious cakes, to Matthias Bäcker, PhD for various AFM images and heated discussions about football, to Sebastian Schusser for several ellipsometric measurements and for being our "organising agency" and last but not least to Jan Oberländer for the fruitful cooperation and for recently being a pleasant officemate.

I take this as an opportunity to thank all students that have significantly contributed to this work. Thank you Benno "Hahnenkönig" Schneider, Sven Heimhalt, Patrick Pütz and Max Koch. I hope that I have been a good supervisor to you. I learned from you as well!

Special thanks are directed to all my friends not namely mentioned here for their moral support. Christian and Alex, I will not forget the numerous fishing trips that, no matter whether they ended up successfully or empty-handed, have been a lot of fun for me!

Despite the geographical distance, my family was always nearby. My parents deserve my utmost appreciation for always believing in me, for their continuous love and their support in my decisions. Auch möchte ich von Herzen meiner Oma danken, die mich in allen Phasen meiner akademischen Ausbildung in vielerlei Hinsicht unterstützt und damit zum Gelingen dieser Arbeit beigetragen hat – sei es durch selbstgemachten Apfelgelee oder durch die unermüdliche Nachfrage nach dem absehbaren Ende meiner Doktorarbeit. Danke Oma!

At last, my heartfelt thanks go out to my girlfriend Sophie for her love and patience. She continuously encouraged me to do my best and was always there when I needed her most. I love you!

# Table of Contents

# Abstract

The aseptic processing and packaging of food, in combination with the possibilities of aseptic storage, transport and packaging recycling, represents one of the most sustainable technologies in modern food processing and contributes significantly to reducing the losses of fruits, vegetables and milk and to increase the availability of this food all over the world. In contrast to conventional food processing methods, product and container are continuously sterilised separately and brought together under sterile conditions. This allows for a gentler thermal treatment of the product, while maintaining the benefits of an extended shelf life and the storage without refrigeration. Besides the thermal treatment of the product, the containers are sterilised in order to inactivate potential pathogens and/or food spoilers on the surface of the packaging. Today, hydrogen peroxide ($H_2O_2$) applied in either gaseous or vapour phase, particularly because of its good handling and high environmental compatibility, represents one of the mostly used sterilising agents in the aseptic filling industry. Against this background it is actually surprising that the mechanisms of biocidal action of $H_2O_2$ are rather poorly understood. In order to characterise the effectiveness of the sterilisation by $H_2O_2$, test objects inoculated with an unnaturally high load of microorganisms are taken through the sterilisation process. In retrospect, these are examined for viable bacteria. It seems obvious that this is a very time-consuming and costly procedure.

This work focused on the development of novel strategies for determining the effectiveness of the sterilisation by gaseous $H_2O_2$ by means of a real-time monitoring system. Therefore, a handheld sensor system for the online monitoring of the $H_2O_2$ concentration, which represents an important factor of the sterilisation, has been developed in the first instance. It could be shown that this monitoring system largely meets the technical requirements for field use. The main strategy, however, aimed at identifying the influencing factors of the sterilisation by gaseous $H_2O_2$ – determining in detail the impact of each of these variables on the microbicidal action – and to make them detectable using predominantly commercial gas sensors. The variables of the sterilisation process

include the $H_2O_2$ concentration, humidity, gas temperature, flow rate and time of exposure. Initially, different types of gas sensors, including a calorimetric type, different metal-oxide semiconductor (MOX) as well as an electrochemical gas sensor have been identified as potential candidates for monitoring the factors which are involved in the sterilisation. Furthermore, the inactivation kinetics of bacterial spores by gaseous $H_2O_2$ have been investigated in several series of microbiological tests using *Bacillus atrophaeus* (formerly *Bacillus subtilis*) spores. In a first approach, a correlation between the microbicidal effectiveness and the signal output of two commercial gas sensors via one parameter, namely the $H_2O_2$ concentration, was established. Nevertheless, since the sterilisation is not solely dependent on the $H_2O_2$ concentration, other factors had to be taken into account. The second approach meanwhile aimed no more to establish a parameter-dependent correlation, but rather a direct correlation between sensor response and microbicidal action. In a first work on this topic, the sensing characteristics of several sensor types have been analysed with respect to their sensitivity towards the influencing factors of the sterilisation process. These are the $H_2O_2$ concentration, the humidity, the gas temperature and the gas flow rate. In parallel, microbiological tests have been carried out.

It could be shown that the sensors in test equally responded to the influencing factors of the sterilisation. Additionally, oriented on the concept of an electronic nose, the feasibility of determining the microbicidal effectiveness on the basis of chemical images obtained from the sensor output, by applying pattern recognition, has been demonstrated. In a second work on this topic, the same sensors had been used, but the field of examined parameters has been defined more precisely and the number of measurement points has been increased considerably in order to obtain a higher statistical significance of both, the sensory measurements and microbiological tests. Thus, it was possible to establish two models, which correlate the sensor responses of the calorimetric gas sensor and two different types of MOX sensors with the microbicidal action within a wide parameter field. Based on this, a multi-sensor system for monitoring the effectiveness of the sterilisation process by gaseous $H_2O_2$ is proposed.

The content of this thesis concludes with a study on the sensing mechanisms of different types of metal oxides towards $H_2O_2$, since a vast number of sensors used in this project belong to the group of MOX sensors. Therefore, pure $SnO_2$ and $WO_3$ as well as Pt- and Pd-doped $SnO_2$ films were deposited on a self-developed array structure. It could be demonstrated that the doping with catalytically active materials significantly increases the sensitivity of MOX sensors towards $H_2O_2$. In this way, even low concentrations of $H_2O_2$ down to the ppm range can be detected. Thus, these sensors can be adopted for other fields of application where the detection of rather low concentrations is required, e.g., in the exhaust system of aseptic sterilisation devices or for environmental control in the vicinity of $H_2O_2$ deploying processes.

# Nederlandse samenvatting

De aseptische verwerking en verpakking van voedsel in combinatie met aseptische bewaring en transport en de recyclage van de verpakkingsmaterialen zijn belangrijke duurzame technologieën in de voedingsindustrie. Hierdoor wordt immers het verlies van bv. fruit, groenten en melkproducten in sterke mate gereduceerd wat de wereldwijde beschikbaarheid van deze voedingsmiddelen duidelijk ten goede komt. In tegenstelling tot de eerder klassieke methoden worden vandaag het voedingsproduct en zijn verpakkingsmateriaal eerst apart gesteriliseerd alvorens beide met elkaar in contact worden gebracht onder eveneens steriele condities. Dit maakt een mildere thermische behandeling van het product mogelijk terwijl het voordeel van een langdurige bewaring zonder koeling behouden blijft. Naast de warmtebehandeling van het voedingsproduct dient te verpakking gesteriliseerd te worden om potentiële pathogene of bedervende kiemen te inactiveren. Hierbij geniet waterstofperoxide ($H_2O_2$) vandaag de voorkeur: Het kan zowel als gas als in de dampfase op een veilige en gecontroleerde manier worden gebruikt en is bovendien milieuvriendelijk zodat het nu het meest courante steriliserende medium is in het aseptische afvullen van voedsel.

Voor deze achtergrond is het daarom verrassend dat de biocide werkingsmechanismen van $H_2O_2$ in feite nog steeds slechts gedeeltelijk begrepen zijn. Om de efficiëntie van de sterilisatie door $H_2O_2$ te analyseren worden testvoorwerpen doorgaans eerst met buitengewoon hoge concentraties aan micro-organismen geïnoculeerd om vervolgens het aantal overlevende kiemen te bepalen nadat het testobject het sterilisatieproces doorlopen heeft. Dergelijke testcycli zijn echter niet enkel tijdrovend maar ook kostenintensief.

In het kader van deze thesis werden daarom nieuwe strategieën ontwikkeld om de efficiëntie van sterilisatie door $H_2O_2$ in de gasfase te bepalen waarbij de klemtoon op "real-time monitoring" ligt en het gebruik van gassensoren. Als eerste stap werd een "handheld" sensorsysteem ontworpen om $H_2O_2$ concentraties continu te kunnen opvolgen en het werd bovendien aangetoond

dat dit instrument aan de technische vereisten voor analyses binnen een productieomgeving voldoet. Het hoofdoogmerk lag vervolgens op het identificeren van de verschillende, bijkomende factoren die de sterilisatie-efficiëntie van $H_2O_2$ gas mede bepalen – het achterhalen van de impact van elk van deze factoren afzonderlijk – en hun kwantitatieve analyse door hoofdzakelijk commercieel beschikbare (gas-) sensoren. De variabele parameters van een sterilisatieprotocol omvatten niet enkel de $H_2O_2$ concentratie zelf maar ook de relatieve vochtigheid, de gastemperatuur, het gasdebiet en de blootstellingstijd. Belangrijk in deze is het feit dat "co-factoren" zoals vochtigheid en temperatuur niet enkel de sterilisatie-efficiëntie beïnvloeden maar ook de precisie waarmee een gassensor op bepaalde $H_2O_2$ concentraties reageert. In deze context werden dan ook verschillende types van gassensoren nader op hun toepasbaarheid geëvalueerd, in het bijzonder een calorimetrische sensor, verschillende MOX-sensoren (metaal-oxide halfgeleiders) en een elektrochemische gas-sensor. Tegelijkertijd werd de biocide werking van blootstelling aan $H_2O_2$ gas op bacteriële kiemen onderzocht aan de hand van microbiologische testreeksen op basis van de *Bacillus atrophaeus* (ook bekend onder de vroegere naam "*Bacillus subtilis"*).

Als eerste aanzet kon een correlatie worden vastgesteld tussen de microbiocide efficiëntie en de signaaloutput van twee commerciële gassensoren op de basis van een parameter, namelijk de concentratie van $H_2O_2$. Omdat sterilisatieprocessen echter niet enkel van deze concentratie alleen afhangen moesten ook de andere parameters in rekening worden gebracht. Vervolgens werd getracht om los van deze parameter-afhankelijke correlatie een rechtstreekse correlatie tussen de sensor-response en de microbiocide werking te achterhalen. Daarom werden het antwoordsignaal en de gevoeligheid van verschillende sensor-types onderzocht met betrekking tot alle factoren die de sterilisatie-efficiëntie beïnvloeden wat ook werd nagegaan in het kader van microbiologische testen. Volgens deze metingen reageren de geteste sensoren op een vergelijkbare maar toch unieke manier op de verschillende sterilisatieparameters. In analogie met het concept van elektronische neuzen en patronenherkenning werd dan ook aangetoond dat het haalbaar is om de

microbiocide efficiëntie te bepalen op basis van de "scheikundige vingerprints" die met een combinatie van verschillende sensortypes worden behaald.

In het vervolg werden dezelfde sensoren opnieuw gebruikt maar dan binnen een nauwkeuriger gedefinieerde parameterruimte en met een veel hogere dichtheid aan meetpunten. Hierdoor werd een hogere statistische significantie bereikt van zowel de sensor-gebaseerde data als van de microbiologische tests. Met deze gegevens konden twee modellen ontwikkeld werden die de sensorrespons van een calorimetrische gassensor en van twee verschillende types van MOX sensoren correleren met de microbiocide werking binnen een breed gebied van de mogelijke sterilisatieparameters. Op deze basis wordt dan ook een multisensor-systeem voorgesteld dat de efficiëntie van sterilisatieprocedés op een betrouwbare wijze kan monitoren.

Het afsluitende hoofdstuk van deze thesis beschrijft een studie op de sensor-mechanismes die in werking treden als verschillende types van metaaloxides worden blootgesteld aan $H_2O_2$. Hiertoe werden zowel zuivere $SnO_2$- en $WO_3$ films alsook Pt- en Pd-gedopeerde $SnO_2$ films op een zelf ontwikkelde multisensor-meetplatform geïntegreerd. Het is duidelijk gebleken dat de dopering met katalytisch actieve elementen tot een belangrijke toename van de gevoeligheid van MOX-sensoren ten aanzien van $H_2O_2$ leidt. Op deze wijze konden bijzonder lage $H_2O_2$ concentraties, tot zelfs in het ppm regime, gedetecteerd worden. Bijgevolg kunnen deze sensoren ook aangepast worden voor het gebruik in andere toepassingsdomeinen waarin juist de lage detectielimieten van belang zijn zoals in de uitlaatleiding van sterilisatieopstellingen of in milieuanalyses.

# Chapter 1

## Introduction

This chapter deals with the fundamentals of food processing with a focus on aseptic processing and in particular, aseptic sterilisation processes employing gaseous/vapour phase hydrogen peroxide ($H_2O_2$). In addition, standard test methods for testing the effectiveness of aseptic sterilisation processes as well as the state of the art regarding the monitoring of $H_2O_2$ in aseptic sterilisation processes are outlined. Finally, the aim and scope of the present work are presented.

---

Note: Parts of this chapter (**Sections 1.4.2**, **1.4.3** and **1.5.1**) have been submitted for publication as a book chapter:

P. Kirchner, S. Reisert, M. J. Schöning, Calorimetric gas sensors for hydrogen peroxide monitoring in aseptic food processes, Springer series on chemical sensors and biosensors: Gas sensing fundamentals, Springer, Berlin 2013, *in press*, DOI 10.1007/5346_2013_51.

## 1.1 Preface

During the past century, food processing has contributed to make food the basis of a healthy civilisation, help society hurdle hunger and diseases and improve the safety, nutrition, convenience, affordability and availability of foods. The processing and packaging of foodstuff frequently serves multiple objectives, with numerous benefits to the consumer and society [1]:

- Preservation
- Safety
- Quality
- Availability
- Sustainability
- Convenience
- Health and Wellness

Today, most food products reach the consumer in some type of package. Many different types of food packages are used for several different reasons. But ultimately, they have a few things in common. Packaging contributes to the safety of food by protecting the product from contamination of pathogens and food spoilers. Moreover, packaging extends the shelf life of the product by providing a physical barrier to atmospheric oxygen, moisture, light and other agents that would accelerate deterioration of the product. Not in the least, the packaging itself provides the legally required information to the consumer in the form of a label bearing information about the product identity, quantity, ingredients, nutrient content, expiration date, and commercial source [2,3]. One key-technology in modern food packaging is represented by the aseptic processing of food [4].

## 1.2 Aseptic packaging

Aseptic packaging is one of the most important methods for food packaging today, since it significantly increased the safety, quality, availability and convenience of certain foods all around the world. In addition, the amount of energy required for preserving and storing such foods is decreased. The major

difference between aseptic packaging and traditional methods of food packaging, i.e. canning, is that product and packaging material are continuously sterilised separately prior to the filling and sealing. In order to prevent recontaminations of the product, the filling and sealing process takes place under aseptic conditions. The sterilised package is filled with the sterile product and hermetically sealed to produce a shelf-stable final product with extended shelf life and no need for refrigeration. This method has provided continuous improvement in the quality of the packaged product, partly because the products are subject to a much milder heat treatment (flash heating at high temperature but short time) compared to the traditional thermal process [5]. By the thermal flash-heating process, most nutrients, particularly vitamins and most sensory characteristics, like flavour, colour and texture remain to the product [6]. Beside the product treatment, also the packaging sterilisation represents an important factor of the aseptic food process. When reference is made to the term "sterilisation" at this and other points of this thesis, it generally has to be understood in the sense of commercial sterility. According to [7] this means "the absence of microorganisms capable of growing in the food at normal non-refrigerated conditions at which the food is likely to be held during manufacture, distribution and storage". In fact, the term "aseptic", which is referred to a condition in which living pathogenic organisms are absent, would have to be replaced by "antiseptic", which is defined as the prevention of infection by inhibiting the growth of pathogenic microorganisms. Due to the popularity of the term "aseptic packaging", which probably originates from the ideal conception of absolute sterility, it has been retained in the present work.

A variety of sterilisation techniques have been associated with aseptic packaging, including mechanical (washing, wiping, etc.), physical (irradiation, heat, etc.), chemical (ethylene oxide, formaldehyde, propylene oxide, hydrogen peroxide, etc.) and physicochemical (heat or irradiation combined with chemical agents) methods. In either way, hydrogen peroxide represents the most commonly used sterilant for aseptic packages today [8–11]. Therefore, special emphasis will be given to hydrogen peroxide and its use as a sterilant within the next section.

## 1.3 Sterilisation with hydrogen peroxide ($H_2O_2$)

### 1.3.1 General information

The use of hydrogen peroxide ($H_2O_2$) as a disinfectant was first proposed by B. W. Richardson in 1891 [12]. Since, it has been recognised as a decontaminant in a broad field of applications including the treatment of laboratory and medical equipment, pharmaceutical facilities, hospital rooms, animal holding rooms and last but not least food containers [8,13–16]. Applied in aqueous or gaseous forms, hydrogen peroxide exhibits biocidal activity against a variety of organisms including bacterial spores, vegetative bacteria, viruses, amoeba and fungi [13,14,16,17]. Furthermore, it is considered less toxic than other chemical agents such as chlorine dioxide, ethylene oxide and formaldehyde, as it breaks down into water and oxygen. Thus, it is particularly suitable for the sterilisation of food packages, since it minimises the risk of contaminating the product with residues of the sterilising agent [4]. According to [18], $H_2O_2$ represents an almost "ideal decontamination agent" as it fulfils the following requirements:

- Possesses a high activity against a wide spectrum of biological and chemical contaminants
- Offers a quick start of action and long-lasting effect
- It is non-toxic to humans and the environment
- It is compatible with a variety of materials
- Has an unlimited disposal and long-term stability during storage
- It is easily detectable
- It can be purchased at reasonable costs

The properties mentioned are equally applicable to liquid solutions as well as to vapour-phase and/or gaseous $H_2O_2$. However, with respect to the latter, it was proven that $H_2O_2$ in gaseous phase exhibits considerably higher germicidal activity and a faster start of action compared to liquid solutions [19–22]. Moreover, it is applicable on larger areas and rugged surfaces. In the present work, solely sterilisation processes that make use of gaseous $H_2O_2$ are of interest, so that the following information will mainly be related to vapour/gas-phase $H_2O_2$.

### 1.3.2 Mechanism of action of $H_2O_2$

Although vaporised (or gaseous) $H_2O_2$ has been used as a sterilant in the packaging industry since the late 1980s, the exact mechanism(s) of the biocidal action of $H_2O_2$ are rather poorly described in literature. Often is referred to two reviews on the mechanism of action of biocides, which consider $H_2O_2$ an oxidising agent reactive with the biomolecules (proteins, lipids, nucleic acids, etc.) that make up cellular and viral structure/function [8,21]. The damaging of the biomolecules is believed to be produced by a phenomenon called oxidative stress, which is induced by reactive oxygen species (ROS), more precisely, hydroxyl radicals (OH·). These are oxygen derivable radicals having a high capability to produce cellular damage. The formation of hydroxyl radicals by $H_2O_2$ may occur under several conditions:

- Interaction with transition metal ions (copper, iron, etc.) [23]
- In combination with UV irradiation [24,25]
- In a Fenton reaction by participation of intra-/extra-cellular $Fe^{2+}$ [26]

The oxidative stress initiated by the hydroxyl radicals may affect different cell components, leading to irreversible damage. For instance, they may affect the integrity of the cellular membrane due to an oxidation reaction on the lipid bilayer [27]. This leads to a loss in the impermeability of the membrane, disrupting the internal organisation of the cell [28]. Hydrogen peroxide is not a large molecule and thus able to diffuse through the cell membrane [29]. Once inside, it produces hydroxyl radicals according to the mechanisms previously mentioned and affects inner cell constituents. Proteins lose their specific function due to the oxidation of different amino acids such as histidine, tyrosine, cysteine and others [30]. Hydroxyl radicals also produce multiple forms of damage on DNA, including base modifications and the breaking of double strands [30]. Moreover, $H_2O_2$ is an effective agent for the inactivation of bacterial endospores, which inherently feature a high resistance against a variety of treatments, like heat, radiation, pressure and chemicals [31]. It is therefore not surprising that bacterial spores represent the microorganism of choice for testing the effectiveness of sterilisation processes by means of the so-called challenge test. The resistance of the spores is a result of their thick proteinaceous spore coat,

which is highly impermeable to protect the spore's interior. In addition, small, acid-soluble spore proteins protect the DNA. Also, the low water content in the spore core correlates with a high heat resistance [31–33]. Only little literature is found about the exact mechanism of sporicidal inactivation by $H_2O_2$. In one study it was shown that $H_2O_2$ may cause dissolution of the inner and outer spore coat, leading to a disintegration of the spore core [34]. There are other, rather speculative references, but ultimately, the exact mechanisms are still object of research [12].

Amongst the few studies on the sporicidal inactivation mechanism, there have been some works that study the influential parameters to the microbial inactivation by gaseous/vapour-phase $H_2O_2$. Most authors found that the inactivation of spores grows with higher concentrations of gaseous $H_2O_2$ [13,14,17,35–37]. In addition, it turns out that processes, which use $H_2O_2$ in combination with hot air, exhibit a higher microbicidal activity [38,39]. Unger *et al.* propose a different model, by applying lower concentrations in combination with a high level of humidity [40]. The latter also describe that sub-visible condensation of $H_2O_2$ on the material to be sterilised was discovered to increase the inactivation rate, whereas dripping condensation should be avoided in order to obtain uniform sterilisation efficiency. Furthermore, various works report on the synergetic effect of $H_2O_2$ in combination with physical excitation, by e.g., infrared [39] and UV-C irradiation [13,41–45] or ionisation by plasma [46,47]. The objective of the combined methods is to enhance the formation of ROS, which in turn are believed to be responsible for the microbial inactivation. Each of the mentioned treatments comprises advantages and disadvantages for certain applications. Thus, the choice of the method is predominantly determined by other factors, such as the time of treatment, material compatibility, surface area, technological complexity and costs.

### 1.3.3 Testing the effectiveness of packaging sterilisation devices

The German Engineering Federation "Verband Deutscher Maschinen- und Anlagenbau e.V." (VDMA) has elaborated a code of practice for testing the effectiveness of packaging sterilisation devices [48]. This document describes methods for testing the packaging sterilisation of aseptic plants by means of $H_2O_2$, the so-called challenge tests, which will be described briefly in this section. These challenge tests require artificial inoculation of packaging material with

microorganisms under controlled conditions, in order to obtain statistically significant test results allowing objective comparisons. As test organisms for processes employing $H_2O_2$ in combination with heat, spores of the species *Bacillus atrophaeus* (ATCC 9372, formerly *B. subtilis*) and *Bacillus subtilis* SA 22, also known as the hay bacillus or grass bacillus, are proposed. There are two different test procedures, the count-reduction test (CRT) and the end-point test (EPT).

In the count-reduction test, the test items infected with the test microorganism are passed through the aseptic plant. In doing so, the number of viable spores is determined before and after the sterilisation. From the difference in microorganism counts, the logarithmic cycle reduction (LCR), also called log-rate, may be determined as follows:

$$LCR = log(mean\ initial\ count) - log(final\ count) \quad (1.1)$$

Each test item should have an initial microorganism count of at least $10^5$ spores. In the end-point test, the packaging is artificially inoculated with test microorganisms as in the CRT, but in this case in three graduated infection stages each being greater by a power of ten than the one before. The main difference with respect to the CRT is that in the EPT the artificially infected packaging is filled with a sterile culture medium matched to the test microorganism and after an incubation phase, only the number of unsterile packaging units is determined. Beyond the effectiveness of the packaging material sterilisation, the EPT provides information about the entire process, from supplying the product and filling through recontamination-free closure of the packaging. The packaging units according to the EPT should have an initial microorganism count of at least $10^2$,$10^3$ and $10^4$ spores. In case of the EPT, the LCR may be calculated using most probable number (MPN) methods as suggested by Moruzzi *et al.* [49].

## 1.4 $H_2O_2$ monitoring in aseptic sterilisation processes – state of the art

### 1.4.1 Conventional methods

A number of different strategies for monitoring $H_2O_2$ in gaseous or vapour phase have emerged during the last years, such as infrared spectroscopy, colorimetry,

mass spectroscopy, chemiluminescense as well as amperometric methods. However, most of these methods are not applicable for monitoring the $H_2O_2$ concentration in package sterilisation processes as they are merely be used for the detection of low $H_2O_2$ concentrations and/or do not withstand the harsh environmental conditions [50]. Therefore, only the most practicable methods will be discussed in the following.

### 1.4.2 Calorimetric sensor for the detection of $H_2O_2$

A first sensor for the purpose of monitoring $H_2O_2$ in gaseous phase at elevated temperatures, as employed in aseptic sterilisation processes, has been introduced by Näther in 2009 [51,52]. This calorimetric type of sensor consists of a differential set-up of two temperature sensors (Pt100 elements) built up on a transistor outline (TO 8) socket (see Fig. 1.1). One of the Pt100 elements is coated with a catalyst, typically $MnO_2$, whilst the other Pt100 is coated with a material for passivation, e.g., perfluoroalkoxy (PFA).

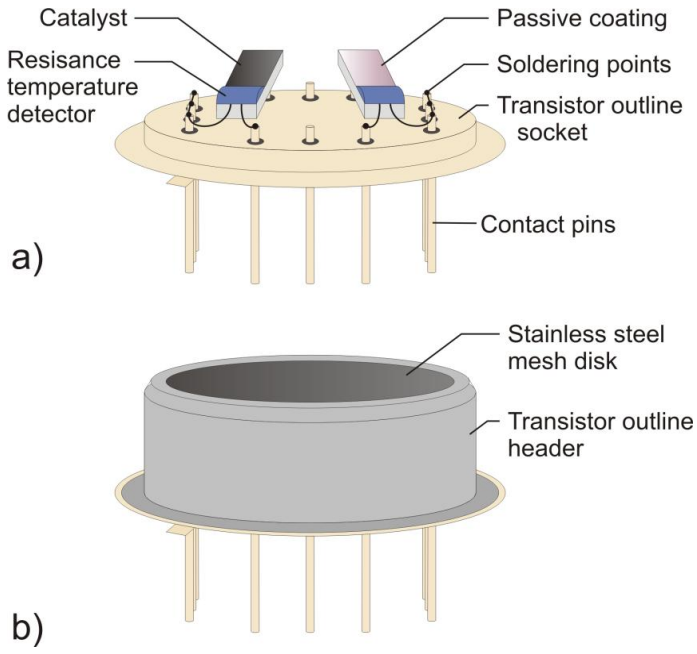


**Figure 1.1:** Schematic of the calorimetric sensor arrangement for monitoring $H_2O_2$; a) calorimetric differential set-up on transistor outline (TO 8) socket and b) sensor shielded by a TO header and a stainless steel mesh disk (Figure adapted from [50]).

The sensing principle is based on an exothermic reaction of $H_2O_2$ on the catalyst, causing a rise in the temperature on the catalytically activated Pt100. The net reaction at the sensor can be described by the following equation:

$$2H_2O_2(g) \rightarrow 2H_2O(g) + O_2(g) + \Delta_R H \quad (1.2)$$

with $\Delta_R H$ (reaction enthalpy) of -105.3 kJ/mol and *(g)* referring to gaseous phase.

Since the sensor is built up in a differential arrangement, the sensor signal (difference between the temperature of the activated and passivated Pt100) is independent of the gas temperature. The sensor signal is in linear correlation to the $H_2O_2$ concentration. Its characteristic may be described as follows:

$$\Delta T_{signal} = s \cdot c_{H2O2} + \Delta T_0 \quad (1.3)$$

Here, $s$ is the sensitivity, $c_{H2O2}$ is the $H_2O_2$ concentration and $\Delta T_0$ is the temperature off-set. For further information on the sensing principle and practical application of this sensor by means of a handheld sensor system for online monitoring of $H_2O_2$ in aseptic sterilisation processes is referred to **Chapter 2** of this thesis.

1.4.3 Calorimetric thin film sensors

Besides the sensor system for the online monitoring of the $H_2O_2$ concentration, efforts on the development of chip-based calorimetric sensors for the local detection of the $H_2O_2$ concentration on the items to be sterilised have been made. Here, a fast sensor response for the in-line monitoring during a short contact time of the package with the gaseous $H_2O_2$ as well as a flat sensor design for its fixation on the particular item are required. Even if the sensor arrangements are developed for two different areas of application, both of them are based on the same catalytic detection principle, namely a differential set-up of a catalytically activated and a passivated temperature-sensitive device. A first generation of these chip-based calorimetric sensors has been realised on silicon substrates, wherein the temperature-sensitive elements were based on either thin-film resistors [53] or thermocouples [54]. Though, due to their high thermal

mass, accompanied with a relatively long response time in the range of seven seconds, they did not meet the requirements for an in-line measurement with a short contact time of the analyte to be detected.

However, a second generation of thin-film sensors has been realised on a flexible polyimide sheet with a thickness of 25 µm [55]. The reason for using polyimide instead of conventional silicon as sensor substrate relies on the low thermal conductivity of 0.147 $Wm^{-1}K^{-1}$ (compared to 156 $Wm^{-1}K^{-1}$ for silicon) to guarantee a high sensitivity by avoiding the heat transfer between the active and passive sensor segment. In addition, polyimide shows a chemical inertness against hydrogen peroxide and an acceptable mechanical stability as well as a sufficient thermal endurance up to 400 °C. As catalyst, a dispersion of manganese(IV) oxide has been chosen, whereas the electrical insulation was achieved by a SU-8 photo resist layer on top of the resistance structures. A sample of this type of sensor is depicted in Fig. 1.2.

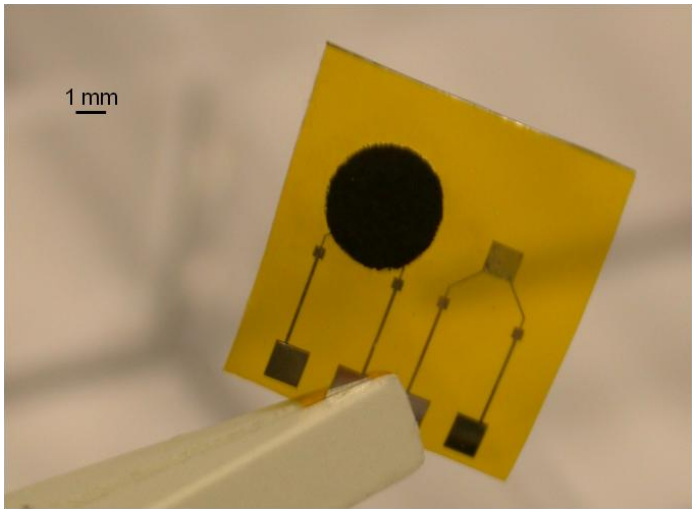


**Figure 1.2:** Calorimetric gas sensor based on a differential set-up of a catalytically activated (left) and a passivated (right) temperature-sensitive thin-film resistance, realised on a 25 µm polyimide sheet with a size of 10 x 10 mm² (Figure adapted from [50]).

With the polyimide-based sensor, sensitivities up to approximately 7.1°C/% v/v could be achieved in the range between 0 to 8% v/v $H_2O_2$ in the gaseous phase [56], which is comparable to the "TO 8" sensors for online monitoring. The

response time ($t_{90}$) of the polyimide-based sensors was determined to be 5.7 s. That said, the response is faster by a factor of approximately 6 compared to the sensors built up on a TO socket. Advantageously using a new "read-out" strategy for evaluation of the sensor signal now offers the possibility to quantitatively monitor the $H_2O_2$ concentration on-line as well as in-line in a single package during each sterilisation step [57]. Another promising feature of these foil sensors relies on their flexibility, allowing them to be installed in nearly any position on the packaging material, including edges and corners.

To exploit the full potential of these foil-based sensors and to make them suitable for in-line monitoring, for example, by integrating them into a test package, which can be carried through the sterilisation process, an adequate signal transmission has to be adapted still. In this context, a wireless transmission by means of an RFID (radio frequency identification) circuit seems to be an appropriate option. One proposal for such a circuit is as follows [53], consisting of a:

- Transmission system, containing a passive RFID transponder (inside the aseptic filling system), inductively coupled to an RFID transceiver (outside of the aseptic filling system)
- Calorimetric $H_2O_2$ gas sensor embedded inside of a test package and connected to a transponder

If sensor and transponder are fabricated on chip level together with an integrated low-power circuit, the transceiver could not only be used for reading the sensor data, but also to power the transponder circuit via electromagnetic induction. This way, an additional power supply is not required on the part of the test package.

Besides the technical sophistication of the thin-film calorimetric sensor based on polyimide foil, Kirchner *et al.* have recently introduced a method for monitoring the microbicidal effectiveness of gaseous $H_2O_2$ on the basis of this sensor [58]. Thereby, the sensor signal was correlated to the achieved LCR of *Bacillus atrophaeus* within a certain range of process parameters. This work also reflects the relationship between the growing microbicidal effectiveness with increasing $H_2O_2$ concentration, which has been reported by several independent studies (see **Section 1.3.2**).

## 1.5 Aim and scope of the work

### 1.5.1 Initial situation

The steady increase in the output of production of aseptic filling goods, increasing cost pressure as well as the consumers demand for safe foods require a sustainable solution in terms of the quality management of aseptic filling processes. One of the most critical factors represents the sterilisation of the packaging material. To the present day it has not succeeded to establish appropriate rapid tests for the monitoring of sterilisation processes employing $H_2O_2$ vapour as sterilant on the market, although this represents one of the most frequently used techniques. Recognised methods for determining the effectiveness of sterilisation propose the use of artificially inoculated packaging with a high load of spores, which show an increased resistance against the sterilising agent, taking them through the sterilisation process. The decrease in viable spore count after the sterilisation is then used a measure of the sterility. However, this method is very labour intensive and time consuming, since the samples have to be incubated for at least 24 hours prior to counting. Thus, a process control by means of a real-time monitoring seems virtually impossible.
The first sensor for monitoring sterilisation processes employing gaseous $H_2O_2$ at elevated temperatures and $H_2O_2$ concentrations up to 8% v/v has been introduced by Näther [51,52] (see **Section 1.4.2**). With this sensor, the $H_2O_2$ concentration in aseptic sterilisation processes could for the first time selectively be detected in the relevant concentration range. Mostly in parallel to the present work, the development of chip-based calorimetric sensors for the detection of $H_2O_2$ concentrations inside a package was done by Kirchner [50,59]. The works of Näther and Kirchner so far represent milestones with respect to the parametric monitoring of sterilisation processes employing $H_2O_2$.

However, as mentioned earlier, the sterilising effect by hydrogen peroxide is not solely attributed to its presence or concentration. It has been found that other parameters such as humidity, temperature, the presence of catalysts, etc. and particularly the interplay of these factors, can affect the sterilisation significantly. Considering the sterilisation process a complex multi-component system that needs to be monitored, the use of a multi sensor seems recommended. In general, a multi-sensor system may be understood as a

combination of different sensory functions which differ in their specificity and sensitivity, combined in a single device. At first glance, one might think that it would be most obvious to combine such sensors that could provide the highest specificity towards a given parameter when detecting it in a multi-component medium (MCM), in this case the sterilisation medium. However, the possibilities to find a set of sensors that is optimised to detect components in such a MCM are restricted by the fact that the specificity of a sensor is only partial. It should also be noted that the precise mechanism of microbial inactivation and the contribution of individual factors are not yet known in detail. It is believed that the biocidal action of $H_2O_2$ arises from the decomposition of the same and resulting short-living, reactive intermediates. These intermediates, mainly hydroxyl radicals, are related to a high potential of microbial inactivation. It seems therefore not satisfactory to deduce the effectiveness of the sterilisation process solely on the basis of parametric data such as the $H_2O_2$ concentration or temperature.

A promising approach could therefore be not to identify the individual parameters themselves, but the sum of their impact onto the sterilisation process. This admittedly abstract approach can be transferred to the scientifically much debated concept of an "electronic nose". In the course of this, usually an array of different, not necessarily selective, but highly sensitive sensors are combined. Thereby, the sensor response is not necessarily intended to serve as a quantitative measure of a physical quantity. Rather it can be understood as a chemical image, specific to the present situation. In combination with pattern recognition, such systems are nowadays used to mimic the human sense of smell, e.g., for the identification of odours, which was ultimately eponymous for this sensor concept. Ultimately, the use of electronic noses is not limited to the detection of odours. In principle, they can be applied to almost any situation related to gas detection, for example, they had been used for:

- Assessing the freshness and ripeness of fruits [60,61]
- Distinguishing between different types of coffee beans and roasting levels [62–64]
- Evaluating the shelf life of several dairy products (milk, yoghurts, cheese) [65–67]

- Quality assessment of smoked salmon [68,69]
- Determining the age of wine [70]
- Identification of wood samples [71]
- The sensorial analysis of human breath for quick diagnosis of certain diseases such as pneumonia or asthma [72,73]

The number of different types of sensors used for electronic sensing (e-sensing) purposes is just as numerous as their areas of application, as a view to the literature reveals. The metal-oxide semiconductor sensor (MOX) can be seen as the "standard sensor" in this field [74–76]. However, the same diversity is found for other transducers, such as surface acoustic wave (SAW) sensors [77], metal-oxide field-effect transistors (MOSFETs) [78], charge-couple device (CCD) sensors [79,80], mass spectrometry [81,82], gas chromatography [77,83] and infrared spectroscopy [84,85].

Besides multi sensors that make use of a single transducer principle there are also combined systems. Using only one transducer limits the resolution of such an array, since only a limited class of materials with their sensing characteristics is available. On the other hand, the combination of all types of available sensors may in turn lead to an excess of useful dimensions in the sensor response. Thus, rather the noise level is increased instead of obtaining new information, partly because of the sensitivity towards unimportant factors. It is therefore favourable to select the sensors specific to the desired application, which in turn requires certain prior knowledge of the analytical data.

Concerning the aseptic sterilisation process with gaseous $H_2O_2$, the selection of suitable sensors faces some difficulties in several aspects. First of all, the sensors must exhibit certain robustness against the harsh process conditions in order to enable continuous operation. In addition, they should be available at reasonable costs and operable with low technical effort. On the other hand, although the variables of the sterilisation process can be identified, there has still been a lack of suitable detection methods, for example, monitoring $H_2O_2$ at elevated concentrations and temperatures. Moreover, the mechanisms of microbial inactivation are still not well understood, which in turn restricts the identification of a suitable target dimension that could be correlated to the biocidal action. In sum, these could be the reasons why monitoring systems,

except for standard measuring procedures (e.g. monitoring of the temperature), were not associated with sterilisation processes employing gaseous $H_2O_2$ to the present day.

With regard to the sterilisation process, a promising strategy for monitoring its effectiveness could be as follows: On the one hand, combine sensors that monitor important variables of the sterilisation process with a high specificity, i.e., the $H_2O_2$ concentration and temperature. This could be done with the previously presented calorimetric sensor. On the other hand, the response of less specific, but all in all much more sensitive sensors may deliver useful information on the reactions or mechanisms intended to be involved in the microbial inactivation. These are, in particular, oxidising species derived from the decomposition of $H_2O_2$. In ideal case, the sensor response even correlates to the microbial inactivation. One group of sensors that potentially meet these requirements is represented by the MOX sensors [86]. Going even one step further, one could try to detect the final products of the decomposition of $H_2O_2$, namely $H_2O$ and $O_2$, in order to obtain evidences on the reactivity of the sterilant. Since $H_2O_2$ already represents a large proportion of the sterilant (an aqueous solution is evaporated), it seems reasonable to focus on $O_2$. A rather selective way of monitoring $O_2$ is by making use of an electrochemical type of sensor that is best known from the automotive industry as "lambda probe". The combination of these sensors thus represents a sophisticated way to assess the processes involved in the microbial inactivation. However, in order to allow a statement on the effectiveness of the sterilisation and correlating it to the sensor responses, the potential of microbial inactivation must first be determined for different process conditions using referenced test procedures, i.e., the CRT with spores of *B. atrophaeus*. Ideally, these tests are carried out in parallel to the sensory measurements. In the second instance, a correlation between the sensor response and the effectiveness of sterilisation could be established.

### 1.5.2 Content of the work

The objectives of the present work can be divided into two parts. First: One focus was to foster the practical application of the introduced calorimetric sensor in terms of an online monitoring of aseptic sterilisation devices. Second: The main objectives of this work were the targeted examination of the factors influencing the sterilisation by $H_2O_2$ and the identification of commercially

available gas sensors as possible candidates for monitoring the overall effectiveness of sterilisation. The content of this thesis has formally been divided into seven chapters, with the chapters 2 to 6 referring to original publications of the author of this thesis*:

**Chapter 2** describes the development and characterisation of a handheld sensor system for the online monitoring of $H_2O_2$ in aseptic sterilisation processes. The sensor system makes use of the calorimetric gas sensor described in **Section 1.4.2**. The sensor's response towards $H_2O_2$ as well as other important sensor characteristics, such as the long-term stability, response time and cross-sensitivities, are evaluated. Measurements were therefore carried out at a test rig as well as at a manufacturer's aseptic plant.

**Chapter 3** deals with a sensor system consisting of two commercially available gas sensors, namely a metal-oxide semiconductor gas sensor (TGS 816) and an electrochemical solid-electrolyte gas sensor (SO-A0-250) that are studied with respect to their response towards $H_2O_2$. Additionally, microbiological challenge tests with *Bacillus atrophaeus* have been carried out and a correlation between sensor response and microbicidal effectiveness is established via the $H_2O_2$ concentration.

In **Chapter 4**, the microbiological tests have been carried out in a larger extent, investigating the influence of $H_2O_2$ concentration, humidity, gas temperature and flow rate on the logarithmic cycle reduction of *B. atrophaeus*. In parallel, the response of six gas sensors, including three different types of sensors, towards the same parameters is evaluated, while the sensing mechanisms of the sensors and the influence of each parameter are discussed in detail. The obtained values of logarithmic cycle reduction are compared with chemical images generated by the sensors in a qualitative approach. Based on the relationship found between the sensor signals and the inactivation of spores, a multi-sensor system for the

*** To facilitate the readability of this thesis, the publications are not fully reproduced in their original wording: Recurring information has been shortened while additional information is provided when appropriate.**

evaluation of the aseptic sterilisation process by means of an electronic nose is proposed.

**Chapter 5** addresses the same sensors that had been investigated in Chapter 4, while on the basis of the experience from the previous works, the inactivation kinetics of *B. atrophaeus* is examined in substantially more detail in the relevant range. For this purpose, a methodical calibration experiment was carried out, which allows a more targeted investigation of the parameters influencing the sterilisation with gaseous $H_2O_2$. Finally, two different types of sensors are identified as possible candidates for monitoring the effectiveness of sterilisation in a quantitative way. Therefore, two different mathematical models that correlate the sensor signals to the biocidal action are presented.

**Chapter 6** focuses on the sensing mechanisms of metal-oxide semiconductor gas sensors in presence of $H_2O_2$. We note that the exact compositions of the commercially available sensors used in this work are unknown. In order to study the response of these sensors towards $H_2O_2$ more precisely, various metal oxides, namely $SnO_2$ and $WO_3$ as well as the influence of dopants were investigated in a further experiment. Therefore, a sensor array containing four sensing structures was realised on an 8 x 8 mm² sapphire chip. It is shown that the metal-oxide semiconductor gas sensors are suitable for detecting $H_2O_2$ down to the ppm concentration range. The highest sensitivity is achieved with Pt-doped $SnO_2$.

The concluding **Chapter 7** summarises the main findings of this work and discusses potential further actions and challenges.

## 1.6 Experimental considerations

This section provides general information on the sensing principle of the sensors used in this work. Furthermore, the experimental set-up as well as the preparation and evaluation of the microbiological tests are described.

### 1.6.1 Sensing principle of the sensors appearing in this thesis

Three different types of gas sensors have been used in this thesis. These are: A calorimetric-type gas sensor for the detection of $H_2O_2$, metal-oxide semiconductor gas sensors and an amperometric-type solid-electrolyte gas sensor for the detection of $O_2$. Their basic sensing mechanisms will be outlined in the following.

#### 1.6.1.1 Calorimetric $H_2O_2$ sensor

The calorimetric $H_2O_2$ sensor used in this thesis is based on a differential set-up of two temperature sensors (Pt100) that are mounted on a transistor outline (TO 8) socket. The sensing mechanism of this sensor has already been described in **Section 1.4.2**. Additional information on the sensor fabrication and its characteristics will be provided in **Chapter 2** of this thesis.

#### 1.6.1.2 Metal-oxide semiconductor sensors

Metal-oxide semiconductor gas sensors were introduced in the early 1960s by a Japanese Engineer named Taguchi. Even if a large number of different designs of these sensors have emerged in the meantime, basically nothing has changed with respect to its functional structure. The sensitive material consists of either an n-type (e.g., $SnO_2$, $WO_3$) or p-type (e.g., CuO) metal oxide, which is deposited in thin layers on a supporting material (substrate). The supporting material contains electrodes (e.g., interdigitated structures), which contact the active layer, enabling the measurement of its electrical properties, for example the resistance of the active layer. Since the majority of sensors used today consist of $SnO_2$, the sensing mechanism of MOX will exemplarily be explained at this point on behalf of all n-type metal-oxide semiconductors.

The sensing mechanism is related to the interaction of either oxidising or reducing gases at the metal-oxide surface, resulting in a change in the electrical resistance of the active layer. This mechanism is primarily depending on the presence of oxygen. At temperatures below about 150 °C, oxygen is initially

physisorbed at the crystal surface, which still has no effect on the electrical conductivity. With rising temperature, the oxygen dissociates and is increasingly ionised by donor electrons from the metal oxide. It is now chemisorbed to the surface. At the same time, the remaining positive charges lead to a formation of a space-charge layer. This space-charge layer serves as a potential barrier against free electron movement. The reactions responsible for the changes in the conductivity of the sensor take place at the grain boundaries of the polycrystal. The conductivity of the active layer is thereby attributed to the potential barrier. If a reducing gas (e.g., CO) is presented, it comes to a reaction with the chemisorbed oxygen. As a consequence, the surface density of the negatively charged oxygen decreases. The released electrons are returned to the semiconductor. Thus, the height of the barrier at the grain boundary is reduced, which in turn is associated with a decrease in the electrical resistance of the metal oxide. In contrast, upon exposure to oxidising gases (e.g., $O_3$), the formation of additional surface groups leads to an increase of the potential barrier, increasing the resistance of the active layer. Exemplarily, the mechanisms at the inter-grain barrier in the absence of gases and in the presence of a reducing gas are schematically depicted in Fig. 1.3. Here, Φ represents the surface barrier potential in eV.

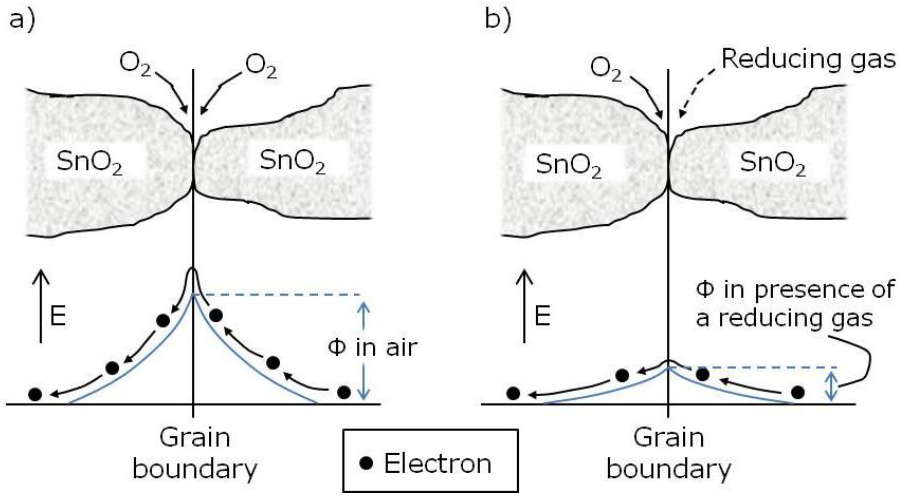


**Figure 1.3:** Model of the inter-grain potential barrier of an $SnO_2$ sensor in the absence of gases a) and in the presence of a reducing gas b) (this figure has been adapted from [87]).

It is obvious from these mechanisms, that MOX are not very specific, since in principle, almost any redox-active species will contribute to the change in the signal. Nevertheless, the low selectivity of these sensors can be increased by different strategies. Thus, for example, gas specific reactions may be enhanced by means of catalytically active additives, e.g., Pd and Pt. These dopants provide additional surface binding sites. Here, two mechanisms can be distinguished, which explain the contribution of impurities to increase the specificity and sensitivity: One is represented by the so-called spillover effect, which is based on the catalytic action of the incorporated impurities. By the binding of gas components on the foreign atoms, the activation energy is lowered for certain reactions. The products of these reactions may in turn further react with the adsorbates at the metal-oxide interface. The second effect is based on the chemisorption of charged molecules directly at the binding sites of the dopants. The charge transfer between the impurity atoms and the adsorbate, in turn, affects the potential barrier in the semiconductor. The selectivity of MOX may further be influenced by the operating temperature. One reason for this is the temperature-dependent occupancy of the binding sites, which means a shift in the ratio of potential reactants. Furthermore, the equilibria of the various surface reactions may be shifted by the change of the thermal energy of the adsorbates.

The response of MOX upon exposure to reacting gases is given by the following kinetic:

$$R_s = R_0[C]^{-\beta} \tag{1.4}$$

Here $R_s$ is the sensor resistance at a certain concentration $[C]$, $R_0$ is the resistance of the sensor in air and $\beta$ is equal to the power law exponent, specific to each sensor. These sensors are often applied for the detection of combustible gases, whereby the measurement range of the concentration can extend over several orders of magnitude. Typically, in such situations the sensor resistance is plotted as a function of the gas concentration in a log-log scale, wherein the sensor characteristic is represented as a straight line. However, in a rather narrow measuring range, the sensor characteristics can be approximated by linear models without loss in accuracy.

1.6.1.3 Oxygen sensor based on zirconia

Oxygen sensors, formally also referred to as lambda probes, are best known from the automotive industry. In contrast to the sensors used therein, which are operated in a potentiometric mode, the sensor used in this work is based on the amperometric principle.

The central part of this sensor is represented by a zirconia ($ZrO_2$) layer that, depending on the doping, is conductive for oxygen ions at temperatures above about 300 °C. It is therefore termed a solid electrolyte. To improve the carrier mobility in the solid electrolyte, the layer is usually doped with yttria ($Y_2O_3$). In order to adjust the operating temperature of the sensor, a heating element is integrated in the zirconia layer. The solid electrolyte is on both sides connected to porous platinum electrodes, which in the amperometric mode are applied with an operating voltage. The sensor is operated in a diffusion-limited mode. Therefore, the zirconia layer at the cathode is connected to the gas via a diffusion barrier. If the sensor is heated to the operating temperature, ionisation of the oxygen at the three-phase boundary between cathode, solid electrolyte and gas takes place:

$$O_2 + 4\,e^- \Rightarrow 2\,O^{2-} \tag{1.5}$$

Due to the applied voltage between the electrodes, the oxygen ions are transported to the anode, were the corresponding reverse reaction occurs:

$$2\,O^{2-} \Rightarrow O_2 + 4\,e^- \tag{1.6}$$

The oxygen ions in the solid electrolyte thus close the electric circuit. The transport of oxygen to the sensor surface is limited by the diffusion barrier. A schematic of the sensor structure and its sensing mechanism is depicted in Fig. 1.4.

Since the diffusion rate is dependent on the partial pressure of oxygen and on the permittivity of the barrier, the sensitivity and measuring range of the sensor can be adjusted by the design of the diffusion barrier. The resulting current serves as the sensor signal, which shows a logarithmic dependency from the partial oxygen pressure:

$$I_S = k \cdot ln\left(1 - \frac{[O_2]}{100}\right) \quad (1.7)$$

Here, $I_S$ is the sensor current, $[O_2]$ is the oxygen concentration and $k$ is a constant. The sensor constant $k$ is specific to each individual sensor. It may be determined by a single-point calibration in air ($[O_2]$≈21%).

The sensor is very specific to oxygen. However, the sensor reaction may be affected by redox-active species at the sensor surface. This becomes even more favoured at high operating temperatures of the sensor. Likewise, the sensor signal may be falsified by the humidity, due to the electrolytic splitting of water into hydrogen and oxygen, which is also favoured by elevated temperatures and the voltage applied at the electrodes.

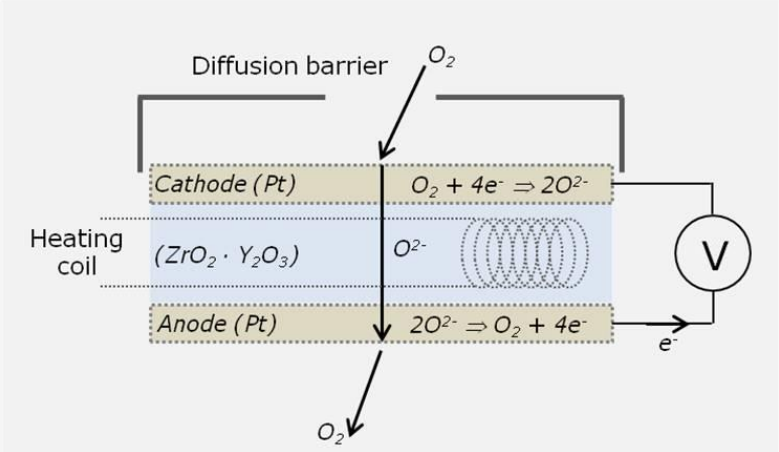


**Figure 1.4:** Schematic of the sensor structure and sensing mechanism of a solid-electrolyte ($ZrO_2$) based $O_2$ sensor.

1.6.2 Experimental set-up

In the following subsections, the experimental set-up for the sensory and microbiological measurements will be described. Parts of this section have been adapted from the **Chapters 2-5**.

1.6.2.1 Test apparatus

For the sensor characterisation and microbiological testing a test apparatus for the generation of gaseous hydrogen peroxide, which basically corresponds to a

sterilisation unit of an aseptic filling plant, has been developed. A model of the test apparatus is shown in Fig. 1.5.

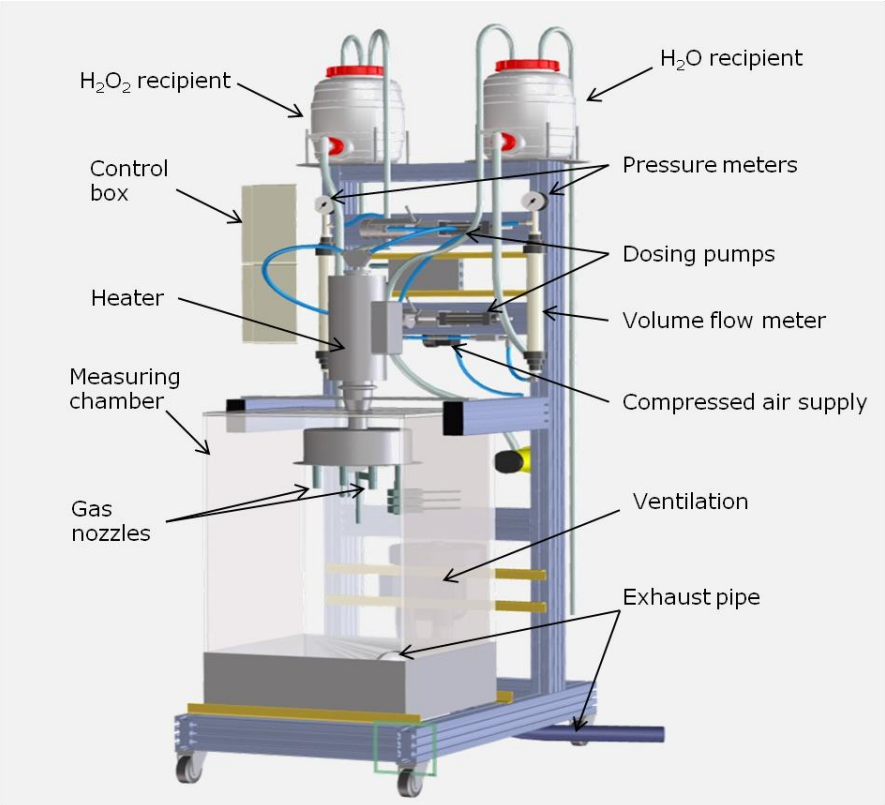


**Figure 1.5:** Model of the experimental set-up used for the sensor characterisation and microbiological testing.

The test apparatus consists of a heater (Thermocoax, WK 409, P=2x3 kW), two dosing piston pumps (486 µl/stroke) that are actuated via hydraulic cylinders (Rexroth, PRA 0320125) for hydrogen peroxide solution and water, a manual pressure valve and volume flow meter (Kobold, KSM1010, 3-34 $m^3/h$) to provide a steady flow of compressed air (5-20 $m^3/h$) and a measuring chamber to which the sterilising gas is fed by four gas nozzles. The heater and dosing pumps are operated by a control relay (Easy, 822-DC-TC). To adjust a certain concentration of $H_2O_2$ in the measuring chamber, the provided air stream is fed by an aqueous hydrogen peroxide solution of 35% w/w. In order to simulate the utilisation of lower concentrated $H_2O_2$ solutions, the air stream can additionally

be fed with water. The mixture of air and aqueous $H_2O_2$ solution is subsequently evaporated in the heater. The evaporated mixture is further heated up to the adjusted temperature up to a maximum of 330 °C and then, evenly dispensed to the measuring chamber by four gas nozzles. The installed ventilation provides a continuously discharge (70 m³/h) of the sterilising gas from the measuring camber. Details on the set parameters of each test series will be provided in the respective chapters.

1.6.2.2 Sensor mounting

For the measurement series with the commercially available gas sensors (**Chapters 3-5**) a sensor mounting has been installed on one of the gas nozzles inside the measuring chamber (see Fig. 1.6).

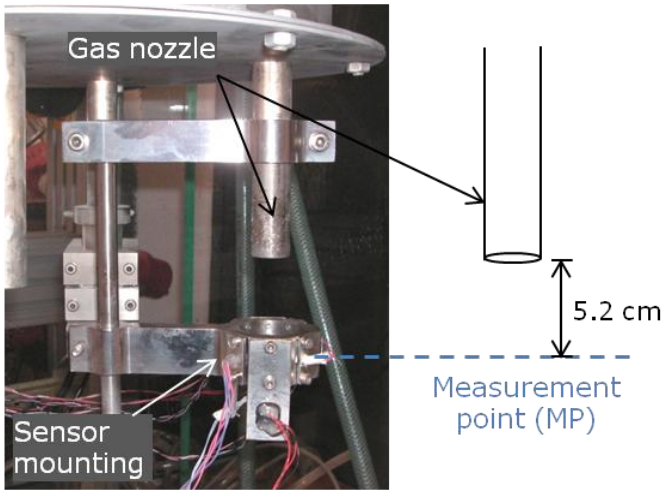


**Figure 1.6:** Photograph of the sensor mounting installed at one of the gas nozzles (inner diameter 16 mm) and schematic of the sensor position (measurement point) in the gas stream.

With this mounting the sensors a positioned equidistantly in the gas stream at a fixed measurement point (MP), 5.2 cm below the outlet of the gas nozzle. To ensure that the measurements are transferable to relevant applications, the measuring point was chosen similar to the test point of industrial processes. Also, in order to obtain information on the true gas temperature at the MP, an additional temperature sensor (Pt100, Jumo PCA 1.2005.1L) has been installed at this point.

1.6.2.3 Hydraulic slide

In order to carry out the microbiological measurements (**chapters 3-5**) a hydraulic slide for an automated, time-controlled sample-insert was implemented in the measuring chamber. A hydraulic cylinder inserts the microbiological samples (*Bacillus atrophaeus* spores immobilised on aluminium strips) into the measuring chamber for an adjustable period of time (via the control relay Easy 822-DC-TC). The exposure time of the samples to the sterilising gas was varied between 150-500 ms during the various studies. Inside the chamber, the measuring point (MP) for the microbiological samples was, equally to that of the gas sensors, defined at a distance of 5.2 cm under a separate nozzle. Photographs of the hydraulic slide in exposed position from inside the chamber (left) and in neutral position from outside the chamber (right) are depicted in Fig. 1.7.

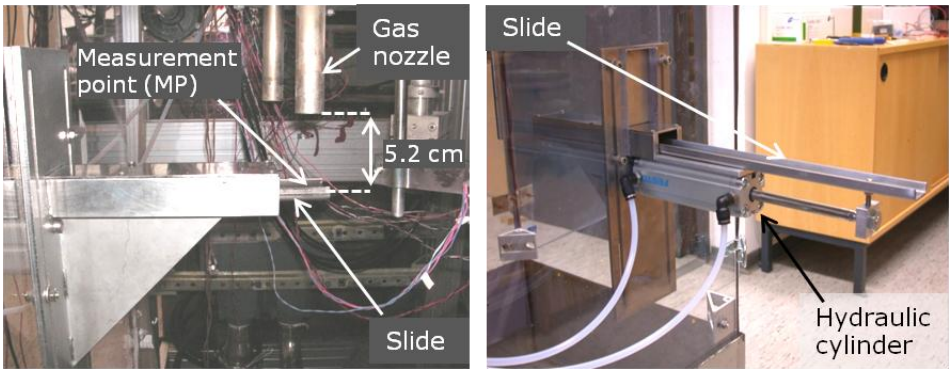


**Figure 1.7:** Photograph of the hydraulic slide in exposed position under the nozzle (left) and in neutral position protected from the $H_2O_2$ stream (right).

1.6.3 Microbiological tests

The microbiological tests described in this thesis have been carried out according to the count-reduction test (CRT) procedure. For a general description of the test method is referred to **Section 1.3.3**. In the following, mainly the preparation and handling of the microbiological samples will be outlined.

As test organism, spores of the species *Bacillus atrophaeus* have been chosen. It is the test organism of choice regarding the sterilisation by hydrogen peroxide, as it is a non-pathogen and offers an increased resistance against the sterilising agent [48, 88]. As test samples, aluminium strips with a size of approximately

5x20 mm have been prepared. The naturally grown thin surface layer of aluminium oxide on the test strips ensures the bioinertness of the test samples. Each strip was at one end inoculated with 10 µl of a spore suspension (spores of *Bacillus atrophaeus* in 70% ethanol) and dried at room temperature in a germ-free environment. The average initial count of spores on the test strips is depending on the initial spore suspension and has to be determined prior to each test series. For the microbiological samples used in this thesis, the initial spore count was in the order of $10^6$ (exact numbers will be provided in the respective chapters). A scanning electron microscopy (SEM) image of an aluminium strip inoculated with $\approx 1*10^6$ spores of *Bacillus atrophaeus* is depicted in Fig. 1.8. The spores have a rod-like shape and are approximately 1µm in length and 0.5µm in width.

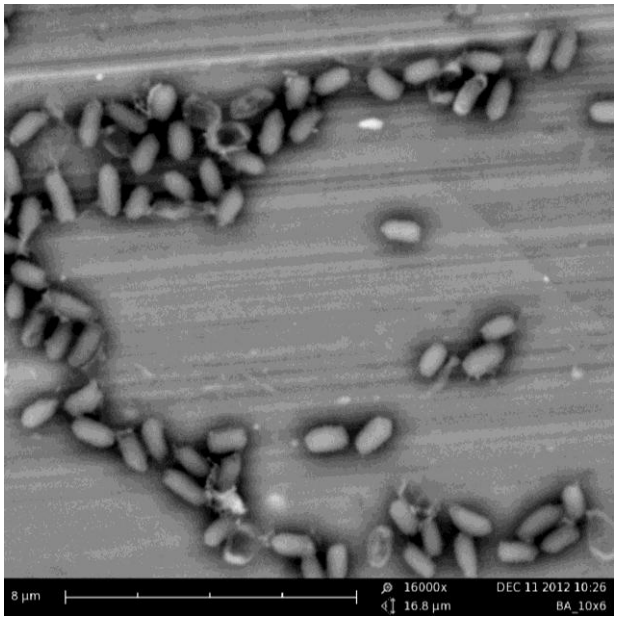


**Figure 1.8:** SEM image of *Bacillus atrophaeus* spores immobilised on an aluminium strip. The white scale bar corresponds to 8 µm.

For the microbiological testing, one strip at a time was glued to the slide (see **Section 1.6.2.3**) at the untreated end with adhesive tape and inserted into the measuring chamber for a pre-defined exposure time (150-500 ms). The exposure times and number of samples taken for each setting of the machine parameters are given in the respective chapters. After the exposure, the sample

(the lower end with adhesive tape previously removed) was put in a test tube with 10 ml of a lactated Ringer's solution. Afterwards, the test tubes are treated in an ultrasonic bath for 10 minutes in order to strip off the spores from the sample. Subsequently, different dilutions of each spore suspension have been prepared. It is necessary to prepare different dilutions of each sample in order to obtain a countable number (< 300) of colony forming units (CFU) on the agar plate. In this work, dilutions up to $1{:}10^4$ have been prepared. Out of each dilution two agar plates were cultivated with 1 ml of the spore suspension and incubated at 37 °C for 24 h. After the incubation time, the number of CFU, whereby each of the CFU is originated from one viable spore, was determined. From the number of CFU on each plate, the logarithmic cycle reduction (LCR), also referred to as log-rate, can be calculated according to Eq. 1.1 (see **Section 1.3.3**). For calculating the LCR the dilution of the spore suspension has to be considered. Fig. 1.9 exemplarily shows a plate with agar culture media and grown colonies of *Bacillus atrophaeus*.

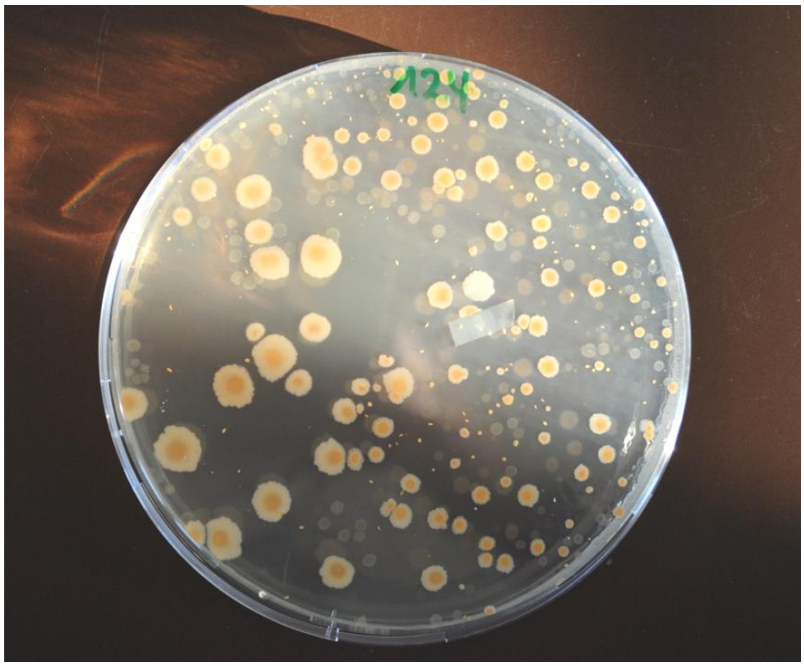


**Figure 1.9:** Photograph of an agar plate (diameter 145 mm) grown with approximately 300 colonies of *Bacillus atrophaeus* after an incubation time of 24 h at 37 °C.

**1.7 References**

[1] J.D. Floros, R. Newsome, W. Fisher, Feeding the world today and tomorrow: The importance of food science and technology, Comprehensive Reviews in Food Science and Food Safety 9 (2010) 572–599.

[2] F.A. Paine, The Packaging User's Handbook, Blackie; AVI, Glasgow, New York, 1991.

[3] G.L. Robertson, Food Packaging: Principles and Practice, Third edition, Taylor & Francis Group, 2012.

[4] S.D. Holdsworth, Aseptic Processing and Packaging of Food Products, Elsevier Applied Science; Elsevier Science Pub. Co., London, New York, 1992.

[5] P. Suppakul, J. Miltz, K. Sonneveld, S. Bigger, Active packaging technologies with an emphasis on antimicrobial packaging and its applications, Journal of Food Science 68 (2003) 408–420.

[6] David, Jairus R. D, R.H. Graves, V.R. Carlson, Aseptic Processing and Packaging of Food: A Food Industry Perspective, CRC Press, Boca Baton, 1996.

[7] Codex Alimentarius Comission, Code of hygienic practice for aseptically processed and packaged low-acid food, 1993.

[8] G. McDonnel, A.D. Russell, Antiseptics and disinfectants: Activity, action, and resistance, Clinical Microbiology Reviews 12 (1999) 147–179.

[9] J. Rogers, C. Sabourin, Y. Choi, W. Richter, D. Rudnicki, K. Riggs, M. Taylor, J. Chang, Decontamination assessment of *Bacillus anthracis*, *Bacillus subtilis*, and *Geobacillus stearothermophilus* spores on indoor surfaces using a hydrogen peroxide gas generator, Journal of Applied Microbiology 99 (2005) 739–748.

[10] A.D. Russell, Bacterial spores and chemical sporicidal agents, Clinical Microbiology Reviews 3 (1990) 99–119.

[11] R.T. Toledo, F.E. Escher, J.C. Ayres, Sporicidal properties of hydrogen peroxide against food spoilage organisms, Applied Environmental Microbiology (1973) 592–597.

[12] E. Linley, S.P. Denyer, G. McDonnell, C. Simons, J.-Y. Maillard, Use of hydrogen peroxide as a biocide: New consideration of its mechanisms of biocidal action, Journal of Antimicrobial Chemotherapy 67 (2012) 1589–1596.

[13] N.A. Klapes, D. Vesley, Vapor-phase hydrogen peroxide as a surface decontaminant and sterilant, Applied Environmental Microbiology 56 (1990) 503–506.

[14] R.A. Heckert, M. Best, L.T. Jordan, G.C. Dulac, D.L. Eddington, W.G. Sterritt, Efficacy of vaporized hydrogen peroxide against exotic animal viruses, Applied Environmental Microbiology 63 (1997) 3916–3918.

[15] J. Krause, G. McDonnell, H. Riedesel, Biodecontamination of animal rooms and heat-sensitive equipment with vaporized hydrogen peroxide, Contemporary Topics in Laboratory Animal Science 40 (2001) 18–21.

[16] G.L. French, J.A. Otter, K.P. Shannon, N.M. Adams, D. Watling, M.J. Parks, Tackling contamination of the hospital environment by methicillin-resistant *Staphylococcus aureus* (MRSA): A comparison between conventional terminal cleaning and hydrogen peroxide vapour decontamination, Journal of Hospital Infection 57 (2004) 31–37.

[17] M.D. Johnston, S. Lawson, Otter J. A., Evaluation of hydrogen peroxide vapour as a method for the decontamination of surfaces contaminated with *Clostridium botulinum* spores, Journal of Microbiological methods 60 (2005) 403–411.

[18] W.A. Rutala, D.J. Weber, Disinfection of endoscopes: Review of new chemical sterilants used for high-level disinfection, Infection Control & Hospital Epidemiology 20 (1999) 69–76.

[19] I. Ansari, A. Datta, An overview of sterilization methods for packaging materials used in aseptic packaging systems, Food and Bioproducts Processing 81 (2003) 57–65.

[20] H. Reuter, Aseptisches Verpacken von Lebensmitteln - Grundlagen und Stand der Technik, Chemie Ingenieur Technik 58 (1986) 785–793.

[21] G. McDonnell, Peroxygens and Other Forms of Oxygen: Their Use for Effective Cleaning, Disinfection, and Sterilization, in: P.C. Zhu (Ed.), New Biocides Development, American Chemical Society, Washington DC (2007) 292–308.

[22] M. Finnegan, E. Linley, S.P. Denyer, G. McDonnell, C. Simons, J.-Y. Maillard, Mode of action of hydrogen peroxide and other oxidizing agents: Differences between liquid and gas forms, Journal of Antimicrobial Chemotherapy 65 (2010) 2108–2115.

[23] N. Howlett, S. Avery, Induction of lipid peroxidation during heavy metal stress in *Saccharomyces cerevisiae* and influence of plasma membrane fatty acid unsaturation, Applied Environmental Microbiology 63 (1997) 2971–2976.

[24] D.W. Sundstrom, B.A. Weir, T.A. Barber, H.E. Klei, Destruction of pollutants and microorganisms in water by UV light and hydrogen peroxide, Water Pollution Research Journal of Canada 27 (1992) 57–68.

[25] N.G. Potapchenko, V.V. Illyashenko, V.F. Gorchev, O.S. Savluk, Synergistic effects of hydrogen peroxide and ozone oxidizers with UV-radiation in studies of the survival rate of *Escherichia coli* 1257 cells, Journal of Water Chemistry and Technology 15 (1993) 146–151.

[26] J. Imlay, S. Chin, S. Linn, Toxic DNA damage by hydrogen peroxide through the Fenton reaction in vivo and in vitro, Science 240 (1988) 640–642.

[27] T.A. Dix, J. Aikens, Mechanisms and biological relevance of lipid peroxidation initiation, Chemical Research in Toxicology 6 (1993) 2–18.

[28] P. Moradas-Ferreira, V. Costa, P. Piper, W. Mager, The molecular defences against reactive oxygen species in yeast, Molecular Microbiology 19 (1996) 651–658.

[29] B. Halliwell, J. Gutteridge, Oxygen toxicity, oxygen radicals, transition metals and disease, Biochemical Journal 1 (1984) 1–14.

[30] G. Storz, M. Christman, H. Sies, B. Amnes, Spontaneous mutagenesis and oxidative damage to DNA in *Salmonella typhimurium*, Proceedings of the National Academy of Sciences of the USA 24 (1987) 8917–8921.

[31] P. Riesenman, W. Nicholson, Role of the spore coat layers in *Bacillus subtilis* spore resistance to hydrogen peroxide, artificial UV-C, UV-B, and solar UV radiation, Applied Environmental Microbiology 66 (2000) 620–626.

[32] B. Setlow, C.A. Setlow, P. Setlow, Killing bacterial spores by organic hydroperoxides, Journal of Industrial Microbiology and Biotechnology 18 (1997) 384–388.

[33] B. Setlow, P. Setlow, Binding of small, acid-soluble spore proteins to DNA plays a significant role in the resistance of *Bacillus subtilis* spores to hydrogen peroxide, Applied Environmental Microbiology 59 (1993) 3418–3423.

[34] S. Shin, E. Calvisi, Beaman T.C., H. Pankratz, P. Gerhardt, R. Marquis, Microscopic and thermal characterization of hydrogen peroxide killing and lysis of spores and protection by transition metal ions, chelators, and antioxidants, Applied Environmental Microbiology 9 (1994) 3192–3197.

[35] C. Forney, R. Rij, R. Denis-Arrue, J. Smilanick, Vapor phase hydrogen peroxide inhibits postharvest decay of table grapes, HortScience – A publication of the American Society for Horticultural Science 1991 (12) 1512–1514.

[36] L. Hall, J.A. Otter, J. Chewins, N.L. Wengenack, Use of hydrogen peroxide vapor for deactivation of *Mycobacterium tuberculosis* in a biological safety cabinet and a room, Journal of Clinical Microbiology 45 (2007) 810–815.

[37] M. Kokubo, T. Inoue, J. Akers, Resistance of common environmental spores of the genus *Bacillus* to vapor hydrogen peroxide, PDA Journal of Pharmaceutical Science and Technology 5 (1998) 228–231.

[38] J. Wang, R. Toledo, Sporicidal properties of mixtures of hydrogen peroxide vapor and hot air, Food Technology 40 (1986) 62–67.

[39] P. Engelhard, U. Kulozik, Packstoffentkeimung mittels Wasserstoffperoxid – Methoden und Kombinationsverfahren, Chemie Ingenieur Technik 78 (2006) 1717–1722.

[40] B. Unger-Bimczok, V. Kottke, C. Hertel, J. Rauschnabel, The influence of humidity, hydrogen peroxide concentration, and condensation on the inactivation of *Geobacillus stearothermophilus* spores with hydrogen peroxide vapor, Journal of Pharmaceutical Innovation 3 (2008) 123–133.

[41] S. Esplugas, J. Giménez, S. Contreras, E. Pascual, M. Rodŕiguez, Comparison of different advanced oxidation processes for phenol degradation, Water Research 36 (2002) 1034–1042.

[42] J.-W. Kang, K.-H. Lee, A kinetic model of the hydrogen peroxide/UV process for the treatment of hazardous waste chemicals, Environmental Engineering Science 14 (1997) 183–192.

[43] A. Lopez, A. Bozzi, G. Mascolo, J. Kiwi, Kinetic investigation on UV and UV/$H_2O_2$ degradations of pharmaceutical intermediates in aqueous solution, Journal of Photochemistry and Photobiology A: Chemistry 156 (2003) 121–126.

[44] V.J. Pereira, H.S. Weinberg, K.G. Linden, P.C. Singer, UV degradation kinetics and modeling of pharmaceutical compounds in laboratory grade and surface water via direct and indirect photolysis at 254 nm, Environmental Science and Technology 41 (2007) 1682–1688.

[45] M. Swaminathan, M. Muruganandham, M. Sillanpaa, Advanced oxidation processes for wastewater treatment, International Journal of Photoenergy 2013 (2013) 1–3.

[46] M.N. Bathina, S. Mickelsen, C. Brooks, J. Jaramillo, T. Hepton, F.M. Kusumoto, Safety and efficacy of hydrogen peroxide plasma sterilization for repeated use of electrophysiology catheters, Journal of the American College of Cardiology 32 (1998) 1384–1388.

[47] S. Vassal, L. Favennec, J.J. Ballet, P. Brasseur, Hydrogen peroxide gas plasma sterilization is effective against *Cryptosporidium parvum* oocysts, American Journal of Infection Control 26 (1998) 136-138.

[48] Verband Deutscher Maschinen- und Anlagenbau e.V., Code of Practice: Filling machines of VDMA hygiene class V: Testing the effectiveness of packaging sterilization devices, Frankfurt, 2008.

[49] G. Moruzzi, W.E. Garthright, J.D. Floros, Aseptic packaging machine pre-sterilisation and package sterilisation: Statistical aspects of microbiological validation, Food Control 11 (2000) 57–66.

[50] P. Kirchner, S. Reisert, M. Schöning, Calorimetric Gas Sensors for Hydrogen Peroxide Monitoring in Aseptic Food Processes, Springer, Heidelberg, *in press*, DOI 10.1007/5346_2013_51.

[51] N. Näther, Entwicklung eines $H_2O_2$-Messverfahrens für die Überwachung der mikrobioziden Wirksamkeit bei der Sterilisation aseptischer Verpackungen, Dissertation, Marburg, 2009.

[52] N. Näther, H. Henkel, A. Schneider, M.J. Schöning, Investigation of different catalytically active and passive materials for realising a hydrogen peroxide gas sensor, Physica Status Solidi (a) 206 (2009) 449–454.

[53] P. Kirchner, B. Li, H. Spelthahn, H. Henkel, A. Schneider, P. Friedrich, J. Kolstad, M. Keusgen, M.J. Schöning, Thin-film calorimetric $H_2O_2$ gas sensor for the validation of germicidal effectivity in aseptic filling processes, Sensors and Actuators B: Chemical 154 (2011) 257–263.

[54] P. Kirchner, Y.A. Ng, H. Spelthahn, A. Schneider, H. Henkel, P. Friedrich, J. Berger, M. Keusgen, M.J. Schöning, Gas sensor investigation based on a catalytically activated thin-film thermopile for $H_2O_2$ detection, Physica Status Solidi (a) 207 (2010) 787–792.

[55] P. Kirchner, J. Oberländer, P. Friedrich, J. Berger, G. Rysstad, M. Keusgen, M.J. Schöning, Realisation of a calorimetric gas sensor on polyimide foil for applications in aseptic food industry, Sensors and Actuators B: Chemical 170 (2012) 60–66.

[56] P. Kirchner, J. Oberländer, P. Friedrich, J. Berger, H.-P. Suso, A. Kupyna, M. Keusgen, M.J. Schöning, Optimisation and fabrication of a calorimetric gas sensor built up on a polyimide substrate for $H_2O_2$ monitoring, Physica Status Solidi (a) 208 (2011) 1235–1240.

[57] P. Kirchner, J. Oberländer, H.-P. Suso, G. Rysstad, M. Keusgen, M.J. Schöning, Towards a wireless sensor system for real-time $H_2O_2$ monitoring in aseptic food processes, Physica Status Solidi (a) 210 (2013) 877–883.

[58] P. Kirchner, J. Oberländer, H.-P. Suso, G. Rysstad, M. Keusgen, M.J. Schöning, Monitoring the microbicidal effectiveness of gaseous hydrogen peroxide in sterilisation processes by means of a calorimetric gas sensor, Food Control 31 (2013) 530–538.

[59] P. Kirchner, Thin-film calorimetric gas sensors for hydrogen peroxide monitoring in aseptic food processes, Dissertation, Marburg, 2013.

[60] L.P. Pathange, P. Mallikarjunan, R.P. Marini, S. O'Keefe, D. Vaughan, Non-destructive evaluation of apple maturity using an electronic nose system, Journal of Food Engineering 77 (2006) 1018–1023.

[61] A.H. Gómez, G. Hu, J. Wang, A.G. Pereira, Evaluation of tomato maturity by electronic nose, Computers and Electronics in Agriculture 54 (2006) 44–52.

[62] T. Aishima, Discrimination of liquor aromas by pattern recognition analysis of responses from a gas sensor array, Analytica Chimica Acta 243 (1991) 293–300.

[63] M. Pardo, G. Niederjaufner, G. Benussi, E. Comini, G. Faglia, G. Sberveglieri, M. Holmberg, I. Lundstrom, Data preprocessing enhances the classification of different brands of Espresso coffee with an electronic nose, Sensors and Actuators B: Chemical 69 (2000) 397–403.

[64] M. Falasconi, M. Pardo, G. Sberveglieri, I. Riccò, A. Bresciani, The novel EOS835 electronic nose and data analysis for evaluating coffee ripening, Sensors and Actuators B: Chemical 110 (2005) 73–80.

[65] S. Labreche, S. Bazzo, S. Cade, E. Chanie, Shelf life determination by electronic nose: Application to milk, Sensors and Actuators B: Chemical 106 (2005) 199–206.

[66] M. Navratil, C. Cimander, C.-F. Mandenius, On-line multisensor monitoring of yogurt and filmjolk fermentations on production scale, Journal of Agricultural Food Chemistry 52 (2004) 415–420.

[67] T. Jeorgos, P.V. Nielsen, Electronic nose technology in quality assessment: Monitoring the ripening process of danish blue cheese, Journal of Food Science 70 (2005) E44–E49.

[68] G. Olafsdottir, E. Chanie, F. Westad, R. Jonsdottir, C.R. Thalmann, S. Bazzo *et al.*, Prediction of microbial and sensory quality of cold smoked atlantic salmon (*Salmo salar*) by electronic nose, Journal of Food Science 70 (2005) S563.

[69] J. Haugen, E. Chanie, F. Westad, R. Jonsdottir, S. Bazzo, S. Labreche, P. Marcq, F. Lundby, G. Olafsdottir, Rapid control of smoked Atlantic salmon (*Salmo salar*) quality by electronic nose: Correlation with classical evaluation methods, Sensors and Actuators B: Chemical 116 (2006) 72–77.

[70] C. di Natale, F.A.M. Davide, A. D'Amico, G. Sberveglieri, P. Nelli, G. Faglia, C. Perego, Complex chemical pattern recognition with sensor array: The discrimination of vintage years of wine, Sensors and Actuators B: Chemical 25 (1995) 801–804.

[71] A.D. Wilson, D.G. Lester, C.S. Oberle, Application of conductive polymer analysis for wood and woody plant identifications, Forest Ecology and Management 209 (2005) 207–224.

[72] N.G. Hockstein, E.R. Thaler, D. Torigian, Miller, Wallace T Jr, O. Deffenderfer, C.W. Hanson, Diagnosis of pneumonia with an electronic nose: Correlation of vapor signature with chest computed tomography scan findings, Laryngoscope 114 (2004) 1701–1705.

[73] S. Dragonieri, R. Schot, B.J. Mertens, S. Le Cessie, S.A. Gauw, A. Spanevello, P.J. Sterk, An electronic nose in the discrimination of patients with asthma and controls, Journal of Allergy and Clinical Immunology 120 (2007) 856–862.

[74] M. Egashira, Y. Shimizu, Odor sensing by semiconductor metal oxides, Sensors and Actuators B: Chemical 13 (1993) 443–446.

[75] H. Nanto, H. Sokooshi, T. Kawai, Aluminum-doped ZnO thin film gas sensor capable of detecting freshness of sea foods, Sensors and Actuators B: Chemical 14 (1993) 715–717.

[76] N. El Barbri, E. Llobet, N. El Bari, X. Correig, B. Bouchikhi, Electronic nose based on metal oxide semiconductor sensors as an alternative technique for the spoilage classification of red meat, Sensors 8 (2008) 142–156.

[77] E. Staples, Electronic nose simulation of olfactory response containing 500 orthogonal sensors in 10 seconds, in: 1999 IEEE Ultrasonics Symposium. Proceedings. International Symposium, Caesars Tahoe, NV, USA, pp. 417–423.

[78] F. Winquist, H. Sundgren, I. Lundstrom, A practical use of electronic noses: Quality estimation of cod fillet bought over the counter, in: International Solid-State Sensors and Actuators Conference - TRANSDUCERS '95, Stockholm, Sweden, pp. 695–698.

[79] Y. Kuang, D.R. Walt, Monitoring "promiscuous" drug effects on single cells of multiple cell types, Analytical Biochemistry 345 (2005) 320–325.

[80] S.R. Kain, M. Adams, A. Kondepudi, T.T. Yang, W.W. Ward, P. Kitts, Green fluorescent protein as a reporter of gene expression and protein localization, Biotechniques 19 (1995) 650–655.

[81] R. Jonsdottir, G. Olafsdottir, E. Martinsdottir, G. Stefansson, Flavor characterization of ripened cod roe by gas chromatography, sensory analysis, and electronic nose, Journal of Agricultural Food Chemistry 52 (2004) 6250–6256.

[82] Supriyadi, K. Shimizu, M. Suzuki, K. Yoshida, T. Muto, A. Fujita, N. Tomita, N. Watanabe, Maturity discrimination of snake fruit (*Salacca edulis Reinw*.) cv. *Pondoh* based on volatiles analysis using an electronic nose device equipped with a sensor array and fingerprint mass spectrometry, Flavour and Fragrance Journal 19 (2003) 44–50.

[83] E. Jellum, O. Stokke, L. Eldjarn, Application of gas chromatography, mass spectrometry, and computer methods in clinical biochemistry, Analytical Chemistry 46 (1973) 1099–1106.

[84] T.A.T.G. van Kempen, W.J. Powers, A.L. Sutton, Technical note: Fourier transform infrared (FTIR) spectroscopy as an optical nose for predicting odor sensation, Journal of Animal Scienc 80 (2002) 1524–1527.

[85] S. Armenta, N.M. Coelho, R. Roda, S. Garrigues, M. de la Guardia, Seafood freshness determination through vapour phase Fourier transform infrared spectroscopy, Analytica Chimica Acta 580 (2006) 216–222.

[86] X. Liu, S. Cheng, H. Liu, S. Hu, D. Zhang, H. Ning, A survey on gas sensing technology, Sensors 12 (2012) 9635–9665.

[87] Figaro USA Inc., Manufacturer data sheet, Operating principle of Figaro Gas Sensors (revised 6/03), www.figarosensor.com/products/general.pdf (21.11.2013).

[88] S.A. Burke, J.D. Wright, M.K. Robinson, B.V. Bronk, R.L. Warren, Detection of molecular diversity in *Bacillus atrophaeus* by amplified fragment length polymorphism analysis, Applied and Environmental Microbiology 70 (2004) 2786–2790.

# Chapter 2

## Development of a handheld sensor system for the online measurement of hydrogen peroxide in aseptic filling systems

Physica Status Solidi (a), 2010, Vol. 207, pp. 913-918

Steffen Reisert[1], Hartmut Henkel[2], Andreas Schneider[2], Daniel Schäfer[2], Peter Friedrich[3], Jörg Berger[4] and Michael J. Schöning[1]

1) Institute of Nano- and Biotechnologies, FH Aachen, 52428 Jülich, Germany

2) von Hoerner & Sulger GmbH, 68723 Schwetzingen, Germany

3) Aseptiksysteme & Foodtechnology, 52441 Linnich, Germany

4) filldesign GmbH, 41199 Mönchengladbach, Germany

## 2.1 Abstract

A handheld sensor system for the online measurement of hydrogen peroxide in aseptic sterilisation processes has been developed. It is based on a calorimetric-type gas sensor that consists of a differential set-up of two temperature sensors, of which one is catalytically activated and the second one is passivated and used as reference. The sensor principle relies in detecting a rise in temperature on the active sensor due to the exothermic reaction of $H_2O_2$ on the catalytic surface. To characterise the sensor system towards $H_2O_2$ sensitivity and other influencing factors, measurements have been carried out both at an experimental set-up and a manufacturer's sterilisation machine. Physical sensor characterisation was done by means of the optical microscopy.

## 2.2 Introduction

The aseptic filling of pre-sterilised foodstuff has reached a high level of technical sophistication and is growing in importance [1]. Among other methods, hydrogen peroxide vapour is used as surface decontaminant for food packages [2, 3]. Due to its environmental compatibility it offers various advantages over other chemical disinfectants. Hydrogen peroxide mainly decomposes to water and oxygen [1,4]. The microbial reduction process by hydrogen peroxide vapour is carried out at temperatures above 200 °C and concentrations of $H_2O_2$ up to 10% v/v in gaseous phase. Vapour phase hydrogen peroxide was shown to have effective antimicrobial properties and to inactivate bacteria, fungi, viruses and highly resistant spores [4-7]. In various studies it was shown that there is a correlation between the concentration of hydrogen peroxide and the microbial reduction of microorganisms [7-11].

For industrial applications it is very useful to monitor the hydrogen peroxide concentration and gas temperature during microbial reduction processes, not only to achieve a more efficient utilisation of hydrogen peroxide, but also to detect faults during the microbial reduction process, e.g., the use of water instead of an aqueous hydrogen peroxide solution or a failure in the dosage of $H_2O_2$.

Various concepts for the realisation of a hydrogen peroxide sensor have been proposed during the last years. Organic materials, like catalase, have been applied to detect $H_2O_2$. These sensors offer a high specificity and very low detection limits, but can not be used at elevated temperatures and high hydrogen peroxide concentrations [12-14]. A further approach relies on the use of semiconductor gas sensors. In this case, the high cross-sensitivity of semiconductor sensors to oxidising and reducing gases can be used to detect hydrogen peroxide. These sensors tolerate gas temperatures up to 500 °C and high concentrations of hydrogen peroxide, but the disadvantages of these sensors can be strong drift and high cross-sensitivity towards humidity [15-20].

In this work, a calorimetric-type gas sensor has been used for the detection of hydrogen peroxide. It is the sensor of choice regarding sensitivity, stability, measuring range and maximum temperature. Also it can be produced at low costs [21-23]. The sensor system developed has been designed as a handheld

sensor system. It offers the advantage of portability compared to permanently installed monitoring systems.

## 2.3 Experimental

### 2.3.1 Test equipment

To investigate the sensor properties, an experimental set-up for the generation of hydrogen peroxide vapour, similar to industrial apparatuses, has been used. The detailed description of the experimental set-up is shown in **Section 1.6.2.1**.

As for industrial processes, depending on the product to be sterilised, a wide range of parameters is used; a set of parameters, which represent the most common settings, has been chosen to carry out the sensor characterisation. In case of the four nozzle set-up, gas streams between 7.5 and 15 m³/h, which correspond to gas streams between 1.785 and 3.75 m³/h per nozzle, have been selected. The gas temperature was varied between 150 and 330 °C. An aqueous hydrogen peroxide solution of 35% w/w technical grade has been used. Amounts between 250 and 1100 µl/s have been fed to the carrier gas stream. Thereby, hydrogen peroxide concentrations up to 7.4% v/v in the gaseous phase have been realised.
In further investigations within the scope of a field experiment, measurements have been performed at an industrial aseptic filling machine of an established manufacturer, which uses a similar evaporation unit.

### 2.3.2 Sensor principle and fabrication

To realise a calorimetric gas sensor for the detection of hydrogen peroxide, a differential set-up, consisting of a catalytically activated and a passivated temperature sensor, similar as described in [21] has been chosen. The sensor principle relies in detecting a rise in temperature on the catalytically active surface, due to the exothermic reaction of $H_2O_2$ on the same, while the passivated temperature sensor is at ambient (gas) temperature. Fig. 2.1 shows a sketch of the sensor principle. In the same work, different catalysts and passivation materials have been investigated. It was shown, that manganese oxide powder was the most suitable catalyst in terms of activity (temperature increase) and stability. As passivation material Perfluoroalkoxy (PFA) has been

chosen. The same material was used as adhesion promoter for the manganese oxide powder on the active temperature sensor.

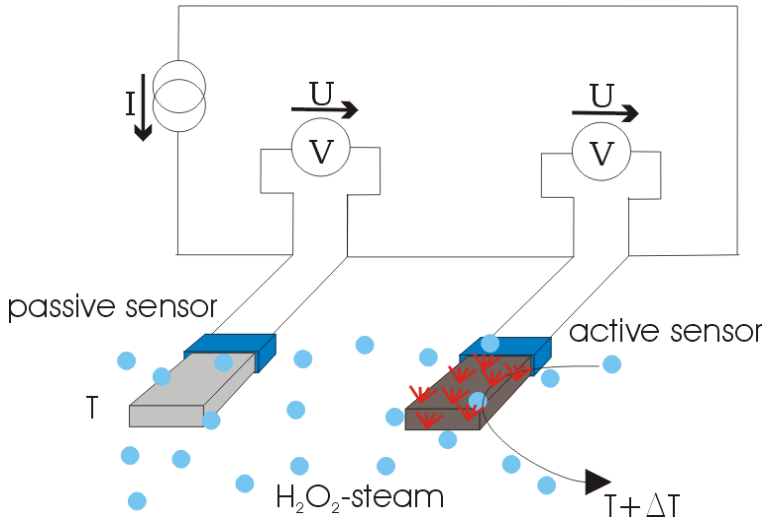


**Figure 2.1:** Sketch of the differential sensor principle.

As temperature transducers, commercially available Pt100 chip sensors have been utilised. The differential set-up was build up in a TO-8 transistor housing. Fig. 2.2 shows the sensor housing a), the active and passive temperature sensor on the transistor socket b), a close-up view on the passive sensor c) and active sensor d), as well as an enlarged view on the catalyst e).

The Pt100 chip sensors were soldered on the contact pins of the transistor socket. Afterwards, the sensors have been treated with PFA and manganese oxide powder, respectively. After this treatment, the active and passive sensor have been characterised by means of 3-D video microscopy as shown in Fig. 2.2 c)-e). As can be seen in Fig. 2.2 c), the whole sensor surface is covered by the PFA. Though there are a few air enclosures in the coat, which most probably resulted from a too fast heating during the coating process. However, these enclosures did not show a negative influence on the passivation characteristics of the sensor, but may have an effect on the sensors response time. On the other hand, in Fig. 2.2 d) the surface of the active sensor is shown. The manganese oxide particles cover the whole surface on the front part sensitive

area of the sensor. On the close-up perspective on the active surface in e) it can be seen that the catalyst surface is rather rough, which is favourable as the contact area of the catalyst is larger.

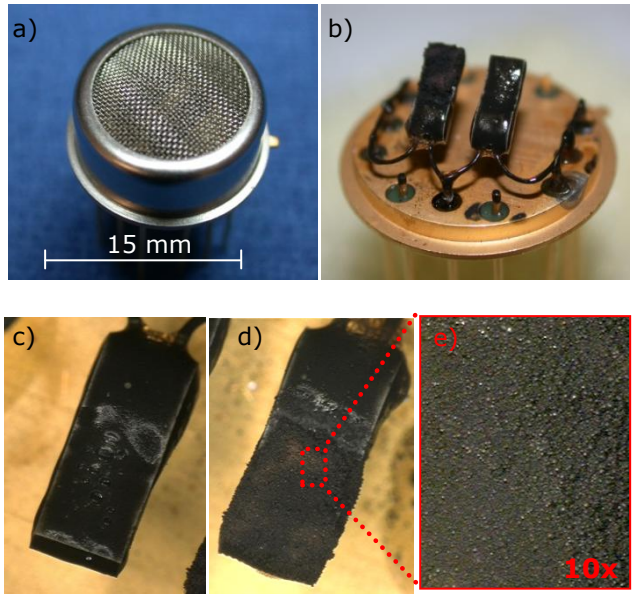


**Figure 2.2:** Photography of the sensor housing a), the active and passive temperature sensor on the transistor socket b), close-up view on the passive sensor c) and active sensor d) and enlarged view on the catalyst by an area of appr. 200 x 300 µm² e).

2.3.3 Sensor housing

In a preliminary study it has been shown that the sensor position in the gas stream has an influence on the reproducibility of the sensor signal. For this purpose, a sensor housing has been constructed, which allows to place the sensor in a defined position in the gas stream. Fig. 2.3 shows a section view of the sensor housing.

The sensor housing consists of a tube with a diameter of 44 mm. At the bottom end, the sensor is adjusted in a socket, which is placed at the centre of the tube in vertical position. At the upper end, the housing consists of an adapter with a smaller diameter, in which the gas nozzle of the sterilisation apparatus is inserted. Hence, the sensor position is always the same, i.e., ca. 40 mm from the outlet of the gas nozzle. The sensor housing is affixed to a telescopic rod,

which carries the sensor cables. On the other end it is connected to the handheld readout device.

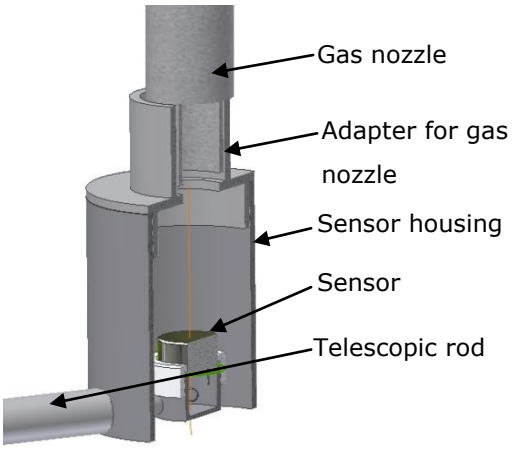


**Figure 2.3:** Section view of the sensor housing. The sensor wiring is connected to the readout unit along the telescopic rod.

2.3.4 Handheld device

In order to read out the sensor data, an electronic handheld unit has been developed by vH&S GmbH (Schwetzingen, Germany). It consists of a current source of 1 mA to supply the Pt100 chip sensors, two analogue-to-digital converters (ADC) to convert the analogue signals of the temperature sensors into discrete numbers, which are then post-processed by a microcontroller. The necessary specifications for the sensor readout unit and conversion factors for signal processing were provided by the author of this thesis (for the full data flow diagram see **Appendix 4**). The system is previously fed with the calibration data of the sensor. Based on this data, the microprocessor will calculate the hydrogen peroxide concentration from the measurement values, obtained by the two temperature sensors. The handheld device is equipped with an electronic display. Fig. 2.4 shows the data flow diagram a) and a photography of the handheld device b).

The electronic unit was programmed in a way that various display options are available. The display parameters are the measured hydrogen peroxide concentration and gas temperature. A plotting of the measurement values over time is also included. The different display views can be changed via the

navigation keys. The calibration data may also include algorithms for data preparation, such as the compensation of temperature influences.

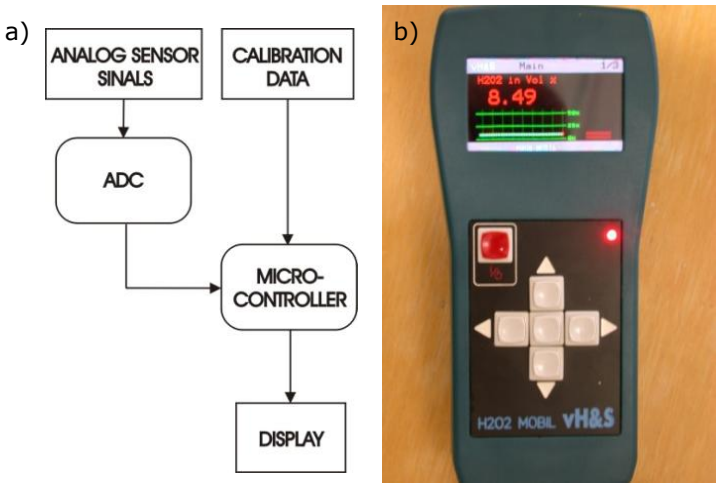


**Figure 2.4:** Data flow diagram a) and photography of the handheld device developed by the vH&S GmbH (Schwetzingen, Germany) b).

## 2.4 Results and discussion

### 2.4.1 Sensor characterisation

The sensor characterisation has been carried out with the test equipment, which is described in **Section 2.3.1**. All measurements have been performed with the sensor housing and the sensor was placed in the gas stream as described in **Section 2.3.3**. For the characterisation of the sensor, the sensitivity towards hydrogen peroxide, the dependency of temperature and gas flow, as well as the response time and the long-term stability were of interest. The sensitivity of the sensor has been investigated at different hydrogen peroxide concentrations. Therefore, amounts of 250 to 1100 µl/s of an aqueous hydrogen peroxide solution have been dosed to a carrier gas stream of 10 m³/h. Subsequently, the aerosol was vaporised in the heater and the gas was heated up to a temperature of 270 °C. Thus, concentrations of hydrogen peroxide between 2.3 and 7.4% v/v have been realised. Fig. 2.5 shows the obtained measurement values (temperature difference between active and passive sensor) as a function of the hydrogen peroxide concentration.

The sensor shows a linear behaviour of the hydrogen peroxide concentration in a range up to 8% v/v, which can be described as follows:

$$\Delta T = -3.8 + C_{H2O2} \cdot 8.5 \qquad (2.1)$$

Here, $\Delta T$ is the temperature difference (in °C) between active and passive sensor and $C_{H2O2}$ is the hydrogen peroxide concentration in percent of volume (% v/v). The characteristic parameters of the sensor are the sensor off set of -3.8 °C and the sensitivity of 8.5 °C/ % v/v.

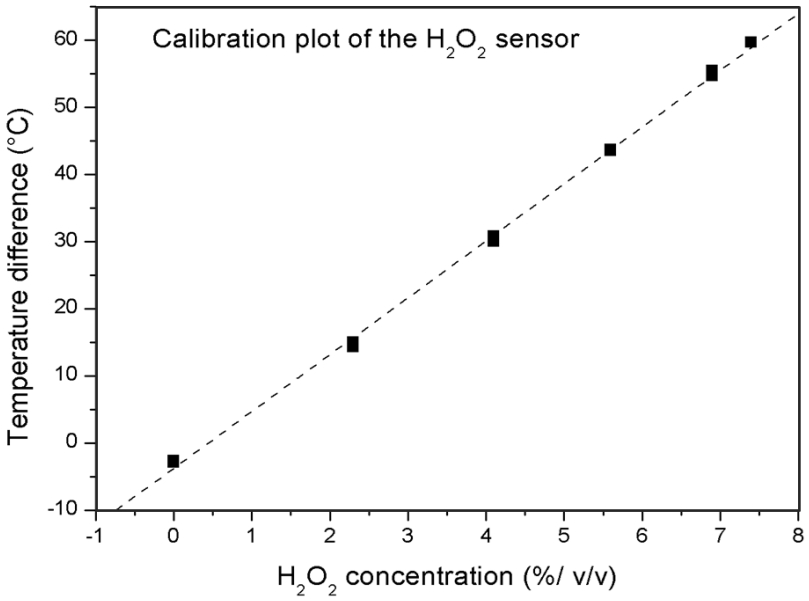


**Figure 2.5:** Calibration plot of the $H_2O_2$ sensor.

In order to characterise the sensor's long-term stability, a recalibration has been performed after the sensor has been exposed to the hydrogen peroxide vapour for around 15 hours. While hydrogen peroxide has a tendency to decompose on its own, it is necessary to add a stabiliser to the solution. In case of the hydrogen peroxide solution that was used in this study, phosphoric acid serves as stabiliser. It is possible that the sensor suffers an aging due to residues of the stabiliser contained in the hydrogen peroxide solution, namely phosphorus and phosphorus containing compounds, which blocks surface sites of the catalyst and

hence, inhibit it. If that is the case, a notable decrease in sensitivity of the sensor (slope of the calibration plot) would be noted. Fig. 2.6 shows the results obtained by the first and second calibration measurement.

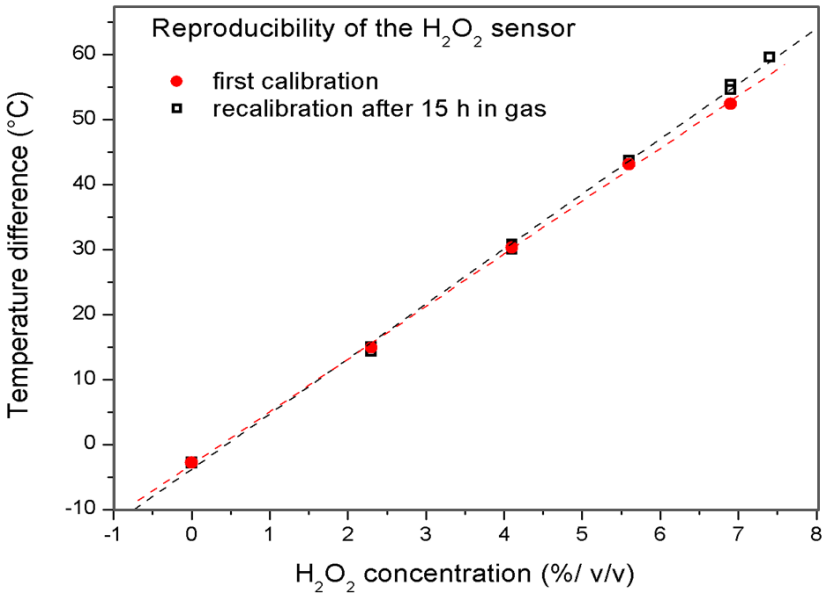


**Figure 2.6:** Comparison of the sensor curve before and after 15 hours of exposure to $H_2O_2$ vapour.

The values obtained during the recalibration after the sensor has been exposed to hydrogen peroxide vapour for 15 hours are almost identical to those obtained during the first calibration. In both cases, a linear regression model was fit to the data. The characteristic parameters of the two curves are shown in Tab. 2.1.

**Table 2.1:** Characteristic parameters of the calibration curves.

| Measurement | Off set (°C) | Sensitivity (°C/ % v/v) |
|---|---|---|
| calibration | -3.1 | 8.1 |
| recalibration | -3.8 | 8.5 |

It was assumed, that the sensitivity would decrease with time due to residues of stabiliser on the active sensor surface. Though, a decrease in sensitivity after 15 hours of exposure to hydrogen peroxide vapour can not be observed. The

sensitivity is actually higher in case of the recalibration. However, the differences in the obtained values are within an acceptable margin of error.
In a further measurement, the influence of gas temperature on the sensor signal has been investigated. Therefore, the gas temperature in the heater has been varied between 150 and 330 °C at a constant concentration of $H_2O_2$ of 4.1% v/v. The values obtained by this measurement are shown in Fig. 2.7. The signals have been normalised to the measured value at the lowest gas temperature of 150 °C and are plotted against the measured temperature at the sensor chip.

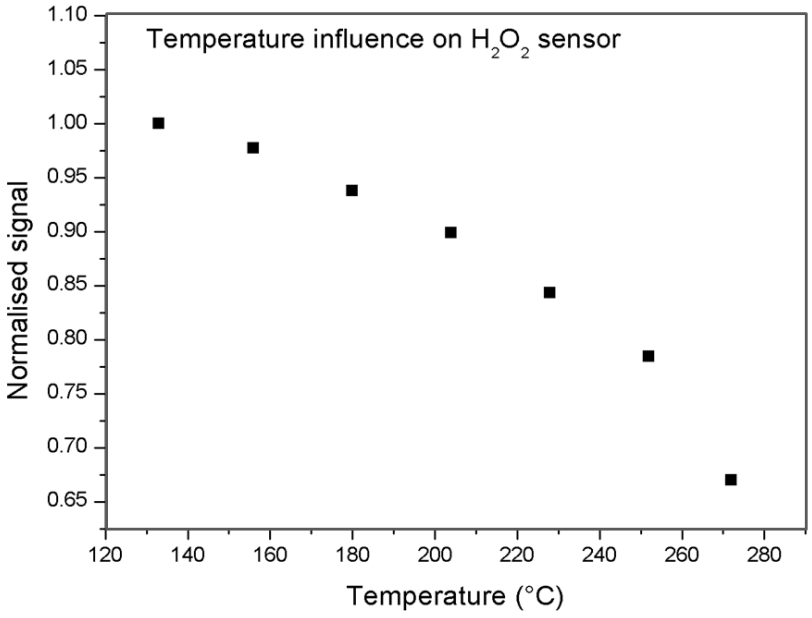


**Figure 2.7:** Measured values at a constant $H_2O_2$ concentration of 4.1% v/v, normalised to the measured value at the lowest gas temperature of 150 °C.

The measurement values are decreasing with increasing gas temperature, whereas the decrease of the signal is increasingly accelerated at higher temperatures. At the highest gas temperature of 330 °C, which corresponds to a temperature of around 270 °C at the sensor, the measured value has decreased to ca. 67% of the initial value. This behaviour was, however, not expected. The Arrhenius's equation, which describes the temperature dependency of the rate constant of a chemical reaction, predicts an increasing rate constant with temperature. Hence, the activity of the catalyst should be increasing with

temperature and in consequence, the temperature difference should be higher at elevated gas temperatures. On the other side, it is known that hydrogen peroxide decomposes to molecular oxygen and water. The decomposition rate of $H_2O_2$ is, however, also accelerated with increasing temperature. Therefore, it is imaginable, that the hydrogen peroxide decomposes on the hot surface of the heater, which can reach a temperature of up to 600 °C and in consequence, the concentration of $H_2O_2$ in the gas is decreasing, resulting in a lower temperature difference at the sensor. Though, to finally evaluate the present question, further investigations have to be done.

In addition, the influence of the gas flow rate on the behaviour of the $H_2O_2$ sensor has been studied. Therefore, the gas flow rate has been varied between 7.5 and 15 m³/h at a constant $H_2O_2$ concentration of 4.1% v/v. The values obtained from this measurement are depicted in Fig. 2.8.

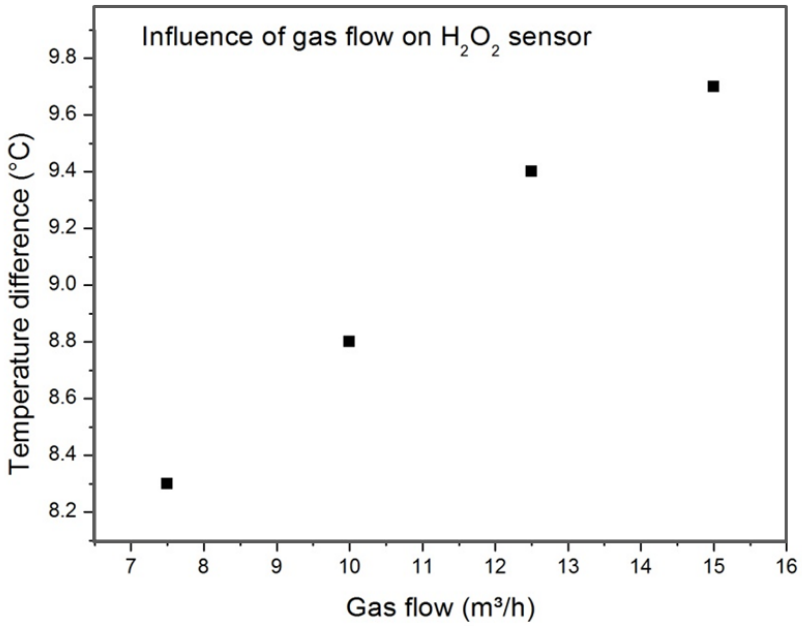


**Figure 2.8:** Influence of the flow rate on the $H_2O_2$ sensor response.

The measurement results shown in Fig. 2.8 were obtained with a second $H_2O_2$ sensor, different from the one that was used for the earlier described measurements. This sensor possesses a lower sensitivity (compare temperature difference at 10 m³/h and 4.1% v/v $H_2O_2$ from Fig. 2.5 and 2.6), but the overall

sensor behaviour was identical. It can be seen that the flow rate has an influence on the sensor's behaviour. The temperature difference is increasing with increasing flow rate. Between the highest flow rate of 15 m³/h and the lowest flow rate of 7.5 m³/h, the difference in the sensor signal is 1.4 °C at a $H_2O_2$ concentration of 4.1% v/v, which corresponds to a difference in sensitivity of 0.34 °C/ % v/v between the highest and the lowest flow rate, or a relative change in sensitivity of 2.1% per m³/h. Assuming that the flow rate is a fixed parameter in aseptic sterilisation processes this influence can be neglected.
Furthermore, the response time of the sensor has been studied. It was shown that the sensor reaches a stable signal (temperature difference between active and passive temperature sensor), 35 seconds after it was placed in the gas stream. According to the manufacturer data sheet of the Pt100 chip sensors, used to realise the $H_2O_2$ sensor, the response time ($t_{90}$) of an individual sensor in air is 16 seconds. It is likely that the response time of the sensor is increased due to the additional coating with PFA and manganese oxide, respectively. The air enclosures in the PFA coat (see **Section 2.3.2**) may also lead to a prolongation of the response time. In a single series of measurement, the absolute accuracy of the sensor is 0.2% v/v. Over a total measurement time of 25 hours, the accuracy was 0.5% v/v. No cross-sensitivity towards humidity was observed. Table 2.2 summarises the most important sensor characteristics.

**Table 2.2:** Main characteristics of the differential calorimetric $H_2O_2$ sensor.

| | |
|---|---|
| Sensitivity | up to 10 °C/ % v/v |
| Measuring range | up to 10% v/v $H_2O_2$<br>up to 330 °C |
| Response time | 35 s |
| Accuracy | ±0.2% v/v $H_2O_2$ (single measurement)<br>±0.5% v/v $H_2O_2$ (life time) |
| Life time | > 25 h |
| Cross-sensitivity $H_2O$ | none |

In further investigations, the sensor system has been tested at a manufacturer's sterilisation machine, by means of a field experiment. Measurements have been

carried out at various hydrogen peroxide concentrations, gas temperatures and flow rates. Thereby, similar sensor behaviour, compared to the measurements at the experimental set-up has been observed. Also it was possible, to immediately detect errors of the sterilisation process, when, for example, the dosage of hydrogen peroxide failed or water was dosed to the carrier gas stream instead of hydrogen peroxide solution.

## 2.5 Conclusions

A handheld sensor system for the detection of hydrogen peroxide, based on a calorimetric gas sensor, has been developed and characterised. The device comprises all necessary electronics for the acquisition and processing of sensor data. Measurements have been performed at an experimental set-up and a manufacturer's sterilisation machine.

The sensor exhibits a high sensitivity and selectivity towards hydrogen peroxide. The linear range of the $H_2O_2$ sensor is between 0 and 8% v/v $H_2O_2$. The influence of gas flow on the sensor signal is negligible within the range of interest. A temperature-dependent behaviour of the sensor signal was observed. Indices could be found, that the decrease in the sensor signal towards higher gas temperatures may be due to the decomposition of hydrogen peroxide at the surface of the heater. The response time of the $H_2O_2$ sensor is 35 seconds. In a single measurement, the sensor accuracy is 0.2% v/v. The absolute accuracy over a life time of 25 hours is 0.5% v/v. Compared to the results in [21], where a similar sensor set-up in a TO housing was used, an improvement in the sensor characteristics, especially regarding sensitivity, accuracy and long-term stability, was achieved. Furthermore, investigations on the response time and the influence of flow rate have been performed. While in earlier works [21-23] the sensor was permanently placed in the gas stream, the developed handheld sensor system offers the advantage of portability.

It was shown, that reproducible measurement values were obtained. Malfunctions in the sterilisation process at the manufacturer's sterilisation machine have been detected. Based on the information about the measured hydrogen peroxide concentration and gas temperature obtained by the handheld sensor system, machine parameters can be set to optimise the sterilisation efficiency.

In further field experiments at the manufacturer's sterilisation machine, it is envisaged to make more detailed investigations on the sensor properties, especially the sensitivity, accuracy and long-term stability.

### 2.6 Investigation of different polymers as passivation material

In a further study with the participation of the author of this work, three polymers have been investigated as possible passivation materials of the calorimetric sensor, namely the photoresist SU-8 (Nano$^{TM}$ SU-8 from MicroChem) and the fluoropolymers PFA (DuPont$^{TM}$ PFA 857-110) and FEP (Dyneon$^{TM}$ FEP 6300G Z) [24]. The fluoropolymer (DuPont$^{TM}$ PFA 857-110) corresponds to the PFA that has been used for the fabrication of the sensor presented in this chapter. In order to study the chemical inertness against $H_2O_2$ (exposure to $H_2O_2$), the hygroscopic properties (contact angle measurement) as well as the morphology (SEM), the polymers have been spin-coated on a silicon substrate with an additional insulation layer of silicon oxide (500 nm). A summary of the physical and chemical properties of the materials used is given in Table 2.3.

**Table 2.3:** Chemical and physical properties of SU-8 photoresist, PFA and FEP (adapted from [24]).

| Polymer | Density ($g/cm^3$) | Max. service temp. (°C) | Melting/ degradation temp. (°C) | Thermal conductivity ($W \cdot °C^{-1} \cdot m^{-1}$) | Water absorption (%) |
|---|---|---|---|---|---|
| SU-8 photo resist | 1.075-1.238 | 300-315 | ~380 | 0.2-0.3 | 0.55-0.65 |
| Perfluor-alkoxy (PFA) | 2.150 | 260 | 300-310 | 0.195 | <0.03 |
| Fluorinated ethylene propylene (FEP) | 2.150 | 205 | 250-280 | 0.24 | <0.01 |

All polymers provided good adhesion on the substrate. The SU-8 resist showed an enclosed surface, whereas the surfaces of the fluoropolymers (FEP and PFA) showed slight agglomerates in the range of 120 nm (see Fig. 2.9).

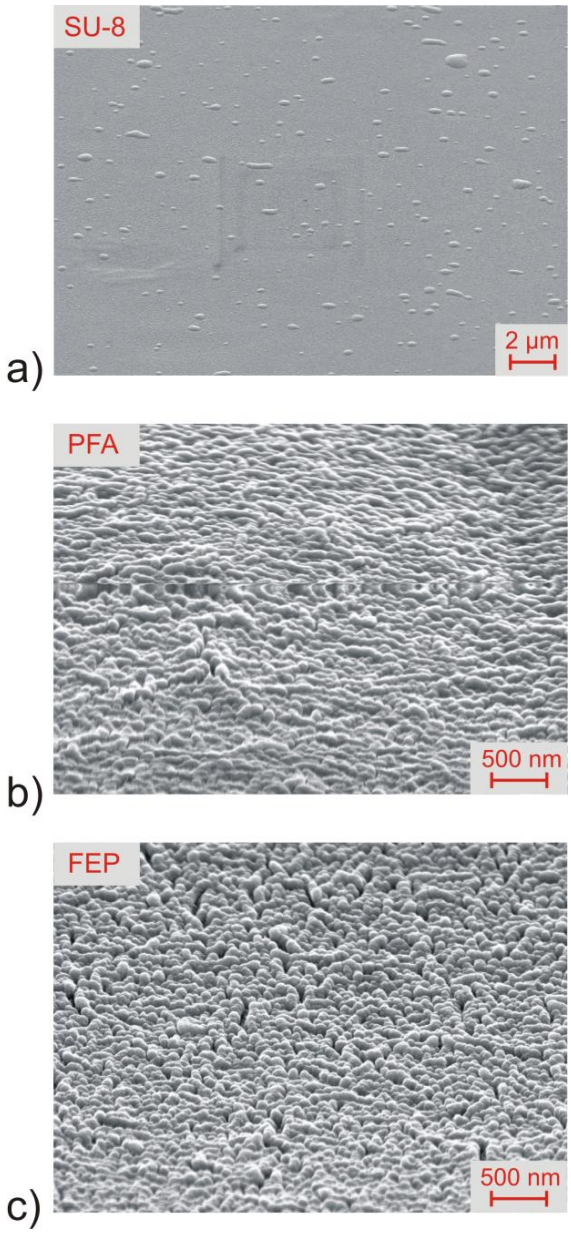


**Figure 2.9:** SEM images of (a) spin-coated SU-8 photo resist, (b) perfluoroalkoxy (PFA) and (c) fluorinated ethylene propylene (FEP) (adapted from Kirchner *et al.* [24]).

The contact angle measurements revealed hydrophilic properties in case of the SU-8 layer and hydrophobic properties in case of the fluoropolymers (see Fig. 2.10 and Tab. 2.4).

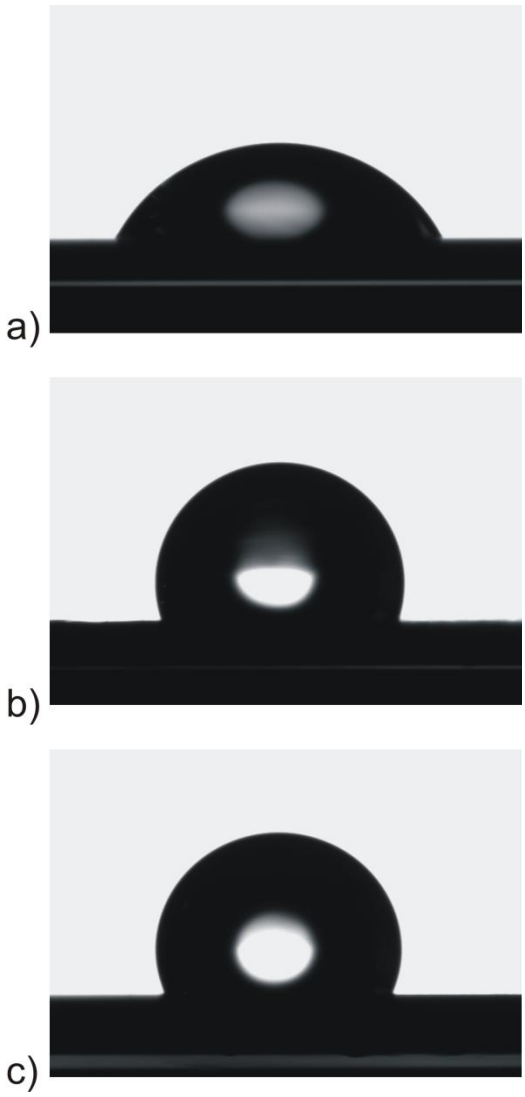


**Figure 2.10:** Contact angle measurements of a 4 µl water droplet on the polymer coatings; water droplet on (a) SU-8 photoresist, (b) FEP and (c) PFA layer (adapted from Kirchner *et al.* [24]).

**Table 2.4:** Contact angle and average film thickness of the spin-coated polymeric layers (adapted from Kirchner *et al.* [24]).

| Polymer | Average contact angle | Average film thickness (µm) |
|---|---|---|
| SU-8 photo resist | 61.6° | 1.7 |
| Perfluoralkoxy (PFA) | 106.3° | 20.4 |
| Fluorinated ethylene propylene (FEP) | 113.5° | 4.1 |

All materials in test showed good passivation characteristics and chemical inertness in presence of $H_2O_2$ and $H_2O$. Evidences could be found that the absorption or micro condensation of water on the hydrophilic surface of the photo resist SU-8 may influence the heat transfer on the sensor. The highest thermal insulation was achieved by PFA.

**2.7 References**

[1] S.D. Holdsworth, Aseptic processing and packaging of food products, Elsevier Applied Science; Elsevier Science Pub. Co., London, New York, 1992.

[2] G. McDonnel, A.D. Russell, Antiseptics and disinfectants: Activity, action, and resistance, Clinical Microbiology Reviews 12 (1999) 147–179.

[3] R. Toniolo, P. Geatti, G. Bontempelli, G. Schiavon, Amperometric monitoring of hydrogen peroxide in workplace atmospheres by electrodes supported on ion-exchange membranes, Journal of Electroanalytical Chemistry 514 (2001) 123–128.

[4] R.A. Heckert, M. Best, L.T. Jordan, G.C. Dulac, D.L. Eddington, W.G. Sterritt, Efficacy of vaporized hydrogen peroxide against exotic animal viruses, Applied Environmental Microbiology 63 (1997) 3916–3918.

[5] M. Kokubo, T. Inoue, J. Akers, Resistance of common environmental spores of the genus *Bacillus* to vapour hydrogen peroxide, PDA Journal of Pharmaceutical Science and Technology 5 (1998) 228–231.

[6] N.A. Klapes, D. Vesley, Vapor-phase hydrogen peroxide as a surface decontaminant and sterilant, Applied Environmental Microbiology 56 (1990) 503–506.

[7] G. Graham, J. Rickloff, J. Dalmasso, Sterilization of isolators and lyophilyzers with hydrogen peroxide in the vapor phase, VHP™ Technology: A collection of scientific papers, AMSCO Scientific, Apex, 1992.

[8] V. Sigwarth, A. Stärk, Effect of carrier materials on the resistance of spores of *Bacillus stearothermophilus* to gaseous hydrogen peroxide, PDA Journal of Pharmaceutical Science and Technology 57 (2003) 3–11.

[9] C. Hultman, A. Hill, G. McDonnell, The physical chemistry of decontamination with gaseous hydrogen peroxide, Pharmaceutical Engineering 27 (2006) 22–26.

[10] K. Imai, S. Watanabe, Y. Oshima, M. Kokubo, J. Akers, A new approach to vapor hydrogen peroxide decontamination of isolators and cleanrooms, Pharmaceutical Engineering 26 (2006) 96–104.

[11] B. Unger-Bimczok, V. Kottke, C. Hertel, J. Rauschnabel, The influence of humidity, hydrogen peroxide concentration, and condensation on the inactivation of *Geobacillus stearothermophilus* spores with hydrogen peroxide vapor, Journal of Pharmaceutical Innovation 3 (2008) 123–133.

[12] M. Aizawa, I. Karube, S. Suzuki, A specific bio-electrochemical sensor for hydrogen peroxide, Analytica Chimica Acta 69 (1974) 431–437.

[13] S. Akgöl, A novel biosensor for specific determination of hydrogen peroxide: Catalase enzyme electrode based on dissolved oxygen probe, Talanta 48 (1999) 363–367.

[14] L. Campanella, R. Roversi, M. Sammartino, M. Tomassetti, Hydrogen peroxide determination in pharmaceutical formulations and cosmetics using a new catalase biosensor, Journal of Pharmaceutical and Biomedical Analysis 18 (1998) 105–116.

[15] I. Taizo, A. Sinichi, K. Kawamura, Application of a newly developed hydrogen peroxide vapor phase sensor to HPV sterilizer, PDA Journal of Pharmaceutical Science and Technology 52 (1998) 13–18.

[16] J. Watson, K. Ihokura, G.S.V. Coles, The tin dioxide gas sensor, Measurement Science Technology 4 (1993) 711–719.

[17] P. Clifford, D. Tuma, Characteristics of semiconductor gas sensors I. Steady state gas response, Sensors and Actuators 3 (1982) 233–254.

[18] J. Gutierrez, F. Cebollada, C. Elvira, E. Millan, J. Agapito, Mechanisms of detection on tin oxide gas sensors, Materials Chemistry and Physics 18 (1987) 265–276.

[19] D. Vlachos, P. Skafidas, J. Avaritsiotis, The effect of humidity on tin-oxide thick-film gas sensors in the presence of reducing and combustible gases, Sensors and Actuators B: Chemical 1995 (25) 491–494.

[20] J. Watson, The tin oxide gas sensor and its applications, Sensors and Actuators 5 (1984) 29–42.

[21] N. Näther, H. Henkel, A. Schneider, M.J. Schöning, Investigation of different catalytically active and passive materials for realising a hydrogen peroxide gas sensor, Physica Status Solidi (a) 206 (2009) 449–454.

[22] N. Näther, L.M. Juárez, R. Emmerich, J. Berger, P. Friedrich, M.J. Schöning, Detection of hydrogen peroxide ($H_2O_2$) at exposed temperatures for industrial processes, Sensors 6 (2006) 308–317.

[23] N. Näther, R. Emmerich, P. Friedrich, H. Henkel, A. Schneider, M. Schöning, A novel gas-phase hydrogen peroxide sensor basing on a combined physical/chemical transduction mechanism, Materials Research Society Symposium Proceedings 951 (2007) 63–68.

[24] P. Kirchner, S. Reisert, P. Pütz, M. Keusgen, M.J. Schöning, Characterisation of polymeric materials as passivation layer for calorimetric $H_2O_2$ gas sensors, Physica Status Solidi A 209 (2012) 859–863.

# Chapter 3

## Towards a multi-sensor system for the evaluation of aseptic processes employing hydrogen peroxide vapour ($H_2O_2$)

Physica Status Solidi (a), 2011, Vol. 208, pp. 1351-1356

Steffen Reisert[1], Hanno Geissler[2], Rudolf Flörke[2], Niko Näther[1], Patrick Wagner[3] and Michael J. Schöning[1]

1) Institute of Nano- and Biotechnologies, FH Aachen, 52428 Jülich, Germany

2) SIG Combibloc Systems GmbH, 52441 Linnich, Germany

3) Institute for Materials Research, Hasselt University, 3590 Diepenbeek, Belgium

### 3.1 Abstract

The presented work focuses on the development of a multi-sensor system for the evaluation of aseptic processes employing hydrogen peroxide vapour. In a first step, selected commercially available gas sensors have been investigated on cross-sensitivity towards hydrogen peroxide vapour and humidity. An MOX (TGS 816, *Figaro*) and a solid-electrolyte gas sensor (SO-A0-250, *Electrovac*) (λ-probe) have shown good characteristics in terms of sensitivity towards HPV, considering also reproducibility, long-term drift and stability. Further, the sterilisation effect of HPV has been investigated by means of the microbial reduction test. A correlation between the microbial reduction of *Bacillus subtilis* spores and the sensor response in hydrogen peroxide atmosphere has been established. Based on this correlation the microbial reduction may be estimated by means of the sensor output over a wide range of parameters.

## 3.2 Introduction

The sterilisation of packaging is an important factor in the aseptic processing of foodstuff [1]. Due to its strong antimicrobial properties and environmental compatibility, hydrogen peroxide vapour is the method of choice for the inactivation of microorganisms such as bacteria, fungi, viruses and highly resistant spores [2-7]. The microbial inactivation process by hydrogen peroxide vapour is carried out at temperatures above 200 °C and concentrations of $H_2O_2$ up to 10% v/v. The inactivation of microorganisms by hydrogen peroxide has been the subject of various studies. It was shown that the microbial inactivation favourably occurs at high concentrations of hydrogen peroxide and elevated gas temperatures [7-12].

The effectiveness of aseptic sterilisation processes by hydrogen peroxide vapour may be determined by the so-called challenge test that requires artificial inoculation of packaging materials with microorganisms under controlled conditions in order to obtain statistically significant test results allowing objective comparison [13-14]. Even though this represents a well established and reliable method, it is to some degree unfavourable as probes require a lot of preparation and an inoculation time between 24 hours and a few days.

Several attempts have been made to characterise sterilisation processes by monitoring the influence parameters, such as the hydrogen peroxide concentration or temperature [15-21]. However, monitoring of one single parameter is often not sufficient for an accurate evaluation of a sterilisation process, since there is an interaction between the various influential parameters, such as temperature, pressure, gas flow and humidity, which can have a decisive effect on the inactivation of microorganisms. One promising approach for the evaluation of multi-component chemical media and dynamic processes relies on the use of multi-sensor systems [22]. Concerning such multi-sensor systems, multi-component chemical media could be described not by a sum of the individual components (or corresponding response from the specific sensors) but by some abstract representation – a chemical image – a virtual fingerprint with a set of parameters intrinsical for a given multi-component medium [23]. In this work, an approach for the development of a multi-sensor system for the

evaluation of aseptic processes employing hydrogen peroxide vapour is presented. Chemical images of selected gas sensors in hydrogen peroxide atmosphere are compared with the results of microbiological count-reduction tests of *Bacillus subtilis*. A correlation between the effectiveness of aseptic sterilisation processes and the response of the selected gas sensors could be established via the hydrogen peroxide concentration.

## 3.3 Experimental

### 3.3.1 Test equipment and measuring parameters

To perform the microbiological tests and investigate the sensor properties, an experimental set-up in laboratory scale, similar to industrial apparatuses, has been used for the generation of hydrogen peroxide vapour. A detailed description of the experimental set-up is given in **Section 1.6.2**.

For the sensor characterisation and microbiological testing a set of parameters, which represents common settings for industrial sterilisation processes, has been chosen. All measurements have been carried out at a gas flow rate of 10 m³/h and a gas temperature of 270 °C, but different levels of hydrogen peroxide concentration in gaseous phase. Therefore, on one hand, different amounts of a technical grade aqueous hydrogen peroxide solution of 35% w/w have been fed to the carrier gas stream. On the other hand, measurements have been performed at a constant dosage but different dilutions of the hydrogen peroxide solution. While at the first experiment the ratio between hydrogen peroxide and water in gaseous phase was kept constant, it is different for the latter experiment. In this way, the influence of humidity on the sensor signal and microbial reduction shall be investigated. The highest concentration of hydrogen peroxide in gaseous phase was achieved at a gas flow of 10 m³/h and the maximum possible dosage of 1100 µl/s of a 35% w/w technical grade hydrogen peroxide solution. Four series of measurement have been carried out, each time two measurements for the sensor calibration and the microbiological tests, respectively. The parameters of the four series of measurement are listed in Tables 3.1-3.4. (Constant hydrogen peroxide – water ratio, varying hydrogen peroxide – water ratio).

**Table 3.1:** Parameter for the sensor calibration of measurement 1. Here, the hydrogen peroxide – water ratio is constant.

| Dosage (µl/s) * | 250 | 500 | 750 | 1000 | 1100 |
|---|---|---|---|---|---|
| $C[H_2O_2]$ (% v/v) | 2.3 | 4.1 | 5.7 | 6.9 | 7.4 |
| $C[H_2O]$ (% v/v) | 7.9 | 14.3 | 19.7 | 24.2 | 25.8 |
| $C[H_2O_2]/ C[H_2O]$ | 0.285 | 0.285 | 0.285 | 0.285 | 0.285 |

* Measurements have been carried out at a constant volume flow of 10 m³/h, a constant gas temperature of 270 °C and varying dosage of a 35% w/w technical grade aqueous hydrogen peroxide solution.

**Table 3.2:** Parameter for the sensor calibration of measurement 2. The hydrogen peroxide – water ratio is variable.

| $C_{sol}[H_2O_2]$ (% w/w) * | 15 | 25 | 35 |
|---|---|---|---|
| $C[H_2O_2]$ (% v/v) | 2.2 | 3.9 | 5.6 |
| $C[H_2O]$ (% v/v) | 23.8 | 21.8 | 19.7 |
| $C[H_2O_2]/ C[H_2O]$ | 0.092 | 0.176 | 0.285 |

* Measurements have been carried out at a constant volume flow of 10 m³/h, a constant gas temperature of 270 °C and varying dilutions of a technical grade aqueous hydrogen peroxide solution ($C_{sol}[H_2O_2]$) at a constant dosage of 750 µl/s.

**Table 3.3:** Parameter of the microbiological measurement 1 with a constant hydrogen peroxide – water ratio.

| Dosage (µl/s) * | 300 | 500 | 600 | 900 |
|---|---|---|---|---|
| $C[H_2O_2]$ (% v/v) | 2.6 | 4.1 | 4.7 | 6.4 |
| $C[H_2O]$ (% v/v) | 9.3 | 14.3 | 16.6 | 22.5 |
| $C[H_2O_2]/ C[H_2O]$ | 0.285 | 0.285 | 0.285 | 0.285 |

* Measurements have been carried out at a constant volume flow of 10 m³/h, a constant gas temperature of 270 °C and varying dosage of a 35% w/w technical grade aqueous hydrogen peroxide solution.

**Table 3.4:** Parameter of the microbiological measurement 2 with varying hydrogen peroxide – water ratio.

| $C_{sol}[H_2O_2]$ (% w/w) * | 15 | 25 | 35 | 50 |
|---|---|---|---|---|
| $C[H_2O_2]$ (% v/v) | 1.6 | 2.8 | 4.1 | 6.2 |
| $C[H_2O]$ (% v/v) | 17.4 | 15.9 | 14.3 | 11.7 |
| $C[H_2O_2]/ C[H_2O]$ | 0.092 | 0.176 | 0.285 | 0.530 |

* Measurements have been carried out at a constant volume flow of 10 m³/h, a constant gas temperature of 270 °C and varying dilutions of a technical grade aqueous hydrogen peroxide solution ($C_{sol}[H_2O_2]$) at a constant dosage of 500 µl/s.

3.3.2 Gas sensors

Two types of commercially available gas sensors have been investigated on cross-sensitivity towards hydrogen peroxide vapour: The metal-oxide

semiconductor gas sensor (MOX) TGS 816 from Figaro Engineering (Japan) and the amperometric solid-electrolyte sensor SO-A0-250 from Electrovac AG (Austria). Hydrogen peroxide has strong oxidising properties. Semiconductor gas sensors are known for high sensitivity to reducing and oxidising gases, while in case of the solid-electrolyte sensor a reaction to oxygen, originated from the decomposition of hydrogen peroxide on either the heater surface or even the sensor surface itself, is expected. The TGS 816 was heated with a constant voltage of 5 V, while the SO-A0-250 was operated in a temperature controlled mode at 533 °C according to the manufacturer's data sheet. Both sensors were placed directly in the gas stream, 5.2 cm below the outlet of the gas nozzle (see sensor mounting in **Section 1.6.2.2**).

3.3.3 Microbiological tests

The preparation and handling of the microbiological test samples used for this study is explained in **Section 1.6.3**. The average initial count of spores on the test strips was ≈ $8*10^6$. The test strips were exposed to the sterilisation medium for an effective time of 500 ms (a technically common rate of a sterilisation/filling cycle of aseptic carton packages in a filling line). For each setting, a number of five samples has been taken and the logarithmic reduction (log-rate) of viable spores has been determined according to the count-reduction test (CRT) as described in **Section 1.3.3**.

## 3.4 Results and discussion

3.4.1 Calibration of the gas sensor

To investigate the cross-sensitivity of the gas sensors towards hydrogen peroxide vapour, two series of measurement have been carried out as described in **Section 3.3.1**.

3.4.2 TGS 816

Figure 3.1 shows the results of the TGS 816 obtained from measurements 1 and 2, plotted against the assumed hydrogen peroxide concentration calculated from the mixer flow ratios. The measured data is depicted as relative resistance values $R_S/R_0$. $R_0$ was determined in the hot gas stream at a constant gas flow of 10 m³/h and a gas temperature of 270 °C, without the presence of hydrogen peroxide.

From the measurement values diagrammed in Figure 3.1 it can be seen, that there is a non-linear relationship between the sensor signal and the hydrogen peroxide concentration in case of the measurement 1. On the other hand, a linear relationship can be observed in case of measurement 2, while during both measurements the sensor signal is decreasing with increasing hydrogen peroxide concentration. This seems to be apparently in contradiction to the expectation that n-type metal-oxide semiconductor gas sensors, like the $SnO_2$ sensor used in this work, respond with an increase of the sensor resistance in presence of oxidising gases, like hydrogen peroxide. However, to explain the effect of hydrogen peroxide on the metal oxide surface, several mechanisms have to be considered. Thereby, it is assumed that the change in sensor signal relies not merely on a direct influence of the hydrogen peroxide on the metal oxide surface, but is predominantly attributed to the effect of decomposition products of hydrogen peroxide at the sensor surface.

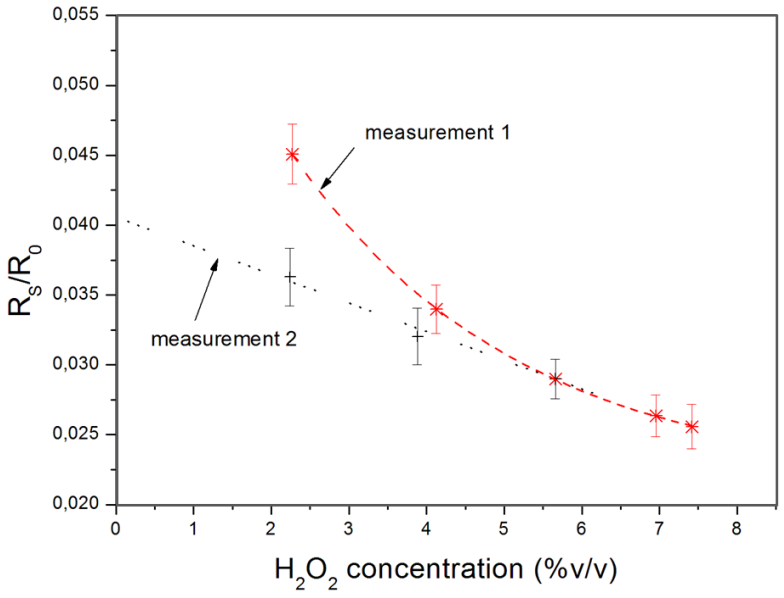


**Figure 3.1:** Sensor signals of the $SnO_2$ semiconductor gas sensor TGS 816 at different concentrations of hydrogen peroxide operated with a constant heating voltage of 5 V, normalised to the resistance value in the hot gas stream (@ 10 m³/h, 270 °C). The measurement 1 refers to Tab. 3.1 and measurement 2 refers to the data of Tab. 3.2.

The decomposition of hydrogen peroxide vapour at ceramic oxide surfaces has been the subject of few earlier investigations [24]. At high temperatures (>400 °C), which is the case at the hot sensor surface, the decomposition of hydrogen peroxide is thought to be initiated by O-O cleavage to give two $OH^{\bullet}$ radicals followed by two reactions.

$$H_2O_2 \rightarrow 2\ OH^{\bullet} \tag{3.1}$$

$$OH^{\bullet} + H_2O_2 \rightarrow HO_2 + H_2O \tag{3.2}$$

$$2HO_2 \rightarrow H_2O_2 + O_2 \tag{3.3}$$

The stoichiometric relationship gives half an oxygen molecule for each decomposed hydrogen peroxide molecule.

$$H_2O_2 \rightarrow H_2O + ½\ O_2 \tag{3.4}$$

The so formed $OH^{\bullet}$ radicals on the oxide surface are of transitory nature, but may act as electron donors and directly increase the conductivity of the metal oxide, in this case tin oxide. This model explains the strikingly decrease of the sensor signal in presence of hydrogen peroxide as shown in Figure 3.1. A similar effect can be observed in the presence of water. When chemisorbed on the tin-oxide surface, water molecules dissociate into hydroxyl species, which again act as electron donors [25-26]. That means hydrogen peroxide and water will contribute to the change in conductivity of the tin oxide in the same way. From the values obtained during measurement 2 it can be seen, that the formation of free hydroxyl radicals being descended from the hydrogen peroxide is predominant for the change in the sensor's conductivity, as the sensor signal is lower for higher hydrogen peroxide concentrations (compare also Table 3.2). The effect of humidity may be observed comparing the obtained values of measurement 1 and 2. The sensor signal at 2.2% v/v $H_2O_2$ derived from measurement 2 is lower compared to that of measurement 1, which comes as a result of the higher level of humidity during measurement 2 but similar concentrations of hydrogen peroxide (compare also Table 3.2).

3.4.3 Solid-electrolyte gas sensor SO-A0-250

The resulting sensor response of the solid-electrolyte gas sensor SO-A0-250 during measurements 1 and 2 in hydrogen peroxide atmosphere is shown in Figure 3.2. The measured oxygen concentration is plotted against the assumed hydrogen peroxide concentration calculated from the mixer flow ratios.

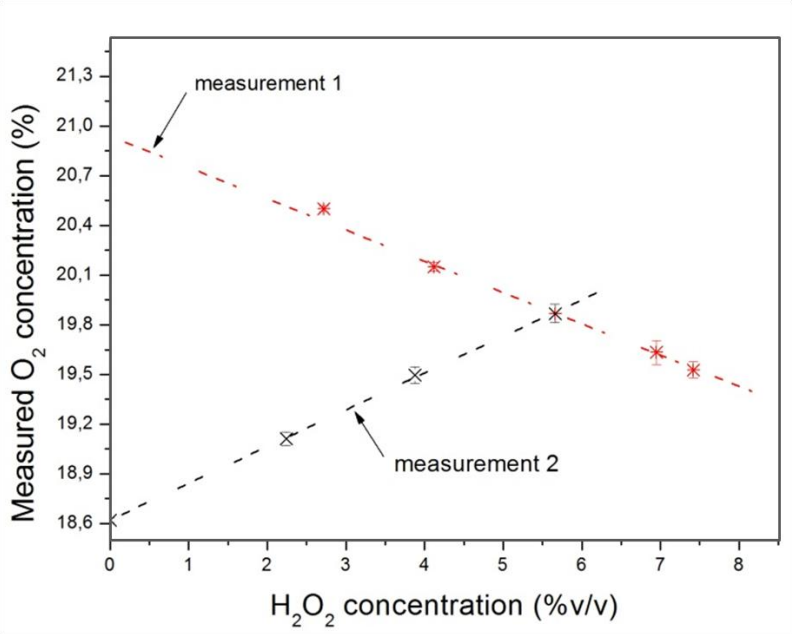


**Figure 3.2:** Measured oxygen concentration of the amperometric solid-electrolyte sensor SO-A0-250 at different concentrations of hydrogen peroxide operated in temperature controlled mode at 533 °C.

The sensor shows a linear behaviour as a function of the hydrogen peroxide concentration. The sensor signal is decreasing towards higher concentrations of $H_2O_2$ during measurement 1, while it is increasing towards higher concentrations during measurement 2. To explain this behaviour, one must consider that the solid-electrolyte gas sensor is sensitive in particular to oxygen and therefore, the sensor signal depends on the oxygen concentration in the medium. The progressively increase of the amount of hydrogen peroxide solution fed to the carrier gas stream leads to a decrease in the relative oxygen content of the gas stream, which explains the declining sensor response in case of measurement 1. On the other hand, the amount of dosed hydrogen peroxide solution was kept

constant during measurement 2, while the dilution was varied from lower to higher concentrations in order to obtain rising hydrogen peroxide concentrations in gaseous phase. In this case, the relative oxygen content of the gas stream is considered to be constant, while the sensor signal is increasing with increasing hydrogen peroxide concentrations. The increase in sensor response observed during measurement 2 may be explained due to a supplementary source of oxygen, which is related to the heterogeneous decomposition of hydrogen peroxide into water and oxygen according to Equation (3.4) at either the heater surface or even at the surface of the sensor itself, which is operated at a temperature of approximately 500 °C. It can be considered that the solid-electrolyte sensor exhibits partial sensitivity towards hydrogen peroxide.

3.4.4 Microbiological tests

The microbiological tests have been carried out as described in **Section 3.3.3**, each parameter with a repetition of five samples. The resulting average log-rates of the microbiological measurements 1 and 2 are shown in Figure 3.3, plotted against the particular hydrogen peroxide concentration.

The results obtained at 0% v/v $H_2O_2$ were taken in the hot gas stream at 270 °C, in absence of hydrogen peroxide. The exposure time to hot air for 500 ms causes only a minimal microbiological reduction of viable spores. The achieved log-rate was in both cases below 0.5. In presence of hydrogen peroxide, the logarithmic reduction rate is significantly increased. For instance, at a concentration of 1.6% v/v $H_2O_2$ during the microbiological measurement 2 the number of viable spores was reduced by two decades during an exposure time of 500 ms. For all further samples from the microbiological measurements 1 and 2, the log-rate is increasing with increasing hydrogen peroxide concentration, except for the sample at 2.6% v/v $H_2O_2$ from the microbiological measurement 1. At the highest $H_2O_2$ concentration of 6.4% v/v the maximum log-rate of 6.9, which means that no viable spores remained, was obtained. Therefore, it was not considered necessary to further increase the hydrogen peroxide concentration.

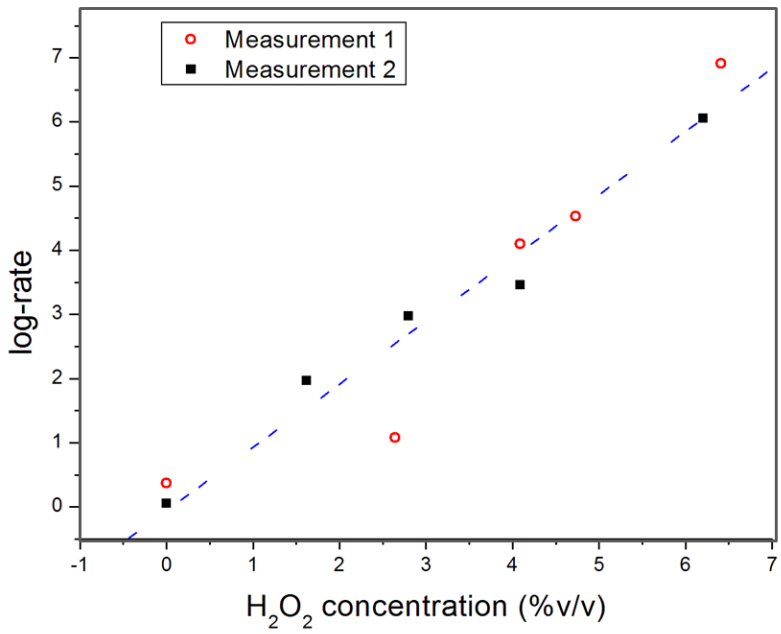


**Figure 3.3:** Logarithmic reduction rates of *Bacillus subtilis* achieved for an exposure time of 500 ms at 270 °C as a function of the hydrogen peroxide concentration. The measurement 1 refers to Tab. 3.3 and measurement 2 refers to the data of Tab. 3.4.

It seems that the inactivation of *Bacillus subtilis* spores is independent from the level of humidity in the sterilisation medium. The logarithmic reduction rate of *Bacillus subtilis* by hydrogen peroxide vapour at a gas temperature of 270 °C can be described as a linear function of the hydrogen peroxide concentration according to the following formula:

$$log\text{-}rate = -0.06 + 0.97\ (\%\ v/v)^{-1} \cdot C[H_2O_2] \qquad (3.5)$$

Here, $C[H_2O_2]$ is the hydrogen peroxide concentration in percent of volume (% v/v).

### 3.4.5 Correlation of log-rate with sensor output

In order to realise a sensor system for the evaluation of aseptic processes employing hydrogen peroxide vapour, a correlation between sensor data and the results of the microbiological tests has to be established.

Based on the known sensor behaviour from the calibration measurements and the relationship found between the hydrogen peroxide concentration and the logarithmic reduction rate, which is described in Equation (3.5), the log-rate may be described as a function of the sensor output of the two sensors in test. Furthermore, additional sensor data and log-rates for all possible combinations of dosed amount of hydrogen peroxide solution between 250 and 1100 µl/s as described in Table 3.1 and respective values of hydrogen peroxide dilutions between 15 and 50% w/w, listed in Table 3.4, have been approximated via the characteristics found during sensor calibration and microbiological test, respectively. From the obtained data an extrapolation was drawn for other possible variations of the gas composition, regarding the hydrogen peroxide concentration and level of humidity. The obtained data are representative for a gas flow of 10 $m^3/h$ and a gas temperature of 270 °C. The resulting graph is shown in Figure 3.4. Thereby, the resulting microbiological log-rate is represented as a coloured scale as a function of the sensor signals of the TGS 816 and SO-A0-250, respectively.

The logarithmic reduction rate of *Bacillus subtilis* spores is represented as a function of the sensor output and diagrammed as coloured scale. From the graph shown in Figure 3.4, the microbial reduction can be determined by means of a given combination of sensor signals. The level of reliability of the approximation derives from the standard deviation of the sensor calibration and the averaging of the log-rate. Based on the established correlation, the resulting log-rate of an unknown gas composition can be determined by reference to the sensor signals with an accuracy of ±0.85 log-rates.

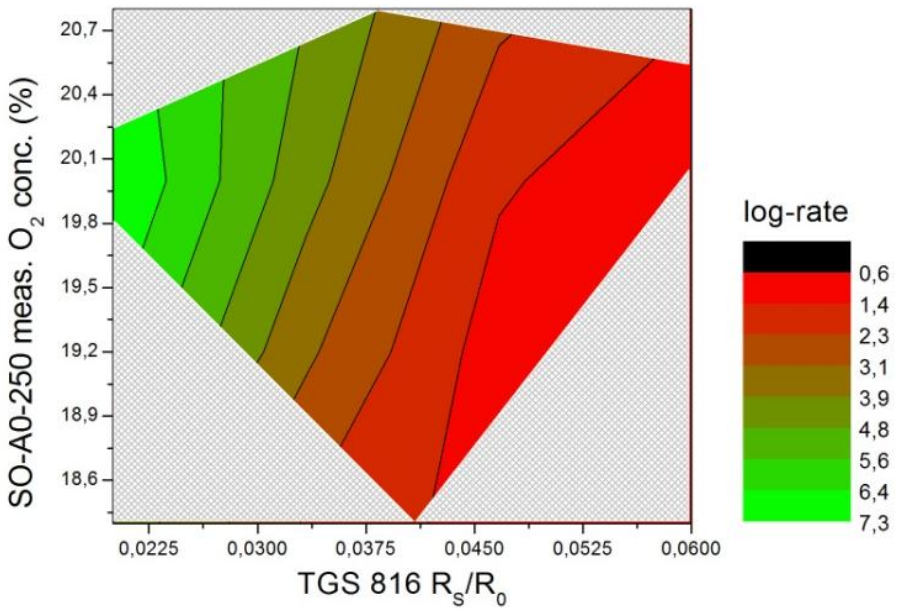


**Figure 3.4:** Extrapolated data set of the logarithmic reduction rate (log-rate) of *Bacillus subtilis* spores as a function of the output values of two commercially available gas sensors (TGS 816 and SO-A0-250).

### 3.5 Conclusion

Two types of commercially available gas sensors have been investigated on cross-sensitivity towards hydrogen peroxide vapour. Additionaly, microbiological count-reduction tests of *Bacillus subtilis* spores have been performed, in order to determine the sterilisation effect of hydrogen peroxide vapour. The calibration of the sensor system and the microbiological tests have been carried at a gas flow of 10 m³/h and a gas temperature of 270 °C. A correlation between the sensor output and the results of the microbiological tests has been established. Based on this correlation, the microbiological reduction rate of an unknown gas composition can be determined by means of the sensor output with an accuracy of ±0.85 log-rates. The developed multi-sensor system is suitable for in-line and real-time analysis of the sterilisation process.

In further studies, the field of parameters shall be extended by other influencing factors of the sterilisation process, namely the temperature and gas flow. Also, the number and type of gas sensors shall be increased in order to obtain more detailed chemical images of the medium to be analysed. The increase in number of sensors and variables requires the introduction of a multivariate analysis, like Fuzzy Logic, Artificial Neural Networks (ANN), or Principal Component Analysis (PCA) in order to handle the captured information. The instrumental systems based on arrays of low-selective/cross-reactive sensors that are used to form chemical images of gaseous multi-component media with further classification and identification using the image recognition techniques has been named 'the Electronic Nose' [27].

### 3.6 Temperature response of the TGS 816

In addition to the measurements discussed in this chapter, the influence of the gas temperature on the response of the metal-oxide semiconductor sensor TGS 816, when exposed to $H_2O_2$, has been analysed. This study was part of an additional article published by the author of this thesis (see ref. [28]). The temperature behaviour of the TGS 816 in presence of 4.1% v/v $H_2O_2$ was investigated in a gas temperature range between 180 and 330 °C. The resulting sensor signals, represented as normalised resistance values, are depicted in Fig. 3.5.

It was found that the sensor resistance was decreasing with increasing gas temperature. The reason for this behaviour may be explained by the heating mode of the sensor. The sensor was heated in a static mode with a constant voltage of 5 V. As a consequence, the temperature of the oxide is subject to temperature changes of the environment, while the temperature of the oxide is increasing progressively with the gas temperature. This is, in fact, in accordance with the general accepted theory, that the resistivity of n-type semiconductors, like the TGS 816, decreases with increasing temperature. Comparative measurements with temperature-controlled semiconductor gas sensors, however, showed no dependence on the sensor signal from the ambient temperature, as long as it is lower than the operating temperature of the sensor. This fact could be used to specifically increase the sensors' temperature

sensitivity in situations where it is desirable, for instance, the characterisation of sterilisation processes which are strongly depending on the temperature

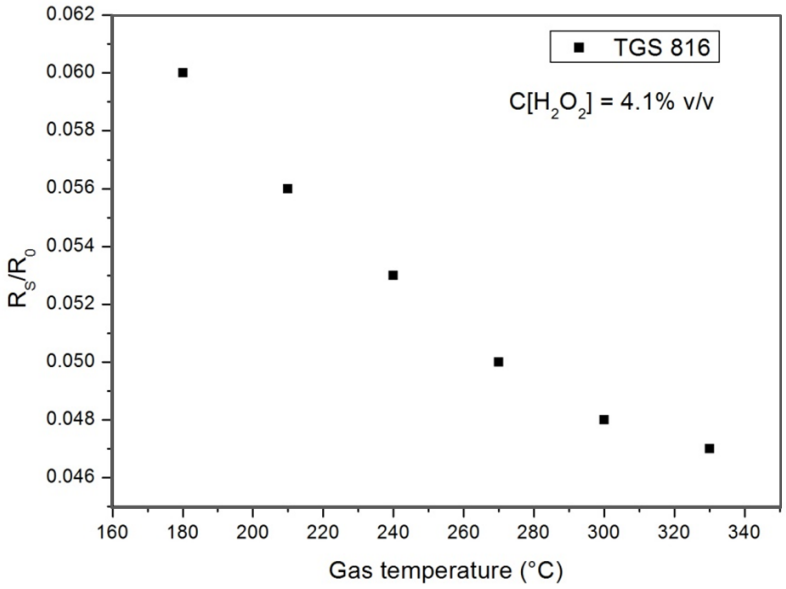


**Figure 3.5:** Normalised sensor signals of the $SnO_2$ semiconductor gas sensor TGS 816 at a constant $H_2O_2$ concentration of 4.1% v/v, but different gas temperatures between 180 and 330 °C, operated with a constant heating voltage of 5 V (adapted from [28]).

**3.7 References**

[1] S.D. Holdsworth, Aseptic processing and packaging of food products, Elsevier Applied Science; Elsevier Science Pub. Co., London, New York, 1992.

[2] G. McDonnel, A.D. Russell, Antiseptics and disinfectants: Activity, action, and resistance, Clinical Microbiology Reviews 12 (1999) 147–179.

[3] R.A. Heckert, M. Best, L.T. Jordan, G.C. Dulac, D.L. Eddington, W.G. Sterritt, Efficacy of vaporized hydrogen peroxide against exotic animal viruses, Applied Environmental Microbiology 63 (1997) 3916–3918.

[4] M. Kokubo, T. Inoue, J. Akers, Resistance of common environmental spores of the genus *Bacillus* to vapour hydrogen peroxide, PDA Journal of Pharmaceutical Science and Technology 5 (1998) 228–231.

[5] R. Toniolo, P. Geatti, G. Bontempelli, G. Schiavon, Amperometric monitoring of hydrogen peroxide in workplace atmospheres by electrodes supported on ion-exchange membranes, Journal of Electroanalytical Chemistry 514 (2001) 123–128.

[6] N.A. Klapes, D. Vesley, Vapor-phase hydrogen peroxide as a surface decontaminant and sterilant, Applied Environmental Microbiology 56 (1990) 503–506.

[7] G. Graham, J. Rickloff, J. Dalmasso, Sterilization of isolators and lyophilyzers with hydrogen peroxide in the vapor phase, VHP™ Technology: A collection of scientific papers, AMSCO Scientific, Apex, 1992.

[8] C. Hultman, A. Hill, G. McDonnell, The physical chemistry of decontamination with gaseous hydrogen peroxide, Pharmaceutical Engineering 27 (2006) 22–26.

[9] V. Sigwarth, A. Stärk, Effect of carrier materials on the resistance of spores of *Bacillus stearothermophilus* to gaseous hydrogen peroxide, PDA Journal of Pharmaceutical Science and Technology 57 (2003) 3–11.

[10] K. Imai, S. Watanabe, Y. Oshima, M. Kokubo, J. Akers, A new approach to vapor hydrogen peroxide decontamination of isolators and cleanrooms, Pharmaceutical Engineering 26 (2006) 96–104.

[11] B. Unger-Bimczok, V. Kottke, C. Hertel, J. Rauschnabel, The influence of humidity, hydrogen peroxide concentration, and condensation on the inactivation of *Geobacillus stearothermophilus* spores with hydrogen peroxide vapor, Journal of Pharmaceutical Innovation 3 (2008) 123–133.

[12] M.D. Labas, C.S. Zalazar, R.J. Brandi, A.E. Cassano, Reaction kinetics of bacteria disinfection employing hydrogen peroxide, Biochemical Engineering Journal 38 (2008) 78–87.

[13] Verband Deutscher Maschinen- und Anlagenbau e.V., Code of practice: Filling machines of VDMA hygiene class V: Testing the effectiveness of packaging sterilization devices, Frankfurt, 2008.

[14] G. Moruzzi, W.E. Garthright, J.D. Floros, Aseptic packaging machine pre-sterilisation and package sterilisation: Statistical aspects of microbiological validation, Food Control 11 (2000) 57–66.

[15] I. Taizo, A. Sinichi, K. Kawamura, Application of a newly developed hydrogen peroxide vapor phase sensor to HPV sterilizer, PDA Journal of Pharmaceutical Science and Technology 52 (1998) 13–18.

[16] N. Näther, H. Henkel, A. Schneider, M.J. Schöning, Investigation of different catalytically active and passive materials for realising a hydrogen peroxide gas sensor, Physica Status Solidi (a) 206 (2009) 449–454.

[17] N. Näther, L.M. Juárez, R. Emmerich, J. Berger, P. Friedrich, M.J. Schöning, Detection of hydrogen peroxide ($H_2O_2$) at exposed temperatures for industrial processes, Sensors 6 (2006) 308–317.

[18] N. Näther, R. Emmerich, P. Friedrich, H. Henkel, A. Schneider, M. Schöning, A novel gas-phase hydrogen peroxide sensor basing on a combined physical/chemical transduction mechanism, Materials Research Society Symposium Proceedings 951 (2007) 63–68.

[19] S. Reisert, H. Henkel, A. Schneider, D. Schäfer, P. Friedrich, J. Berger, M.J. Schöning, Development of a handheld sensor system system for the online measurement of hydrogen peroxide in aseptic filling systems, Physica Status Solidi (a) 207 (2010) 913–918.

[20] S. Corveleyn, G. Vandenbossche, J. Remon, Near-infrared (NIR) monitoring of $H_2O_2$ vapor concentration during vapor hydrogen peroxide (VHP) sterilisation, Pharmaceutical Research 14 (1997) 294–298.

[21] J. Wang, D.A. Mondiek, Sterilant monitoring assembly and apparatus and method using same, US Patent, US6517777 B1, 1999.

[22] B. Snopok, I. Kruglenko, Multisensor systems for chemical analysis: State-of-the-art in electronic nose technology and new trends in machine olfaction, Thin Solid Films 418 (2002) 21–41.

[23] W. Göpel, Chemical imaging: I. Concepts and visions for electronic and bioelectronic noses, Sensors and Actuators B: Chemical 52 (1998) 125–142.

[24] A. Hiroki, J.A. LaVerne, Decomposition of hydrogen peroxide at water−ceramic oxide interfaces, Journal of Physical Chemistry B 109 (2005) 3364–3370.

[25] D. Kohl, Surface processes in the detection of reducing gases with $SnO_2$-based devices, Sensors and Actuators 18 (1989) 71–113.

[26] D. Vlachos, P. Skafidas, J. Avaritsiotis, The effect of humidity on tin-oxide thick-film gas sensors in the presence of reducing and combustible gases, Sensors and Actuators B: Chemical 1995 (25) 491–494.

[27] T. Pearce, Handbook of machine olfaction: Electronic nose technology, Wiley-VCH, Weinheim, 2003.

[28] S. Reisert, H. Geissler, R. Flörke, P. Wagner, T. Wagner, M.J. Schöning, Controlling aseptic sterilization processes by means of a multi-sensor system, Proceedings of the IEEE SSCI (CompSens), Paris, 11-15 April (2011) 18-22.

# Chapter 4

## Characterisation of aseptic sterilisation processes using an electronic nose

International Journal of Nanotechnology, 2013, Vol. 10, pp. 470-484

Steffen Reisert[1], Hanno Geissler[2], Rudolf Flörke[2], Christian Weiler[2], Patrick Wagner[3] and Michael J. Schöning[1]

1) Institute of Nano- and Biotechnologies, FH Aachen, 52428 Jülich, Germany

2) SIG Combibloc Systems GmbH, 52441 Linnich, Germany

3) Institute for Materials Research, Hasselt University, 3590 Diepenbeek, Belgium

### 4.1 Abstract

The presented work describes the development of a multi-sensor system for the evaluation of aseptic sterilisation processes employing hydrogen peroxide vapour by means of an electronic nose. Microbiological count-reduction tests with *Bacillus atrophaeus* spores have been carried out in order to characterise influencing factors of the sterilisation by hydrogen peroxide vapour, namely the hydrogen peroxide concentration, humidity, gas temperature and gas flow. In parallel, three different types of gas sensors have been investigated on sensitivity towards the same parameters. A correlation between the results of the microbiological tests and the response of the gas sensors is drawn.

## 4.2 Introduction

The aseptic food processing is a key-technology in modern food-packaging [1]. It offers high standards in terms of safety and quality. At the same time, an extended preservation of the packaged food without refrigeration is assured. Hydrogen peroxide is the most frequently used agent for food package sterilisation [2,3]. Its ability to decompose into environmental compatible products, these are water and oxygen, make it the sterilant of choice in comparison to other chemical disinfectants [4]. Especially when applied in vapour-phase, hydrogen peroxide is effective against a broad spectrum of microorganisms, including bacteria, fungi, viruses and spores [5-7].

For the sterilisation of aseptic food packages, Hydrogen Peroxide Vapour (HPV) is applied at temperatures above 200 °C and concentrations of $H_2O_2$ up to 8% v/v in gaseous phase. An effective sterilisation of carton packages is of high importance in order to avoid product recontamination by pathogenic microorganisms and to attain a longer shelf-life of the product to be filled. The effectiveness of aseptic sterilisation processes is thereto tested by means of microbiological challenge tests [8, 9]. In implementing these tests, artificially inoculated packages with spores of non-pathogenic microorganisms, which exhibit high resistance against the sterilisation medium, are being exposed to the sterilisation process. Thereby, the reduction of viable microorganisms is a measure for the sterility. In case of the sterilisation by HPV, *Bacillus atrophaeus* spores are used as test organisms. Even though this represents a well-established and reliable method, it is to some degree unfavourable as probes require a lot of preparation and an inoculation time between 24 hours and several weeks. The high throughput of modern aseptic filling plants demands a faster way of monitoring the effectiveness of the sterilisation process during process definition and validation in order to avoid discarding, insufficiently sterilised carton packages during production.

Several attempts of characterising the sterilisation processes by monitoring their influence parameters, like hydrogen peroxide concentration or temperature have been made [10-15]. However, monitoring of one single parameter is often not sufficient for an accurate evaluation of a sterilisation process, since there is an interaction between the various influential parameters, such as temperature, gas flow and humidity, which can have a decisive effect on the inactivation of

microorganisms. One promising approach for the evaluation of multi-component chemical media and dynamic processes relies on the use of multi-sensor systems [16]. Concerning such multi-sensor systems, multi-component chemical media could be described not by a sum of the individual components (or corresponding response from the specific sensors) but by some abstract representation – a chemical image – a virtual fingerprint with a set of parameters intrinsical for a given multi-component medium [17].

Within the scope of this work, a multi-sensor system for the evaluation of aseptic sterilisation processes employing HPV shall be developed. Therefore, microbiological tests with spores of *Bacillus atrophaeus* have been carried out in order to evaluate the influencing factors of the sterilisation by HPV, namely the hydrogen peroxide concentration, humidity, the gas temperature and gas flow. At the same time, three different types of gas sensors have been investigated on their sensitivity towards these factors, in order to obtain chemical images of the sterilisation medium for different parameter sets. Finally, a correlation between the sensor signals and the results of microbiological tests for different gas compositions shall be established using chemical image recognition techniques. Such an instrumental system based on arrays of low-selective/cross-reactive sensors that are applied to form chemical images of gaseous multi-component media with further classification and identification has been named 'the Electronic Nose' [18]. Figure 4.1 depicts schematically the concept of an electronic nose.

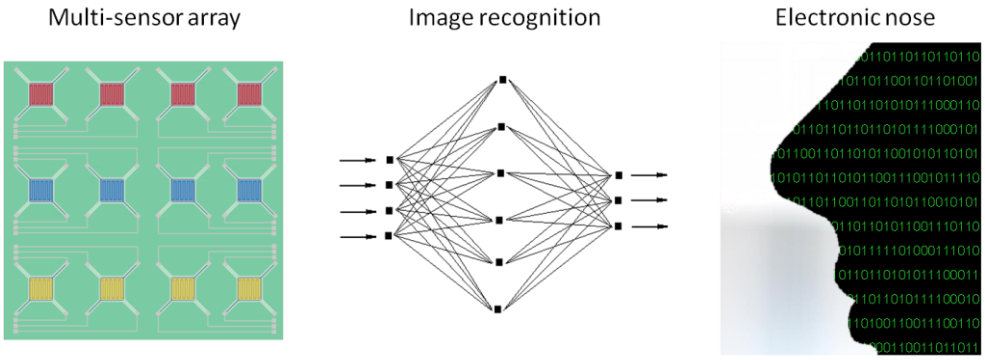


**Figure 4.1:** Concept of an electronic nose: Combining a multi-sensor array with (chemical-)image recognition techniques.

## 4.3 Materials and methods

### 4.3.1 Test apparatus

For the realisation of microbiological tests and calibration of the sensor system, a module for the generation of HPV of a modern aseptic filling machine has been used as described in **Section 1.6.2**.

### 4.3.2 Microbiological tests

For the evaluation of the influencing factors of the microbiological reduction by HPV and calibration of the sensor system, microbiological reduction tests with spores of *Bacillus atrophaeus* have been carried out. Hereto, two different strategies have been pursued. On the one hand, microbiological tests have been carried out according to the count-reduction test (CRT) in order to evaluate the variables of the sterilisation by HPV. On the other hand, tests have been done according to the end-point test (EPT). For a general description of the test procedure is referred to **Section 1.3.3.** As probes by the EPT require less post-processing, the latter ones will be used for the calibration of the sensor system in order to take more samples in a shorter period of time. In both cases, the CRT and EPT, the test organisms have been inoculated on alumina strips. For the CRT, test strips with $\approx 8*10^6$ spores of *Bacillus atrophaeus* have been prepared. In case of the EPT, three different loads with $\approx 10^4$, $10^5$ and $10^6$ spores per strip of the same strain have been used. In this article, the results of the evaluation of the influencing factors obtained by CRT will be presented. A detailed protocol of the test method and inoculation procedure can be found in **Section 1.6.3**. For each setting of machine parameters five microbiological samples have been taken. The maximum achievable log-rate (all spores are inactivated) with an initial bacterial count of $8*10^6$ spores is 6.9.

### 4.3.3 Sensors

When developing a sensor system, first of all, the question of the required sensor functionalities arises. To assess this issue for the desired development of an electronic nose for the evaluation of aseptic sterilisation processes employing HPV, one has to consider the mechanism of microbial inhibition by the sterilisation agent. It is generally considered that the inhibition of microbial growth by hydrogen peroxide is not the direct result of its oxidative properties in its molecular state, but the consequence of the activity of other strongly oxidant,

chemical species derived from it. In fact, hydrogen peroxide is an excellent source of singlet oxygen, superoxide radicals ($O_2^{\bullet -}$) and hydroxyl radicals ($OH^{\bullet}$) that are highly reactive and very toxic for microorganisms [19]. Furthermore, the kinetic of formation of said species is dependent on a number of other influencing factors, like the temperature or the presence of catalysts. This implies that solely monitoring the hydrogen peroxide concentration is not sufficient for a convincing evaluation of the sterilisation process. Another general requirement to sensors is an increased persistence against high gas temperatures of up to 330 °C and particularly, the highly oxidative and corrosive properties of HPV. Against this background, a selection from sensors, with respect to the above mentioned requirements, was chosen.

First, different types of metal-oxide semiconductor gas sensors (MOX) have been selected. Semiconductor gas sensors are known for their high sensitivity to reducing and oxidising gases. The sensing element of these sensors is subject to a change in conductivity when in contact with an oxidising or reducing gas. The selectivity of MOX towards specific groups of gases may be adapted by the type of oxide or additions used. The most common material is tin oxide ($SnO_2$). Also the operating temperature has an influence on the specific selectivity of the oxide. Figure 4.2 (left) depicts schematically the reaction mechanism of this type of sensor towards $H_2O_2$. The MOX was firstly introduced by Taguchi in 1965. Nowadays, it is state-of-the-art to combine several MOX with different oxides/additions and varying operating temperature for the realisation of multi-sensor arrays within the scope of chemical image recognition [20]. Regarding the MOX used in this work, a response to the above mentioned derivates with strong oxidative properties is expected. Radicals act as electron donors and directly increase the conductivity of semiconductor gas sensors [21].

As a second type, a solid-electrolyte sensor, also known as λ-probe was used. The sensing element of this sensor consists of a zirconia ceramic ($ZrO_2$), which is particularly sensitive to oxygen. This sensor should be targeted to detect a rise in the oxygen concentration, which is related to the heterogeneous decomposition of hydrogen peroxide into water and oxygen and therefore,

represents a supplementary source of oxygen. Figure 4.2 (middle) schematically shows the corresponding transducer principle.

The third sensor in test has been a calorimetric hydrogen peroxide sensor, which has been developed in our lab [13, 14] (for a detailed description of this sensor see **Section 1.4.2** and **Chapter 2**). The sensor consists of a differential set-up of a catalytically activated and a passivated temperature sensor. The sensor principle relies in detecting a rise in temperature on the catalytically active surface, due to the exothermic reaction of $H_2O_2$ on the same, while the passivated temperature sensor is at ambient (gas) temperature. This sensor enables the simultaneous monitoring of the hydrogen peroxide concentration up to 8% v/v in gaseous phase and gas temperature. A simplified representation of the reaction mechanism is given in Figure 4.2 (right).

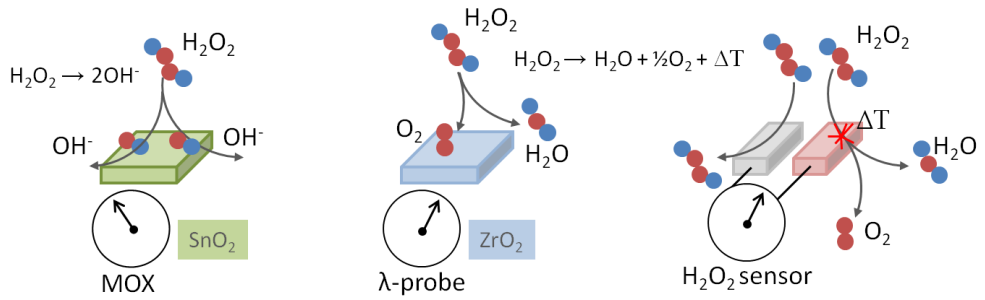


**Figure 4.2:** Reaction mechanism of $H_2O_2$ and its derivatives on the three sensor types (simplified).

4.3.4 Measurements

Four series of measurement have been carried out in order to evaluate the influencing factors of the sterilisation by HPV. Hereby, the influence of the hydrogen peroxide concentration, humidity, gas temperature and gas flow on the microbial reduction of *Bacillus atrophaeus* spores were studied. Same measurements were carried out to investigate the properties of the described sensors in hydrogen peroxide atmosphere. The parameters of each of the four series of measurement are listed in Tables 4.1-4.4. The tables provide information on the air flow set, dosed amount of hydrogen peroxide solution

($D_{sol}$ $H_2O_2$), concentration of the hydrogen peroxide solution ($C_{sol}[H_2O_2]$), gas temperature and calculated $H_2O_2$ concentration in gaseous phase ($C[H_2O_2]$). The latter was calculated from the mixer flow ratio.

**Table 4.1:** Parameter set of the first measurement series (influence of $H_2O_2$ dosage).

| **Measurement 1** | **Parameter** | | | | |
|---|---|---|---|---|---|
| $D_{Sol}$ $H_2O_2$ (µl/s) | 0 | 300 | 500 | 600 | 900 |
| Air flow (m³/h) | 10 | 10 | 10 | 10 | 10 |
| $C_{sol}[H_2O_2]$ (% w/w) | 0 | 35 | 35 | 35 | 35 |
| $C[H_2O_2]$ (% v/v) | 0 | 2.6 | 4.1 | 4.7 | 6.4 |
| Gas temperature (°C) | 270 | 270 | 270 | 270 | 270 |

**Table 4.2:** Parameter set of the second measurement series (influence of $H_2O_2$ dilution).

| **Measurement 2** | **Parameter** | | | | |
|---|---|---|---|---|---|
| $D_{Sol}$ $H_2O_2$ (µl/s) | 500 | 500 | 500 | 500 | 500 |
| Air flow (m³/h) | 10 | 10 | 10 | 10 | 10 |
| $C_{sol}[H_2O_2]$ (% w/w) | 0 | 15 | 25 | 35 | 50 |
| $C[H_2O_2]$ (% v/v) | 0 | 1.6 | 2.8 | 4.1 | 6.2 |
| Gas temperature (°C) | 270 | 270 | 270 | 270 | 270 |

**Table 4.3:** Parameter set of the third measurement series (influence gas temperature).

| **Measurement 3** | **Parameter** | | | | | |
|---|---|---|---|---|---|---|
| $D_{Sol}$ $H_2O_2$ (µl/s) | 500 | 500 | 500 | 500 | 500 | 500 |
| Air flow (m³/h) | 10 | 10 | 10 | 10 | 10 | 10 |
| $C_{sol}[H_2O_2]$ (% w/w) | 35 | 35 | 35 | 35 | 35 | 35 |
| $C[H_2O_2]$ (% v/v) | 4.1 | 4.1 | 4.1 | 4.1 | 4.1 | 4.1 |
| Gas temperature (°C) | 180 | 210 | 240 | 270 | 300 | 330 |

**Table 4.4:** Parameter set of the fourth measurement series (influence of air flow).

| **Measurement 4** | **Parameter** | | | |
|---|---|---|---|---|
| $D_{Sol}$ $H_2O_2$ (µl/s) | 375 | 500 | 625 | 750 |
| Air flow (m³/h) | 7.5 | 10 | 12.5 | 15 |
| $C_{sol}[H_2O_2]$ (% w/w) | 35 | 35 | 35 | 35 |
| $C[H_2O_2]$ (% v/v) | 4.1 | 4.1 | 4.1 | 4.1 |
| Gas temperature (°C) | 270 | 270 | 270 | 270 |

The probes for CRT were exposed to the sterilisation medium at 5 cm below the outlet of the gas nozzle of the test rig for 0.5 seconds, which corresponds to a single step of the sterilisation cycle in modern aseptic filling machines. Each parameter was tested with a repetition of five probes in order to obtain statistically significant results. The sensors were kept permanently into the gas stream at a second nozzle, in the same position as the probes for CRT (see **Section 1.6.2**).

## 4.4 Results and discussion

### 4.4.1 Microbiological tests

Four series of measurement have been carried out according to Tables 4.1-4.4. The resulting log-rates from CRT of the first and second measurement are summarised in Figure 4.3, plotted against the hydrogen peroxide concentration in gaseous phase. While at the first measurement the variation of hydrogen peroxide concentration was achieved by different amounts of hydrogen peroxide solution dosed to the gas stream, different dilutions of the hydrogen peroxide solution have been fed to the gas stream at a constant dosage of 500 µl/s during the second measurement. In this way, the influence of humidity on the microbial reduction shall be investigated. The log-rate at 0% v/v $H_2O_2$ from the first measurement was achieved in the hot gas stream, without the presence of $H_2O_2/H_2O$, whereas during the second measurement an amount of 500 µl/s of water has been fed to the carrier gas stream.

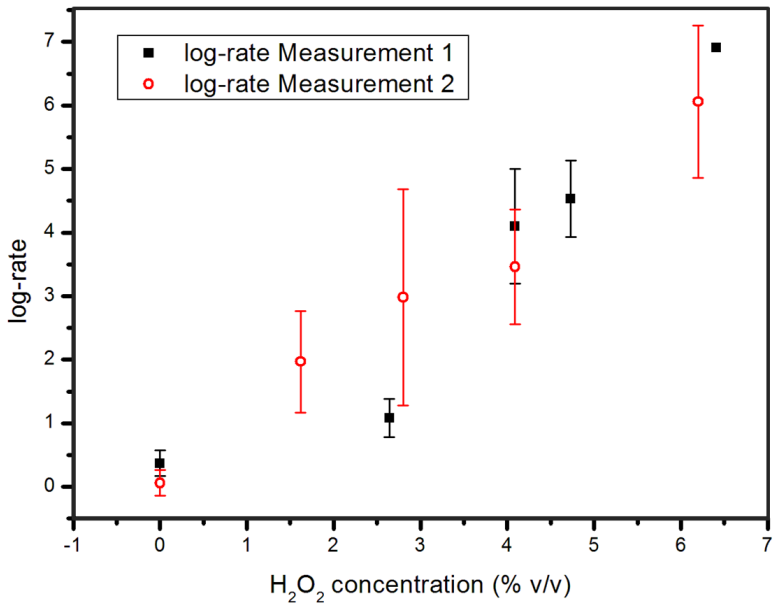


**Figure 4.3:** Resulting log-rates from measurements 1 and 2 (Influence of hydrogen peroxide concentration @ 10 m³/h and 270 °C).

The exposure to hot air/steam at 0% v/v $H_2O_2$ for 500 ms causes only a minimal microbiological reduction of *Bacillus atrophaeus*. The achieved log-rates where in both cases below 0.5. In presence of hydrogen peroxide, the logarithmic reduction rate is significantly increased. For instance, at a concentration of 1.6% v/v $H_2O_2$ during the second measurement the number of viable spores was reduced by two decades during an exposure time of 500 ms. For all further samples from the first and second measurement, the log-rate is increasing with increasing hydrogen peroxide concentration. At the highest $H_2O_2$ concentration of 6.4% v/v the maximum log-rate of 6.9, which means that no viable spores remained, was obtained. It seems that the inactivation of *Bacillus atrophaeus* spores is independent from the level of humidity in the sterilisation medium.

The results of the third microbiological test are shown in Figure 4.4, plotted against the adjusted gas temperature. The parameter setting was according to Table 4.3. The exposure time of the test strips to the sterilisation medium was 500 ms.

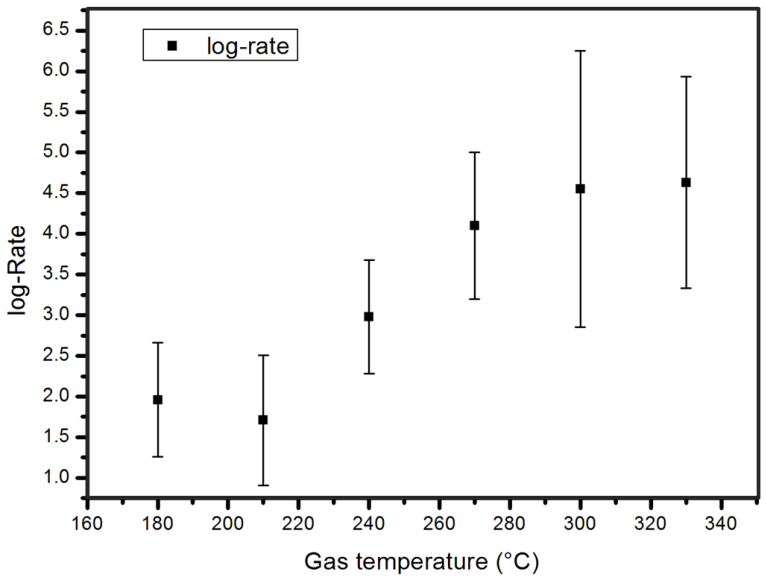


**Figure 4.4:** Resulting log-rates from measurement 3 (Influence of gas temperature @ 10 m³/h and 4.1% v/v $H_2O_2$).

At a gas temperature of 270 °C and a $H_2O_2$ concentration of 4.1% v/v a similar log-rate was achieved as during the first measurement under same conditions

(compare Tables 4.1 and 4.3). Apparently, the achieved microbial reduction at the lowest gas temperature of 180 °C is higher compared to the achieved log-rate at 210 °C. This effect may be explained due to condensation of the hydrogen peroxide on the test strip at relatively low gas temperatures. Subsequently, the condensed $H_2O_2$ will affect the spores even after the test strip has been removed from the gas stream. However, with further increase of the gas temperature higher log-rates were achieved. This observed behaviour confirms that hydrogen peroxide reveals strong antimicrobial properties at high temperatures. Though, an increase of the gas temperature from 300 to 330 °C did not have any effect on the sterilisation efficacy.

The influence of the gas flow has been investigated in the fourth measurement. Therefore, the carrier gas stream was varied between 7.5 and 15 m³/h. At each setting, the dosed amount of hydrogen peroxide solution was adjusted in order to obtain the same $H_2O_2$ concentration of 4.1% v/v in the gaseous phase. The gas temperature was set to 270 °C and the exposure time was 500 ms. The results of the fourth measurement are depicted in Figure 4.5.

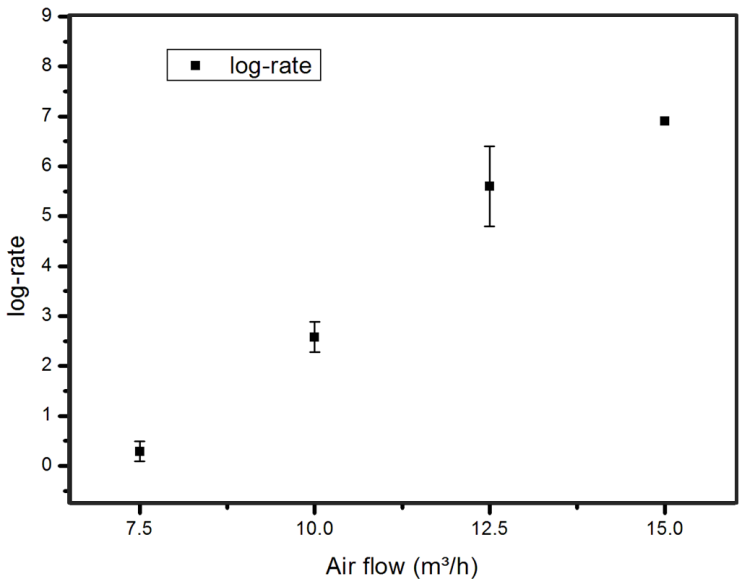


**Figure 4.5:** Resulting log-rates from measurement 4 (Influence of flow rate @ 270 °C and 4.1% v/v $H_2O_2$).

At the lowest gas flow of 7.5 m³/h only a low reduction of less than 0.5 decades was observed. In the following the log rate seems to be linearly increasing with the flow rate until the highest possible log-rate (all spores inactivated) of 6.9 was achieved at the highest gas flow of 15 m³/h. It is assumed that an increase of the flow rate at constant hydrogen peroxide concentration is equatable to an extension of the exposure time. Doubling the flow rate should have the same effect on microbial reduction as doubling the exposure time. Accordingly, it can be deduced, that the microbial reduction of *Bacillus atrophaeus* by HPV is linearly increasing with exposure time.

4.4.2 Sensors

Three types of gas sensors have been investigated on their response towards the influencing factors of the sterilisation by HPV at different concentrations of $H_2O_2$ in gaseous phase, levels of humidity, gas temperatures and flow rates. The sensory requirements and types of sensors in test are described in **Section 4.3.3**. Results of the three types of single sensors in test have been published in [14, 22]. At this point, the results of our studies will be summarised and discussed with respect to the aforementioned challenges.

The developed $H_2O_2$ sensor exhibits a high sensitivity and selectivity towards HPV with a linear relationship between the sensor signal (temperature difference between a catalytically activated and passivated temperature sensor) and the hydrogen peroxide concentration in the gaseous phase. The linear range of the sensor is between 0 and 8% v/v $H_2O_2$ with an absolute accuracy of 0.2% v/v. The sensor response is independent from humidity. When measurements have been carried out at different gas temperatures and constant $H_2O_2$ concentration, a decrease in the sensor signal was observed towards higher temperatures (compare Table 4.3). Our studies have shown, that this decrease in the sensor signal is related to the decomposition of hydrogen peroxide in the heater. The decomposition rate of $H_2O_2$ in the heater was observed to be increasingly accelerated towards higher gas temperatures. Also a minor influence of the gas flow rate on the sensor behaviour was observed, whereby an increase of the sensor signal was observed towards higher flow rates. This effect may be explained by a higher transport rate of $H_2O_2$ to the catalyst surface at higher flow rates. The developed sensor is the first of its kind, suitable for monitoring

hydrogen peroxide in gaseous phase at elevated concentrations of up to 8% v/v $H_2O_2$. Based on the sensing principle of the calorimetric sensor, the gas temperature can be monitored, too.

The response of different commercially available MOX and a solid-electrolyte gas sensor in hydrogen peroxide atmosphere has been discussed in [22]. Concerning the MOX, it was shown that n-type $SnO_2$ sensors in test exhibit a high sensitivity towards hydrogen peroxide. A response of the sensors in steam was observed, too, whereas the signal change was in the same direction when presented in hydrogen peroxide atmosphere. It was lowered by one decade compared to $H_2O_2$. The humidity-dependent behaviour of the MOX has been explained before [21, 23]. The distinct response of the MOX when presented to hydrogen peroxide could be explained by the interaction of hydroxyl radicals on the surface of the sensing element, descended from the decomposition of hydrogen peroxide. Studies on the behaviour of the MOX at different flow rates (compare Table 4.4) did not show any differentiation. The required operating temperature of a MOX is above 250 °C. MOX´s exhibit rather different selectivities at different operating temperatures. When heated in a static mode (constant heating voltage), the sensor will be subject to temperature changes evoked by the environment, once there is a notably change in the ambient temperature. As a consequence, the selectivity coefficient of the sensor will be shifted, which in turn causes a signal change. This behaviour can be used purposefully if a temperature-dependent sensor response is desired. Otherwise, MOX´s can be operated in a temperature-controlled mode.

The λ-probe which has been tested is particularly sensitive to oxygen. During the measurements in hydrogen peroxide atmosphere, an increase in the sensor signal could be observed, which in fact, depends on the $H_2O_2$ concentration. A correlation between the decomposition of hydrogen peroxide and the rise in oxygen concentration can be drawn. It is assumed that hydrogen peroxide serves as source of oxygen when decomposed into water and oxygen. The λ-probe in test was operated in a temperature-controlled mode at a constant temperature of about 500 °C. An influence of the gas temperature on the sensor response has not been observed.

All sensors in test were exposed to the sterilisation medium in sum for a couple of dozen hours over a few months, while they had being exposed to hydrogen peroxide concentrations of up to 8% v/v and gas temperatures of up to 300 °C. A significant change in the sensor behaviour or sensor damage of neither one of the three types of sensors in test could not be observed during this time period.

4.4.3 Correlation

In order to realise a sensor system for the evaluation of the sterilisation efficacy of hydrogen peroxide vapour, a correlation between the results of the microbiological tests and the sensor signals has to be established. Therefore, the resulting log-rate will be contrasted to a chemical image (sum of sensor signals) for each gas composition. One method of displaying multivariate data is based on the use of a radar plot. Hereby, the variables are represented on axes starting from the same point, while each variable expresses the signal of a single sensor for a given gas composition. The values on the axes are connected to their neighbours by a line, which gives the plot a star-like appearance. Each star represents a single observation with a unique pattern for a certain combination of sensor signals. The more differentiated the signals are, the more clearly will differ the shapes of the pattern for each gas composition ("fingerprint").

Radar plots of the resulting sensor signals for each one of the gas compositions listed in Tables 4.1-4.4 have been drawn and were correlated with the respective log-rate achieved during the microbiological tests for the same gas compositions. Exemplarily, the resulting plots of the first measurement (influence of hydrogen peroxide concentration) will be shown here. Figure 4.6, depicts (from left to right) the radar plots of six sensors (four different MOX, λ-probe and $H_2O_2$ sensor) for each gas composition of the first measurement. In order to qualitatively compare the radar plots between each other (scale from 0 to 1), the sensor signals have been normalised to the value obtained in hot air (no dosage). For each plot, the achieved log-rate during the microbiological tests is given. The last one shows all of the achieved patterns in one plot.

From Figure 4.6 it can be seen, that there is a differentiation between the patterns obtained for the different compositions of the sterilisation medium and

the resulting log-rates, respectively, whereas dissimilarities can be recognised at each one of the axes. It follows, that changing of a process parameter, in this case the hydrogen peroxide concentration, equally affects the response of each of the sensors in test. Also, discrete patterns could be obtained for the achieved log-rates.

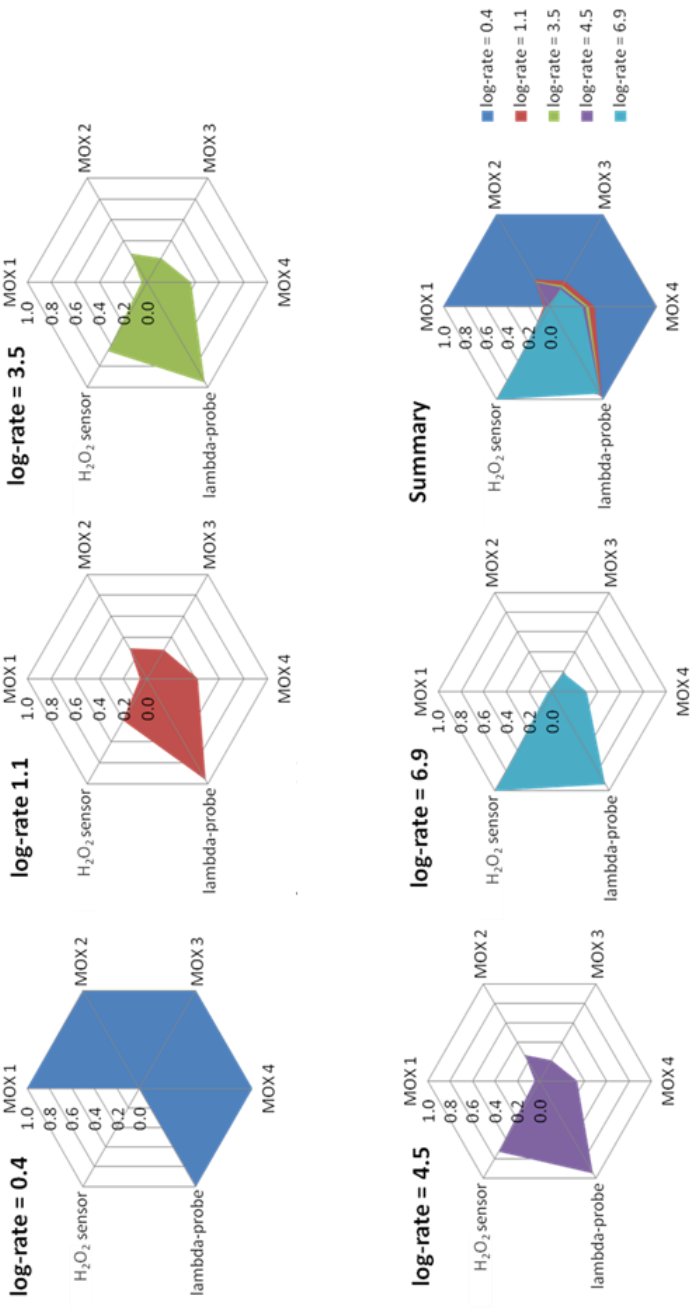


**Figure 4.6:** Radar plots of the resulting sensor signals of six different gas sensors during the first measurement series, correlated with the achieved log-rates during the microbiological tests.

## 4.5 Conclusions

The influencing factors of the microbial reduction of *Bacillus atrophaeus* spores by HPV, namely, the hydrogen peroxide concentration, humidity, gas temperature and flow rate have been studied by making use of the CRT. At the same time, three different types of gas sensors (number n=6) have been investigated on the response towards the same parameters. The comparison of both, the sensory and microbiological measurements reveal that the influencing factors of the sterilisation by HPV equally affect the response of the sensors. This implies the potential use of the sensors in test for the realisation of a multi-sensor system for the evaluation of aseptic processes employing HPV. In further studies, the microbiological tests shall be carried to a larger extend, in view of a more detailed characterisation of the influencing factors of the sterilisation by gaseous HPV. The coming microbiological test will be carried out by making use of the EPT in order to reduce the workload for the microbiological tests. This way, a larger number of probes per parameter could be taken to achieve a higher statistical significance of the microbiological tests. In parallel, the sensory measurements will be performed simultaneously in order to obtain a detailed chemical image of the sterilisation medium at the different parameter settings. Finally, a chemical image recognition technique, like the *Fuzzy Logic* or an *Artificial Neural Network* (ANN) shall be implemented in order to establish a correlation between the sensor signals and the sterilisation efficacy.

**4.6 References**

[1] S.D. Holdsworth, Aseptic processing and packaging of food products, Elsevier Applied Science; Elsevier Science Pub. Co., London, New York, 1992.

[2] G. McDonnel, A.D. Russell, Antiseptics and disinfectants: Activity, action, and resistance, Clinical Microbiology Reviews 12 (1999) 147–179.

[3] R. Toniolo, P. Geatti, G. Bontempelli, G. Schiavon, Amperometric monitoring of hydrogen peroxide in workplace atmospheres by electrodes supported on ion-exchange membranes, Journal of Electroanalytical Chemistry 514 (2001) 123–128.

[4] R.A. Heckert, M. Best, L.T. Jordan, G.C. Dulac, D.L. Eddington, W.G. Sterritt, Efficacy of vaporized hydrogen peroxide against exotic animal viruses, Applied Environmental Microbiology 63 (1997) 3916–3918.

[5] M. Kokubo, T. Inoue, J. Akers, Resistance of common environmental spores of the genus *Bacillus* to vapour hydrogen peroxide, PDA Journal of Pharmaceutical Science and Technology 5 (1998) 228–231.

[6] N.A. Klapes, D. Vesley, Vapor-phase hydrogen peroxide as a surface decontaminant and sterilant, Applied Environmental Microbiology 56 (1990) 503–506.

[7] G. Graham, J. Rickloff, J. Dalmasso, Sterilization of isolators and lyophilyzers with hydrogen peroxide in the vapor phase, VHP™ Technology: A collection of scientific papers, AMSCO Scientific, Apex, 1992.

[8] Verband Deutscher Maschinen- und Anlagenbau e.V., Code of practice: Filling machines of VDMA hygiene class V: Testing the effectiveness of packaging sterilization devices, Frankfurt, 2008.

[9] G. Moruzzi, W.E. Garthright, J.D. Floros, Aseptic packaging machine pre-sterilisation and package sterilisation: Statistical aspects of microbiological validation, Food Control 11 (2000) 57–66.

[10] I. Taizo, A. Sinichi, K. Kawamura, Application of a newly developed hydrogen peroxide vapor phase sensor to HPV sterilizer, PDA Journal of Pharmaceutical Science and Technology 52 (1998) 13–18.

[11] N. Näther, H. Henkel, A. Schneider, M.J. Schöning, Investigation of different catalytically active and passive materials for realising a hydrogen peroxide gas sensor, Physica Status Solidi (a) 206 (2009) 449–454.

[12] N. Näther, L.M. Juárez, R. Emmerich, J. Berger, P. Friedrich, M.J. Schöning, Detection of hydrogen peroxide ($H_2O_2$) at exposed temperatures for industrial processes, Sensors 6 (2006) 308–317.

[13] N. Näther, R. Emmerich, P. Friedrich, H. Henkel, A. Schneider, M. Schöning, A novel gas-phase hydrogen peroxide sensor basing on a combined physical/chemical transduction mechanism, Materials Research Society Symposium Proceedings 951 (2007) 63–68.

[14] S. Reisert, H. Henkel, A. Schneider, D. Schäfer, P. Friedrich, J. Berger, M.J. Schöning, Development of a handheld sensor system system for the online measurement of hydrogen peroxide in aseptic filling systems, Physica Status Solidi (a) 207 (2010) 913–918.

[15] S. Corveleyn, G. Vandenbossche, J. Remon, Near-infrared (NIR) monitoring of $H_2O_2$ vapor concentration during vapor hydrogen peroxide (VHP) sterilisation, Pharmaceutical Research 14 (1997) 294–298.

[16] B. Snopok, I. Kruglenko, Multisensor systems for chemical analysis: State-of-the-art in electronic nose technology and new trends in machine olfaction, Thin Solid Films 418 (2002) 21–41.

[17] W. Göpel, Chemical imaging: I. Concepts and visions for electronic and bioelectronic noses, Sensors and Actuators B: Chemical 52 (1998) 125–142.

[18] T. Pearce, Handbook of machine olfaction: Electronic nose technology, Wiley-VCH, Weinheim, 2003.

[19] M.D. Labas, C.S. Zalazar, R.J. Brandi, A.E. Cassano, Reaction kinetics of bacteria disinfection employing hydrogen peroxide, Biochemical Engineering Journal 38 (2008) 78–87.

[20] J.W. Gardner, P.N. Bartlett, A brief history of electronic noses, Sensors and Actuators B: Chemical 18 (1994) 210–211.

[21] P. Skafidas, D.S. Vlachos, J.N. Avarisiotis, Modelling and simulation of tin oxide based thick-film gas sensors using Monte Carlo techniques, Sensors and Actuators B: Chemical 18 (1994) 724–728.

[22] S. Reisert, H. Geissler, R. Flörke, N. Näther, P. Wagner, M.J. Schöning, Towards a multi-sensor system for the evaluation of aseptic processes employing hydrogen peroxide vapour ($H_2O_2$), Physica Status Solidi (a) 208 (2011) 1351–1356.

[23] D. Vlachos, P. Skafidas, J. Avaritsiotis, The effect of humidity on tin-oxide thick-film gas sensors in the presence of reducing and combustible gases, Sensors and Actuators B: Chemical 1995 (25) 491–494.

# Chapter 5

## Multiple sensor-type system for monitoring the microbicidal effectiveness of aseptic sterilisation processes

*Manuscript under preparation*

Steffen Reisert[1], Hanno Geissler[2], Christian Weiler[2], Patrick Wagner[3] and Michael J. Schöning[1,4]

1) Institute of Nano and Biotechnologies, FH Aachen, 52428 Jülich, Germany

2) SIG Combibloc Systems GmbH, 52441 Linnich, Germany

3) Institute for Materials Research, Hasselt University, 3590 Diepenbeek, Belgium

**5.1 Abstract**

The present work describes a novel multiple sensor-type system for the real-time analysis of aseptic sterilisation processes employing gaseous hydrogen peroxide ($H_2O_2$) as a sterilant. The inactivation kinetics of *Bacillus atrophaeus* by gaseous $H_2O_2$ have been investigated by means of a methodical calibration experiment, taking into account the process variables $H_2O_2$ concentration, humidity and gas temperature. It has been found that the microbicidal effectiveness at $H_2O_2$ concentrations above 2% v/v is largely determined by the concentration itself, while at lower $H_2O_2$ concentrations, the gas temperature and humidity play a leading role. Furthermore, the responses of different types of gas sensors towards the influencing factors of the sterilisation process have been analysed within the same experiment. Based on a correlation established between the inactivation kinetics and the sensor responses, a calorimetric $H_2O_2$ sensor and two different types of metal-oxide semiconductor (MOX) sensors could be identified as possible candidates for monitoring the microbicidal effectiveness of aseptic sterilisation processes employing gaseous $H_2O_2$. Therefore, two linear models that describe the relationship between sensor response and microbicidal effectiveness have been proposed.

## 5.2 Introduction

The origins of aseptic processing can be dated back to more than a century. Nowadays, it represents a key-technology in modern food processing and was recently ranked the No. 1 innovation in food technology [1]. The core elements of aseptic processing are the thermal treatment of the product to be filled, the sterilisation of the container and the filling and sealing in a recontamination free environment in such way that it maintains sterility [2]. In the course of this, the sterilisation of the packaging material is an important criterion. Modern filling machines use hydrogen peroxide ($H_2O_2$) as a sterilant for carton packages.

Previously applied in liquid phase, gas-phase $H_2O_2$ today established as the sterilising agent of choice, since it demonstrated a higher activity compared to liquid-phase $H_2O_2$ [3–6]. It is believed that the microbicidal activity of $H_2O_2$ is based on the activity of products derived from its decomposition. It has been demonstrated that $H_2O_2$ serves as a source of highly reactive species, above all hydroxyl radicals, which cause damage to a variety of microorganisms including highly resistant spores [7–10]. The latter are used as test organisms for determining the sterilisation effectiveness in the context of the so-called challenge test: *Bacillus atrophaeus* is the recommended test organism for sterilisation processes employing $H_2O_2$ in combination with heat, since it inherently has a high resistance against the sterilisation medium [11]. An approved test method is the count-reduction test (CRT). The CRT is carried out using test packages inoculated with an unnaturally high load (at least $10^5$) of *B. atrophaeus*, which are taken to the sterilisation process. The decrease in viable spore count after the sterilisation serves as a measure for the effectiveness of sterilisation. It is usually expressed in powers of ten, the so-called logarithmic cycle reduction (LCR). Although the CRT represents a recognised method, its major disadvantage is the elaborately preparation and post-processing of samples. Solely the incubation period of the spores in ideal case amounts to at least 24 hours. Thus, microbiological tests, like the CRT, cannot be used by means of a real-time monitoring.

It is the aim of this study, to characterise different influencing factors of the sterilisation with gaseous $H_2O_2$ by means of the CRT with *B. atrophaeus*. As

such, the $H_2O_2$ concentration, humidity and temperature have been identified by previous studies [10,12–16]. Moreover, the response of multiple types of gas sensors, namely a calorimetric $H_2O_2$ sensor, different commercially available metal-oxide semiconductor (MOX) gas sensors and an electrochemical gas sensor for the detection of $O_2$, towards the influencing factors of the sterilisation by gaseous $H_2O_2$ have been investigated. For this purpose, a methodical calibration experiment, allowing a detailed investigation of the impact of each of the mentioned influencing factors, has been elaborated. This way, the inactivation kinetics of *B. atrophaeus* and the sensor responses have been analysed for a broad parameter range of the variables $H_2O_2$ concentration in a range between 1.67 and 4.32% v/v, $H_2O$ concentration in a range between 15.10 and 22.60% v/v and the gas temperature ranging from 150 to 330 °C.

Based on the results of the calibration experiment, a correlation between the microbiological effectiveness and the response of the gas sensors has been established. In the end, two different models will be proposed. One is related to the calorimetric gas sensor and covers predominantly the range of higher $H_2O_2$ concentrations (>2% v/v), while the second one is related to the metal-oxide semiconductor gas sensors and may be applied at rather low $H_2O_2$ concentrations (<2% v/v). It will be shown that, by the right choice of sensors in combination with appropriate mathematical models, a sensor system for the real-time monitoring of sterilisation process employing gaseous $H_2O_2$ can be realised.

## 5.3 Materials and methods

### 5.3.1 Experimental set-up

The test apparatus that has been used to investigate the inactivation kinetics of *B. atrophaeus* and to characterise the gas sensors conforms to a sterilisation unit of an industrial aseptic filling machine for large-scale production of food packages and has been described in detail in previous publications [17,18] and in **Section 1.6.2**. The measuring point (MP) for the sensors and microbiological tests was chosen at a distance of 5.2 cm each under a separate nozzle. While the sensors were positioned firmly under one nozzle, the microbiological samples

were introduced via a time-controlled hydraulic slide (see **Section 1.6.2**). The exposure time for the microbiological samples was 150 ms.

5.3.2 Microbiological tests

The microbiological tests have been carried out according to the CRT as described in **Section 1.3.3**. As test samples, *Bacillus atrophaeus* spores inoculated on aluminum strips were used. The initial bacterial count was on average at $2.04*10^6$ CFU (colony forming units) per strip. For each setting of the machine parameters, ten microbiological samples have been taken. The general test procedure and cultivation of the spores is explained in **Section 1.6.3**.

5.3.3 Gas sensors

A calorimetric-type gas sensor for the detection of hydrogen peroxide, which has been developed in the authors' laboratory and different types of commercially available gas sensors, namely four MOX and one electrochemical gas sensor for the detection of $O_2$, also known as lambda probe, have been investigated.

The calorimetric $H_2O_2$ sensor was previously described in detail by several publications of the authors [20,21] (for a detailed description of this sensor see **Section 1.4.2** and **Chapter 2**). In short, it consists of a differential set-up of two temperature sensors, wherein one of the temperature sensors is catalytically activated by $MnO_2$ powder and the second one is passivated by a perfluoroalkoxy (PFA) coating. In presence of hydrogen peroxide, a temperature difference between the catalytically activated and the passivated sensor, caused by the exothermal reaction of hydrogen peroxide on the catalyst, can be detected. The temperature difference is in a linear correlation to the hydrogen peroxide concentration in gaseous phase. Furthermore, the sensor features high specificity to $H_2O_2$ and reproducibility. The commercially available gas sensors employed in this work also have already been described in part by previous publications of the authors [13,14]. It was shown that metal-oxide semiconductor gas sensors exhibit a high sensitivity with respect to the influencing factors of the sterilisation by gaseous hydrogen peroxide. As such, the hydrogen peroxide concentration itself as well as reactive derivatives that originate from the decomposition of hydrogen peroxide, i.e., hydroxyl radicals - which were proven to have a high microbicidal activity - have to be mentioned. The electrochemical sensor primary detects oxygen. Hydrogen peroxide serves

as a possible source of oxygen, which derives from the decomposition of the same [22]. Thus, a change in the oxygen concentration provides information on the reactivity of the sterilising gas. Table 5.1 summarises information on model, manufacturer, sensor type and operation mode of the sensors in test.

**Table 5.1:** Overview of the gas sensors in test.

| | $H_2O_2$ sensor | TGS 816 | TGS 823 | GGS 5333 T | GGS 6333 T | SO A0 250 |
|---|---|---|---|---|---|---|
| Manufacturer * | in-house | Figaro | Figaro | UST | UST | SENSORE |
| Type of sensor ** | calorimetric | MOX | MOX | MOX | MOX | Electro-chemical $O_2$ sensor |
| Heating mode *** | n.h. | $U_{const}$ | $U_{const}$ | $U_{const}$ | $T_{const}$ | $T_{const}$ |

* Figaro = Figaro Engineering (Japan); UST = UST Umweltsensortechnik GmbH (Germany); Sensore = SENSORE Electronic GmbH (Austria)

** MOX = metal-oxide semiconductor

*** n.h. = not heated; $U_{const}$ = constant voltage; $T_{const}$ = constant operating temperature

5.3.4 Calibration experiment

In order to study the inactivation kinetics of hydrogen peroxide on *B. atrophaeus* spores and to determine the sensor characteristics, a methodical calibration experiment has been designed. As influencing factors of the sterilisation process, the $H_2O_2$ concentration, the gas temperature and the humidity were of interest. The assumed values for $H_2O_2$ concentration and humidity ($H_2O$ concentration) correspond to the fraction of their number of molecules (as part of 100) related to the total number of molecules in the gas stream and are given in terms of per cent of volume (% v/v). The chosen calibration data is closely related to the parameters that are used in industrial applications. However, particularly "low" concentrations of $H_2O_2$ in the range between 1 to 5% v/v were of interest for

this study, since the inactivation kinetics at mainly "higher" $H_2O_2$ concentrations (4 to 8% v/v) have been subject of previous works [13–15].

The $H_2O_2$ concentration ($c_{H2O2}$) and humidity ($c_{H2O}$) have been chosen each one in four steps in the range between 1.67 to 4.32% v/v and 15.1 to 22.6% v/v, respectively. The set temperature of the gas stream ($T_{Gas}$) was varied in four steps between 150 and 330 °C. The flow rate of the carrier gas stream was set to a constant value of 10 m³/h, which corresponds to a flow velocity of about 3.5 m/s under standard conditions. Table 5.2 summarises the set of parameters that was chosen for the calibration experiment.

**Table 5.2:** Set of parameters chosen for the calibration experiment.

| $c_{H2O2}$ (% v/v) | $c_{H2O}$ (% v/v) | $T_{Gas}$ (°C) |
|---|---|---|
| 1.67 | 15.10 | 150 |
| 2.48 | 17.60 | 210 |
| 3.35 | 20.20 | 270 |
| 4.32 | 22.60 | 330 |

For the methodical calibration experiment, 40 different measurement points have been selected. In this case, each individual measurement point corresponds to a certain combination of the values from the parameters given in Table 5.2. The measurement points have been chosen according to the scheme shown in Figure 5.1. The coordinates of the points correspond to the values of the parameters. They lie on the edges of a cube (blue) and additionally, four points inside the cube (red) have been defined. The sequence of value change is given by the arrows. For reasons of reproducibility, the vertex points of the cube have been measured two times. The first vertex point (starting point) was measured three times. In sum, a total of 49 measurements has been planned. Each time a parameter is changed, at first constant process conditions have to be reached. This is the case when the sensor signals, in particular the gas temperature, show a constant value. From this point, the measurement time of the sensors was chosen to 300 s. As measurement value for each sensor and

measuring point, the signal of each sensor is averaged over this period. Simultaneously to the sensory measurements, ten microbiological samples were taken for each setting. The contact time of the microbiological samples was chosen uniformly at 150 ms, which turned out to be suitable for studying the inactivation kinetics as the expected microbial reduction of the bacterial spores should be neither too high (total inactivation) nor too low (no inactivation).

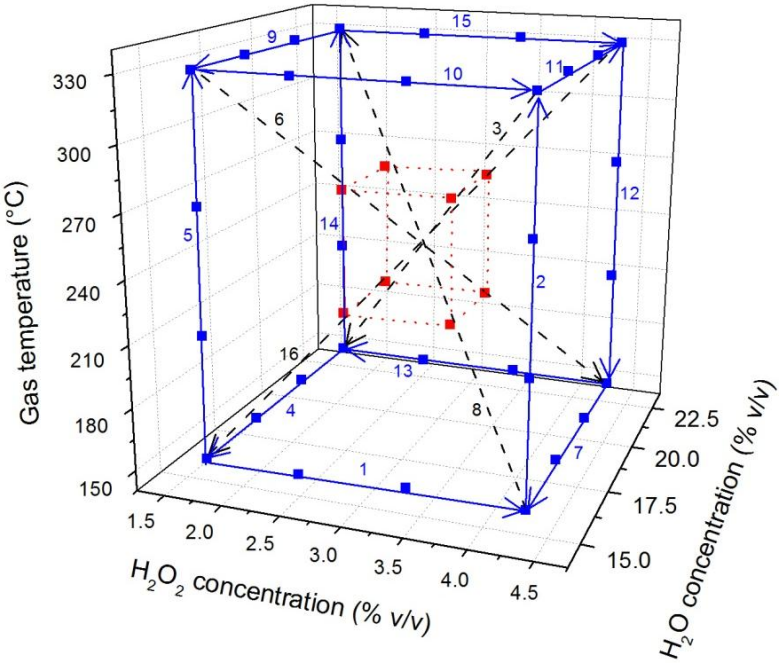


**Figure 5.1:** Scheme of the calibration experiment. The coordinates of the points define the values of the parameters and arrows indicate the order in which the parameters were changed.

## 5.4 Results and discussion

### 5.4.1 Microbiological test

Based on the methodical experiment, the influence of the each parameter ($c_{H2O2}$, $c_{H2O}$ and $T_{Gas}$) on the microbial inactivation was studied. In the following, the results of the microbiological tests will be discussed.

Figure 5.2 shows the overall result of the microbiological test series (according to the scheme shown in Fig. 5.1). Therefore, the obtained LCR is plotted vs. the

corresponding hydrogen peroxide concentration of each measurement point. The values of the respective gas temperature are given by colours (see legend of Fig. 5.2). The values of humidity ($c_{H2O}$) varied between 15.1 and 22.6% v/v within the illustrated measurement but are not further specified (n.s.) for each individual data point in this plot. The dashed horizontal line indicates the maximum achievable LCR (total inactivation).

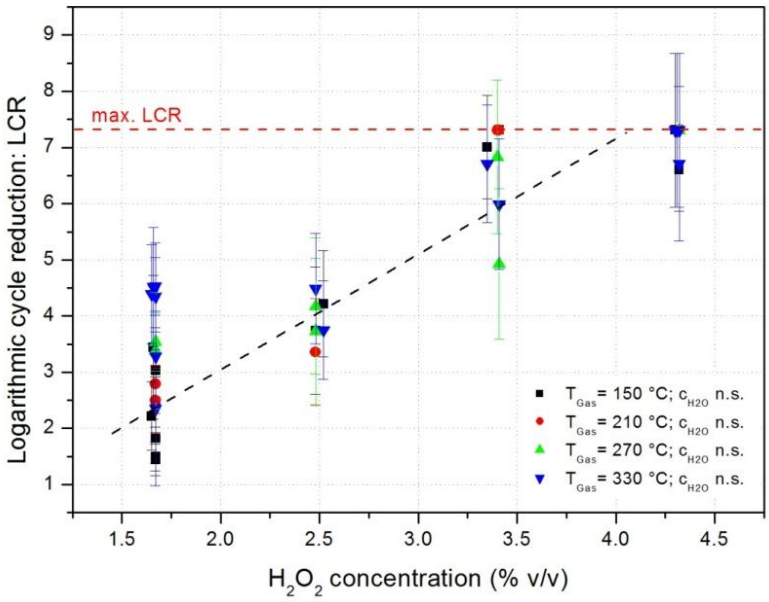


**Figure 5.2:** Logarithmic cycle reduction (LCR) obtained for all 49 measurement points, plotted vs. the hydrogen peroxide concentration ($c_{H2O2}$). Values of gas temperature ($T_{Gas}$) are given by colours (see figure legend) and values of the humidity ($c_{H2O}$) (not specified in the figure) varied between 15.1 and 22.6% v/v, see Fig. 5.1.

In a first approximation, the LCR seems to be increasing linearly with the $H_2O_2$ concentration, whereas the gas temperature does not have much influence on the LCR. Particularly, this is the case for the measurement points with a $H_2O_2$ concentration higher than 2% v/v. For the lowest $H_2O_2$ concentration of 1.67% v/v, the values of the obtained LCR are further apart. To illustrate the linear dependency of the LCR at higher $H_2O_2$ concentrations, a straight line was fitted to the points. The linear dependency of the LCR at mainly higher $H_2O_2$

concentrations, regardless of the gas temperature and humidity, is also confirmed by the results of previous studies [13,15] (see **Chapter 3**).

In order to determine the influence of the gas temperature on the microbial inactivation more accurately, the obtained LCR values are compared to the temperature of the spore carrier, which corresponds to the temperature at the measurement point (MP). Figure 5.3 depicts the obtained LCR as a function of the gas temperature at the particular MP. The values of the respective $H_2O_2$ concentrations are given by colours (see legend of Fig. 5.3) and the values of humidity ($c_{H2O}$), for reasons of available dimensions, are not further specified (n.s.) in this plot.

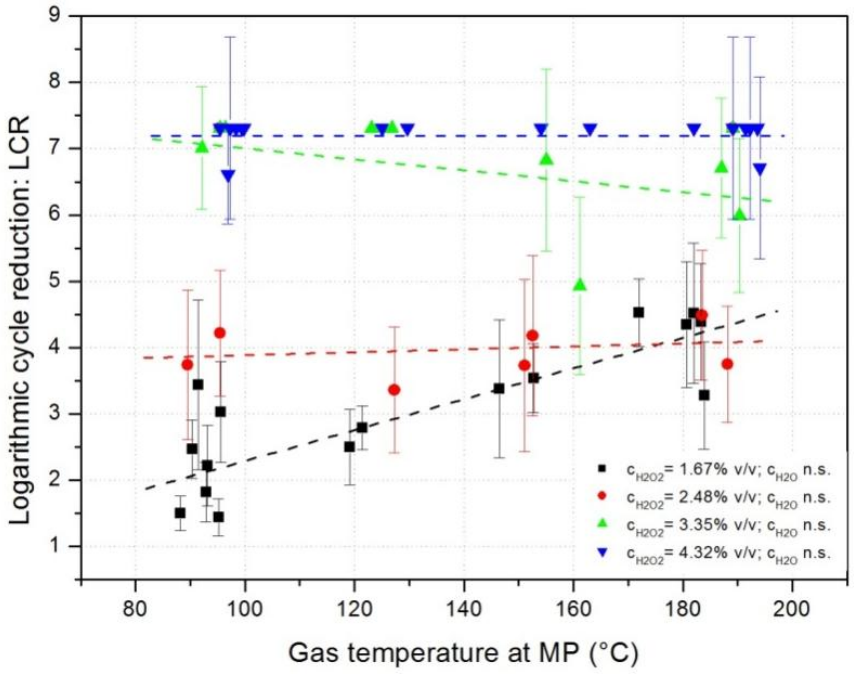


**Figure 5.3:** Logarithmic cycle reduction (LCR) vs. gas temperature at the measurement point (MP). Values of $c_{H2O2}$ are given by colours (see figure legend) and values of the humidity ($c_{H2O}$) (not specified in this figure) are indicated in Fig. 5.1.

For the lowest $H_2O_2$ concentration of 1.67% v/v, the LCR is increasing linearly with the temperature at the MP. At 2.48% v/v $H_2O_2$, the gas temperature at the MP has no influence on the LCR. In contrast, for the next higher value of $H_2O_2$ at 3.35% v/v, the LCR rather seems to be slightly decreasing towards higher temperatures, especially for temperatures above 150 °C at the MP. At the highest $H_2O_2$ concentration the maximum possible LCR was achieved for most of the samples. To illustrate the different temperature behaviour for the various $H_2O_2$ concentrations, straight lines were fitted to the data. It could be shown that predominantly at low $H_2O_2$ concentrations the LCR is affected by the gas temperature. An explanation for the decrease in the LCR towards higher temperatures at 3.35% v/v $H_2O_2$ might be that, at temperatures below its dew point of about 150 °C, condensation of hydrogen peroxide takes place on the spore carrier. The condensed $H_2O_2$ could thus affect the sample in a positive way by means of an extended contact time of the sterilising agent with the spores.
As has already been noted that the humidity only has a minor influence on the LCR, especially at elevated $H_2O_2$ concentrations, a detailed discussion on the influence of humidity on the LCR will focus on the microbiological tests that were carried out at the lowest $H_2O_2$ concentration of 1.67% v/v. Figure 5.4 shows the obtained LCR for different concentrations of water as a function of the gas temperature.

At the lowest gas temperatures of 150 and 210 °C, the obtained LCR values turn out different. Possibly, this is related to condensation effects at low gas temperatures, as discussed earlier. Likewise, Unger-Bimczok *et al.* [12] already found that low concentrations of $H_2O_2$ in combination with a high level of humidity feature a noticeably higher potential of sporicidal inactivation. They also attribute this effect to micro-condensation of $H_2O_2$ on the spore carriers. In the further course, the LCR seems to be increasing together with the gas temperature, independently of the concentration of water. Solely, for a combination of 22.6% v/v $H_2O$ and 1.67% v/v $H_2O_2$, this corresponds to a highly dilute aqueous solution of hydrogen peroxide, the LCR is considerably lower and divergent compared to the other samples at the highest gas temperature of 330 °C. However, because of the low data density and high variance, this effect can only be described phenomenologically.

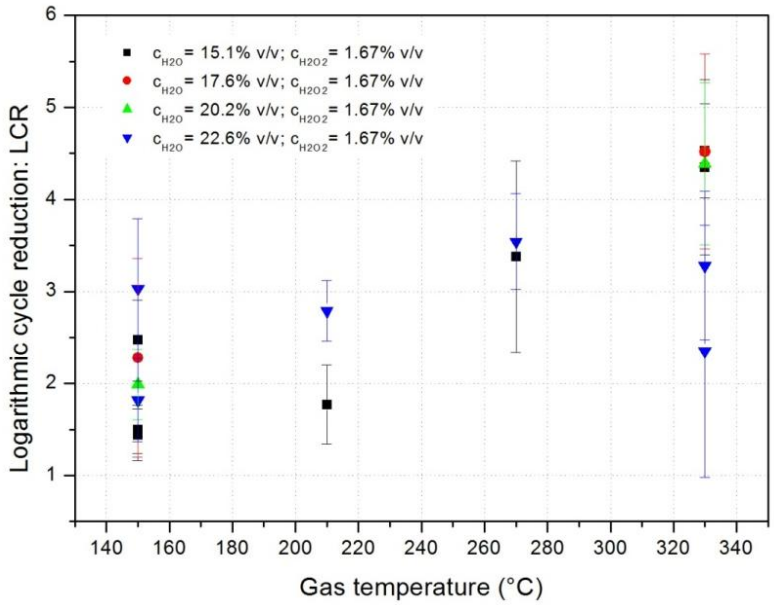


**Figure 5.4:** Logarithmic cycle reduction (LCR) vs. gas temperature at a constant $H_2O_2$ concentration of 1.67% v/v. Values of $c_{H2O}$ are given by colours (see figure legend).

In summary, the microbiological tests demonstrated that, for concentrations of $H_2O_2$ above 2% v/v, the LCR is mainly dependent on the hydrogen peroxide concentration in the gaseous phase. The humidity and gas temperature only play a minor role at elevated $H_2O_2$ concentrations but gain in importance at $H_2O_2$ concentrations below 2% v/v. In this context, it could be shown that the LCR was significantly rising with the gas temperature at the lowest $H_2O_2$ concentration of 1.67% v/v. On the other hand, it was found that highly diluted solutions of hydrogen peroxide (<15% w/w) in combination with high gas temperatures, fairly above the dew point of $H_2O_2$, seem to be less appropriate as a sterilant for vapour-phase sterilisation, since the LCR was lowest and showed the highest variance for this particular combination.

### 5.4.2 Sensors

#### 5.4.2.1 Calorimetric $H_2O_2$ sensor

The measurement data of the calorimetric $H_2O_2$ sensor from the calibration experiment is depicted in Figure 5.5. Therefore, the temperature difference (ΔT)

is plotted vs. the $H_2O_2$ concentration for each one of the measurement points of the calibration experiment. The values of the respective gas temperature are given by colours (see legend of Fig. 5.5). The values of humidity ($c_{H2O}$) varied between 15.1 and 22.6% v/v, but are not further specified (n.s.) for each individual data point in this plot. The dashed lines were fitted to the data, in order to illustrate the linear sensor behaviour.

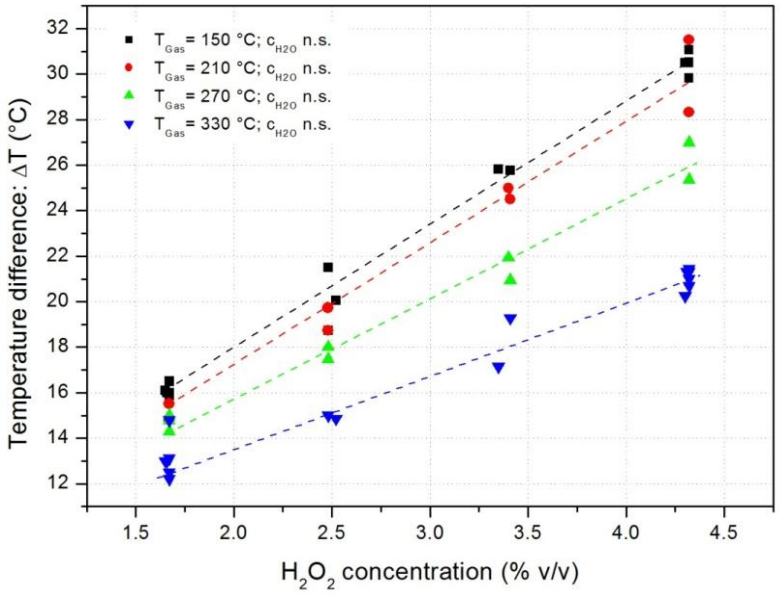


**Figure 5.5:** Resulting temperature difference (ΔT) of the calorimetric $H_2O_2$ sensor obtained for all 49 measurement points, plotted vs. the hydrogen peroxide concentration ($c_{H2O2}$). Values of gas temperature ($T_{Gas}$) are given by colours (see figure legend) and values of the humidity ($c_{H2O}$) (not specified in the figure) varied between 15.1 and 22.6% v/v, see Fig. 5.1.

The response of the $H_2O_2$ sensor is linear for each set of measurement points at a specific gas temperature ($T_{Gas}$), regardless of the level of humidity [$c_{H2O}$]. On the other hand, the sensor has a strong dependence on the gas temperature. In fact, the same behaviour has been found in previous measurements [20]. This phenomenon may be explained by the expansion of the carrier gas with increasing temperature. Assuming constant pressure in the measuring chamber, the volume increases proportional to the gas temperature. At the same time, the

number density of $H_2O_2$ molecules in the gas stream decreases, thus lowering the rate of a reaction at the sensor surface. To overcome this problem, a temperature compensation of the sensor signal can be done. For this purpose, the temperature behaviour of the sensor must be considered in more detail. Therefore, the obtained temperature differences (ΔT) for each one of the four $H_2O_2$ concentrations have been normalised to the temperature difference at the lowest gas temperature of 150 °C. The normalised sensor signal ($\Delta T/\Delta T_{150}$) is then compared to the true gas temperature at the sensor, which corresponds to the signal of the passivated temperature sensor (reference temperature). The normalised sensor signals plotted vs. the reference temperature ($T_{ref}$) are depicted in Figure 5.6.

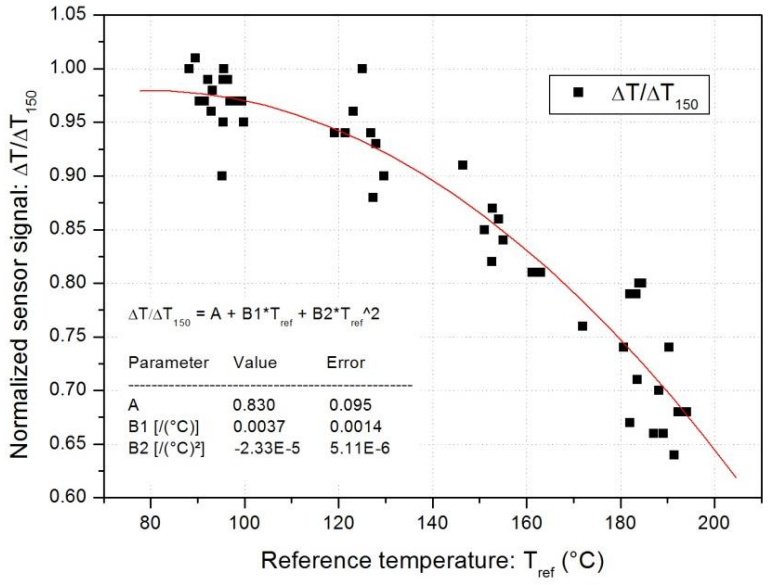


**Figure 5.6:** Normalised sensor signal ($\Delta T/\Delta T_{150}$) of the $H_2O_2$ sensor vs. the reference temperature ($T_{ref}$).

The temperature behaviour of the $H_2O_2$ sensor can be described in good approximation by a second order polynomial regression model according to Equation 5.1:

$$\Delta T/\Delta T_{150} = A + B_1 * T_{ref} + B_2 * T_{ref}^2 \qquad (5.1)$$

With the values for $A$ = 0.83, $B_1$ = 3.7*10$^{-3}$ [/(°C)] and $B_2$ = -2.33*10$^{-5}$ [/(°C)²]. The temperature compensated sensor signal of the $H_2O_2$ sensor ($\Delta T_{comp}$) can now be calculated according to Equation 5.2:

$$\Delta T_{comp} = \Delta T/(\Delta T/\Delta T_{150}) \quad (5.2)$$

The obtained data of the $H_2O_2$ sensor after applying the compensation model is shown in Figure 5.7.

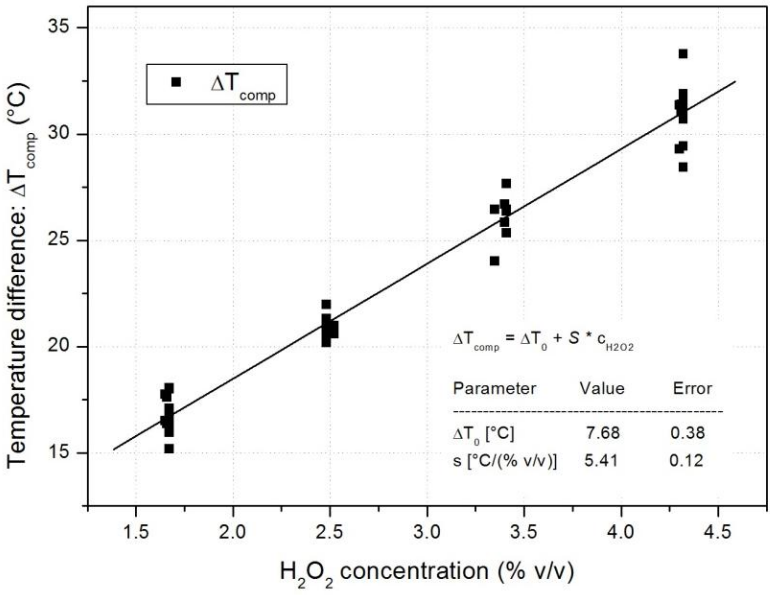


**Figure 5.7:** Compensated sensor signal ($\Delta T_{comp}$) of the $H_2O_2$ sensor vs. the $H_2O_2$ concentration.

The compensated temperature difference ($\Delta T_{comp}$) can be described by a linear model as a function of the $H_2O_2$ concentration according to Equation 5.3:

$$\Delta T_{comp} = \Delta T_0 + S * c_{H2O2} \quad (5.3)$$

Wherein, $\Delta T_0$ corresponds to the sensor's off-set, which amounts to 7.68 °C, $S$ corresponds to the sensor's sensitivity of 5.41 °C/(% v/v) and $c_{H2O2}$ is the hydrogen peroxide concentration in gaseous phase.

In summary, it could be demonstrated that the $H_2O_2$ sensor exhibits a high specificity with respect to the detection of $H_2O_2$ when compared to $H_2O$. The temperature-dependent sensor behaviour can be compensated by a model that takes into account the reference temperature ($T_{ref}$) of the sensor. This way, the $H_2O_2$ sensor can be used over a wide gas temperature range from 150 to 330 °C.

5.4.2.2 Commercially available gas sensors

At this point, exemplarily for the four commercially available metal-oxide semiconductor gas sensors in test, the sensor GGS 5333 T from the Company *UST Umweltsensortechnik GmbH* shall be discussed in detail, because it will later be used for a correlation analysis to the microbicidal effectiveness. More information on the characteristics of the other metal-oxide semiconductor gas sensors and the electrochemical $O_2$ sensor can be found in previous publications of the authors [13,14].

Similar to the $H_2O_2$ sensor, the characteristics of the GGS 5333 T in terms of sensitivity and specificity towards the considered influencing factors of the sterilisation, namely the hydrogen peroxide concentration ($c_{H2O2}$), the humidity ($c_{H2O}$) and gas temperature ($T_{Gas}$), will be presented. In order to investigate the response of the GGS 5333 T upon the exposure of $H_2O_2$, exemplarily the measured data for different $H_2O_2$ concentrations but constant conditions in terms of humidity ($c_{H2O}$ = 15.1 %v/v) and gas temperature ($T_{Gas}$ = 150 °C) will be shown. Figure 5.8 depicts the calibration plot of the GGS 5333 T for different hydrogen peroxide concentrations. The represented sensor signal of the GGS 5333 T sensor in presence of $H_2O_2$ ($R/R0_{GGS,H2O2}$) was normalised to the resistance value in ambient air ($R_0$). The GGS 5333 T exhibits a linear relationship between its resistance and the $H_2O_2$ concentration. Its characteristic can be described by a linear function according to Equation 5.4:

$$R/R0_{GGS,H2O2} = R/R0_{GGS,0} + S_{GGS,H2O2} * c_{H2O2} \quad (5.4)$$

Here, $R/R0_{GGS,0}$ corresponds to the sensor's off-set, which is equal to 0.687 and $S_{GGS,H2O2}$ corresponds to the sensor's sensitivity towards $H_2O_2$, which is equal to -0.046 (% v/v)$^{-1}$.

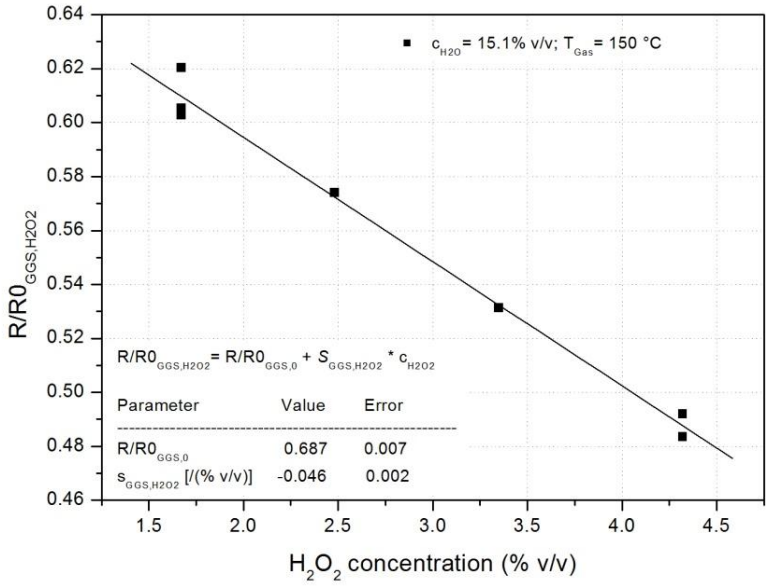


**Figure 5.8:** Calibration plot of the sensor GGS 5333 T for different $H_2O_2$ concentrations at constant conditions of humidity (15.1% v/v) and gas temperature (150 °C).

The sensitivity of the GGS 5333 T sensor towards water will be investigated using the data for constant conditions of $H_2O_2$ concentration ($c_{H2O2}$ = 1.67% v/v) and gas temperature ($T_{Gas}$ = 150 °C). Again, the normalised resistance values will be analysed. Figure 5.9 depicts the calibration plot of the GGS 5333 T for different concentrations of water at constant $H_2O_2$ concentration and gas temperature.

The characteristic of the GGS 5333 T as a function of the $H_2O$ concentration in presence of $H_2O_2$ can be described by a linear function according to Equation 5.5:

$$R/R0_{GGS,H2O} = R/R0_{GGS,0} + S_{GGS,H2O} * c_{H2O} \quad (5.5)$$

Here, $R/R0_{GGS,0}$ corresponds to the sensor's off-set, which is equal to 0.708 and $S_{GGS,H2O}$ corresponds to the sensor's sensitivity towards $H_2O$, which is equal to -0.007 (% v/v)$^{-1}$. The latter one is about 7 times lower as compared to the sensors sensitivity towards $H_2O_2$ ($S_{GGS,H2O2}$).

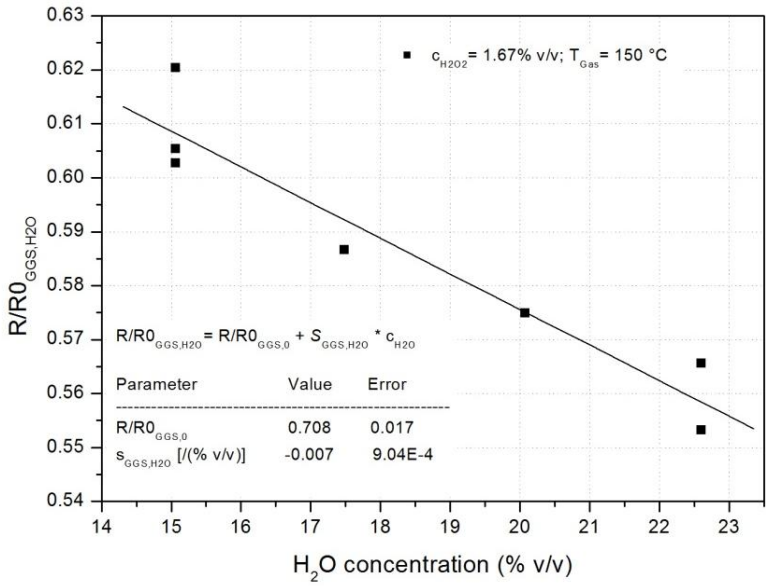


**Figure 5.9:** Calibration plot of the sensor GGS 5333 T for different $H_2O$ concentrations at constant conditions of $H_2O_2$ concentration ($c_{H2O2}$ = 1.67% v/v) and gas temperature ($T_{Gas}$ = 150 °C).

As the GGS 5333 T is operated with a constant heating voltage, the sensors temperature is subject to changes of the gas temperature. Since the temperature of a metal-oxide semiconductor also has an influence on its resistance, the temperature-dependent behaviour of the GGS 5333 T has been determined. Therefore, the data set at constant conditions in terms of $H_2O_2$ concentration ($c_{H2O2}$ = 1.67% v/v) and humidity ($c_{H2O}$ = 15.1% v/v) is analysed. Figure 5.10 shows the normalised resistance values of the GGS 5333 T at constant conditions in terms of $c_{H2O2}$ and $c_{H2O}$ plotted vs. the gas temperature ($T_{Gas}$). In the considered range, the temperature behaviour of the GGS 5333 T can be described by a linear function according to Equation 5.6:

$$R/R0_{GGS,TGas} = R/R0_{GGS,O} + S_{GGS,TGas} * T_{Gas} \quad (5.6)$$

Here, $R/R0_{GGS,0}$ corresponds to the sensor's off-set, which amounts to 0.717 and $S_{GGS,TGas}$ corresponds to the sensor's sensitivity towards the gas temperature, which amounts to $-7{,}31*10^{-4}$ $(°C)^{-1}$. It can be deduced from the values of

$S_{GGS,TGas}$ and $S_{GGS,H2O2}$ that raising the gas temperature by about 63 °C would cause the same change in the sensor signal as an increase of the $H_2O_2$ concentration by 1% v/v.

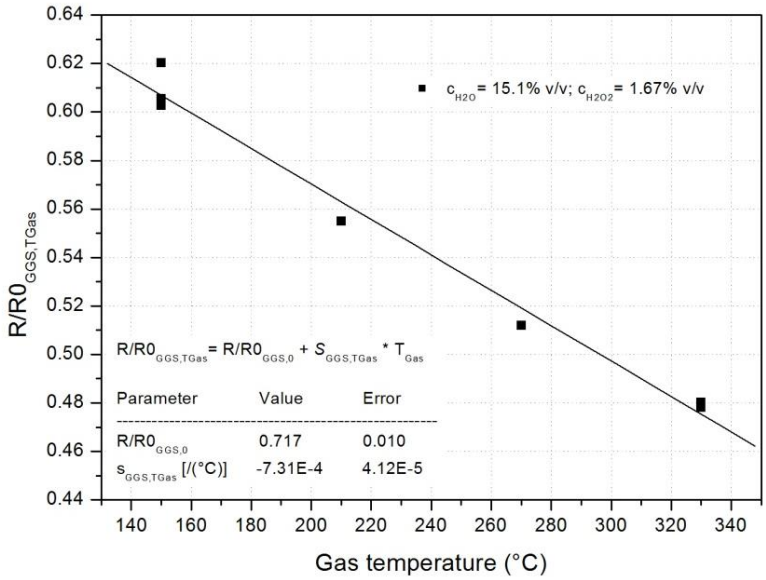


**Figure 5.10:** Temperature behaviour of the sensor GGS 5333 T at constant conditions of $H_2O_2$ concentration ($c_{H2O2}$ = 1.67% v/v) and humidity ($c_{H2O2}$ = 15.1% v/v).

In conclusion, the GGS 5333 T sensor showed a linear correlation between its resistance and the $H_2O_2$ concentration. This is equally true for the $H_2O$ concentration and gas temperature. Whereas the sensor response to $H_2O_2$ is much stronger compared to the influence of humidity, the variation of the gas temperature between 150 and 330 °C approximately caused the same changes in the sensor signal of the GGS 5333 T, like the variation of the $H_2O_2$ concentration in the considered range.

5.4.2.3 Summary of the sensor characterisation

In the following, all gas sensors that had been analysed in this experiment will be compared to each other with respect to their sensitivity, specificity and short-term stability. In order to ensure a comparability of the different types of sensors, the sensitivities and specificities will be compared in a qualitative

manner. The characteristics of all gas sensors in test and information on the type of sensor and heating mode are overviewed in Table 5.3.

**Table 5.3:** Overview of the characteristics of the sensors in test with respect to their sensitivities towards hydrogen peroxide ($S_{H2O2}$), humidity ($S_{H2O}$) and gas temperature ($S_{TGas}$), their specificity and short-term stability.

| | $H_2O_2$-sensor | TGS 816 | TGS 823 | GGS 5333 T | GGS 6333 T | SO A0 250 |
|---|---|---|---|---|---|---|
| Type of sensor * | calorimetric | MOX | MOX | MOX | MOX | Electro-chemical $O_2$ sensor |
| Heating mode ** | n.h. | $U_{const}$ | $U_{const}$ | $U_{const}$ | $T_{const}$ | $T_{const}$ |
| $S_{H2O2}$ *** | ++ | ++ | ++ | ++ | ++ | + |
| $S_{H2O}$ *** | 0 | + | + | + | + | + |
| $S_{TGas}$ *** | + | + | ++ | ++ | 0 | 0 |
| Specificity *** | ++ | + | - | - | + | 0 |
| short-term stability (% of span) | 3% | 3% | 4% | 5% | 7% | 1% |

* MOX = metal-oxide semiconductor

** n.h. = not heated; $U_{const}$ = constant voltage; $T_{const}$ = constant operating temperature

*** ++ = high; + = mid; - = low; 0 = none

With exception of the electrochemical sensor SO A0 250, all sensors in test exhibited a significantly higher sensitivity towards $H_2O_2$ as compared to $H_2O$. In fact, the calorimetric $H_2O_2$ sensor is not sensitive to $H_2O$ and exhibited the highest specificity of all sensors in test with respect to the $H_2O_2$ concentration. It has been shown that all sensors that are either operated unheated or in a constant voltage mode, showed a dependency on the gas temperature. The

sensors GGS 6333 T and SO A0 250, which were operated in a constant temperature mode, did not respond to changes of the gas temperature. Regarding the specificity of the MOX sensors, the TGS 816 and GGS 6333 T exhibit a higher specificity towards $H_2O_2$ as compared to the other two, since they were less sensitive to changes of the gas temperature. The short-term stability of the sensors was determined by comparing the repeatedly measured values at the vertex points of the calibration experiment (see Fig. 5.1). Therefore, the differences of the measured values for each of these points were divided by the span (difference between the highest and the lowest value found during the calibration experiment) and multiplied by 100. The indicated short-term stability corresponds to an average value of all vertex points that have been determined over a measurement period of about 20 hours, spread over three days. Basically, all sensors feature an acceptable short-term stability, except for the GGS 6333 T, for which it was higher than 5%. Although the SO A0 250 was the most stable sensor of all, it did not provide a sufficient sensitivity and specificity for the envisaged application.

### 5.4.3 Correlation model

In order to establish a correlation model between the response of the gas sensors and the LCR, the data of the calibration experiment will be considered. In a first instance, the inactivation kinetics of gaseous hydrogen peroxide on *Bacillus atrophaeus* spores has been studied and the impact of three influencing factors, namely the $H_2O_2$ concentration, humidity and gas temperature, on the microbial inactivation was analysed in detail. One possibility for establishing a correlation is to compare the results by reference to the parametric process variables. Thus, for example, it was shown that for $H_2O_2$ concentrations above 2% v/v the LCR was increasing linearly with the $H_2O_2$ concentration, regardless of the gas temperature or humidity. On the other hand, the $H_2O_2$ concentration can be determined accurately by means of the calorimetric $H_2O_2$ sensor. In this way, a correlation between the signal of the calorimetric gas sensor and the LCR may be established. Recently, Kirchner *et al.* correlated the LCR of *B. atrophaeus* to the signals of a thin-film calorimetric gas sensor that was built-up on a polyimide foil [15]. However, this comparison was done for mainly higher $H_2O_2$ concentrations, a lower number of measurement points and with less statistical significance. Additionally, other than in the older works [15], the

temperature-compensation model will now be considered for the following comparison. Figure 5.11 shows the compensated signals of the $H_2O_2$ sensor ($\Delta T_{comp}$) that were matched to the achieved LCR for each one of the 49 measurement points of the calibration experiment.

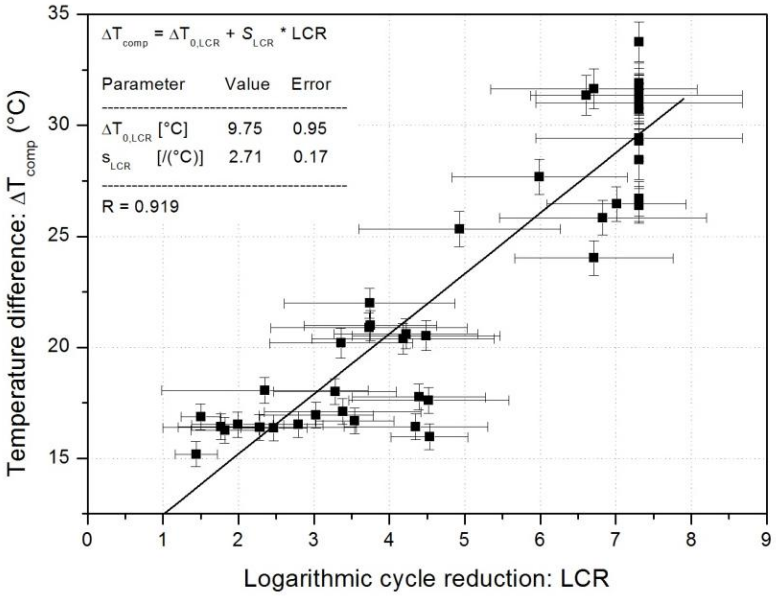


**Figure 5.11:** Compensated signal of the $H_2O_2$ sensor ($\Delta T_{comp}$) plotted vs. the achieved LCR for each one of the measurement points of the calibration experiment.

A linear regression model was applied to the data shown in Fig. 5.11, which can be described by Equation 5.7:

$$\Delta T_{comp} = \Delta T_{0,LCR} + S_{LCR} * LCR \tag{5.7}$$

Here, $\Delta T_{0,LCR}$ is the offset, which amounts to 9.75 °C and $S_{LCR}$ is the sensitivity, which is 2.71 $(°C)^{-1}$. The Pearson´s correlation coefficient (R) obtained from the linear regression is equal to 0.9019, which in turn suggests a good correlation of the data. The proposed model fits fairly well to the data points above $\Delta T_{comp}$ = 20 °C. However, the scatter of the data points below this value is quite large, so this model seems no longer sufficient for values below $\Delta T_{comp}$ = 20 °C. This is

partly a result of the fact that, at low $H_2O_2$ concentrations, not only the concentration of hydrogen peroxide, but also the humidity and the temperature have a strong influence on the microbial inactivation. With regard to the temperature effect at low concentrations of $H_2O_2$, the proposed model could be optimised on the basis of the relationship found between the LCR and the gas temperature at the measuring point (see Fig. 5.3). However, the effect of humidity on the LCR will not be taken into account in this case, as the $H_2O_2$ sensor is not able to detect the humidity.

Since three of the investigated metal-oxide semiconductor gas sensors, in addition to $H_2O_2$ responded on the $H_2O$ concentration and the gas temperature, it was examined whether a direct correlation between the sensor signals and the LCR could be established, in particular for the measurement points with a $H_2O_2$ concentration below 2% v/v. It was found that, in case of the GGS 5333 T and the TGS 823, a linear correlation between the sensor signals and the obtained logarithmic cycle reduction could be established. The corresponding graphs are shown in Figure 5.12 a), in case of the GGS 5333 T and in Figure 5.12 b) for the TGS 823 sensor.

The relationship between the normalised sensor signal and the achieved LCR could, in case of both sensors, be described by a linear function as given by Equation 5.8:

$$R/R0_{x,LCR} = R/R0_{x,0LCR} + S_{x,LCR} * LCR \tag{5.8}$$

Herein, x stands for the respective sensor model, $R/R0_{x,0LCR}$ corresponds to the sensors off-set at 0 LCR and $S_{x,LCR}$ corresponds to the sensor's sensitivity towards the logarithmic cycle reduction. The exact values of the sensor parameters can be obtained from Figure 5.12. The Pearson´s correlation coefficients (R) of the GGS 5333 T and the TGS 823 from the linear regression were equal to -0.922 and -0.921, respectively. Thus, it can be stated that, in the considered range, there is a linear correlation between the sensor signals and the logarithmic cycle reduction for $H_2O_2$ concentrations below 2% v/v.

The correlation analysis has been done for each one of the sensors in test. Here, again the sensitivity with respect to the achieved LCR at low (<2% v/v) and high (>2% v/v) concentrations of $H_2O_2$ ($c_{H2O2}$) has been considered. The sensitivities

of all gas sensors and information on the sensor type and heating mode are overviewed in Table 5.4. Again, the characteristics of the sensors have been assessed in a qualitative manner.

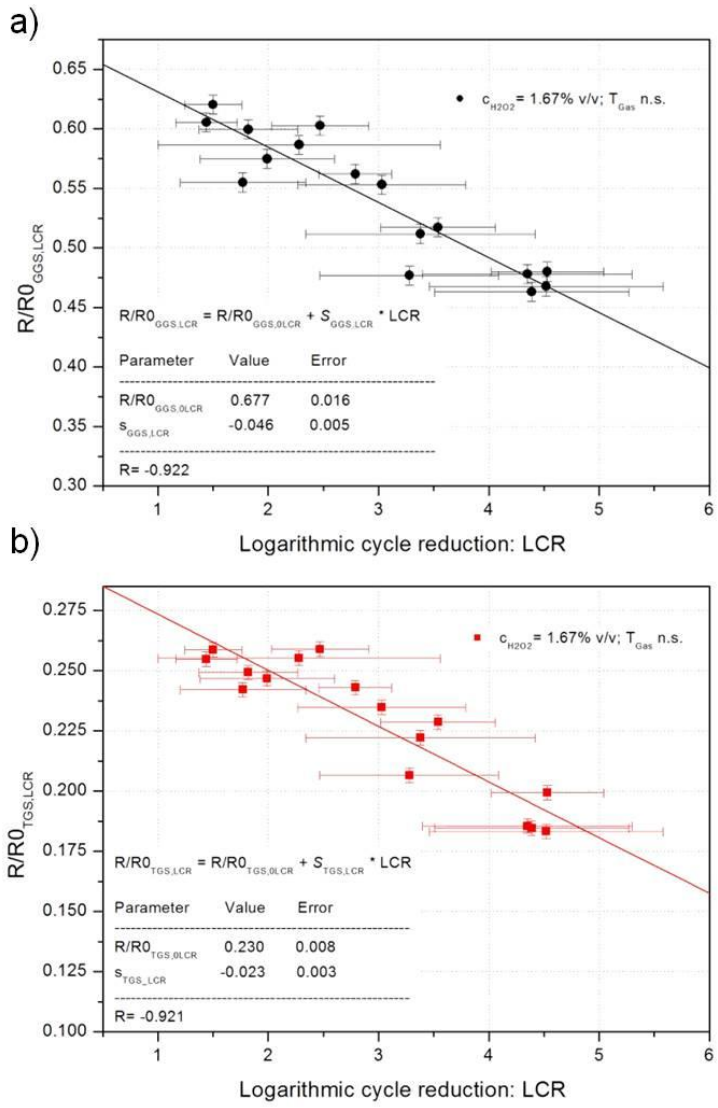


**Figure 5.12:** Correlation between sensor response and achieved logarithmic cycle reduction (LCR) for the measurement points with a $H_2O_2$ concentration of 1.67% v/v, in case of the MOX sensors GGS 5333 T a), and the TGS 823 b).

It has been found that, in the considered range, the determination of the LCR on the basis of the sensors is feasible. Especially, this holds for $H_2O_2$ concentrations higher than 2% v/v in case of the calorimetric $H_2O_2$ sensor and for concentrations of $H_2O_2$ lower than 2% v/v in case of the metal-oxide semiconductor gas sensors GGS 5333 T and TGS 823.

**Table 5.4:** Overview of the characteristics of the sensors in test with respect to their sensitivities ($s_{LCR}$) towards the logarithmic cycle reduction (LCR), once for low (<2% v/v) and once for high (>2% v/v) concentrations of $H_2O_2$.

| | $H_2O_2$-sensor | TGS 816 | TGS 823 | GGS 5333 T | GGS 6333 T | SO A0 250 |
|---|---|---|---|---|---|---|
| Type of sensor * | calorimetric | MOX | MOX | MOX | MOX | Electro-chemical $O_2$ sensor |
| Heating mode ** | n.h. | $U_{const}$ | $U_{const}$ | $U_{const}$ | $T_{const}$ | $T_{const}$ |
| $S_{LCR}$ @ low $c_{H2O2}$ *** | + | - | ++ | ++ | - | 0 |
| $S_{LCR}$ @ high $c_{H2O2}$ *** | ++ | - | - | - | - | 0 |

* MOX = metal-oxide semiconductor

** n.h. = not heated; $U_{const}$ = constant voltage; $T_{const}$ = constant operating temperature

*** ++ = high; + = mid; - = low; 0 = none

### 5.5 Conclusions

The evaluation of the sterilisation process employing gaseous hydrogen peroxide by means of logarithmic cycle reduction tests with *Bacillus atrophaeus* spores demonstrated that the microbicidal effectiveness predominantly is dependent on the $H_2O_2$ concentration deployed, particularly for $H_2O_2$ concentrations above 2% v/v. Such behaviour has already been discussed in earlier studies [13–15]. For $H_2O_2$ concentrations below 2% v/v, the influence of the gas temperature and

the humidity become more important. Thus, it was disclosed that the inactivation of *B. atrophaeus* at a $H_2O_2$ concentration of 1.67% v/v was linearly increasing with the gas temperature. Furthermore, it turned out that for gas temperatures below the dew point of $H_2O_2$, the inactivation of the spores was considerably increased due to condensation of $H_2O_2$ on the spore carrier. An influence by the humidity of the sterilising gas could only be found at the lowest $H_2O_2$ concentration of 1.67% v/v. Lower concentrated aqueous solutions of $H_2O_2$, i.e., 15% w/w, as compared to more concentrated solutions, i.e., 35% w/w, but same concentration of hydrogen peroxide in gaseous phase, were assigned a lower LCR at elevated gas temperatures above the dew point of $H_2O_2$. However, this effect could only be described phenomenologically. In addition, multiple types of gas sensors have been assessed on their capability to measure the microbicidal effectiveness of the sterilising gas by correlating their sensor response to the obtained LCR for each one of the measurement points. It was demonstrated that, after applying a temperature-compensation model, the microbicidal effectiveness at $H_2O_2$ concentrations above 2% v/v could directly be determined by means of the calorimetric $H_2O_2$ sensor. In the lower concentration range (<2% v/v), a good correlation was found for the two metal-oxide semiconductor gas sensors GGS 5333 T and TGS 823, respectively. In contrast to microbiological spore tests, gas sensors enable a fast monitoring in real-time. In conclusion, the presented multi-sensor system in combination with the proposed correlation models represents a useful tool for the evaluation of the biocidal effectiveness of aseptic sterilisation processes employing gaseous $H_2O_2$.

**5.6 References**

[1] J.D. Floros, R. Newsome, W. Fisher, Feeding the world today and tomorrow: The importance of food science and technology, Comprehensive Reviews in Food Science and Food Safety 9 (2010) 572–599.

[2] B.A.H. von Bockelmann, I.L.I. von Bockelmann, Aseptic packaging of liquid food products: A literature review, Journal of Agricultural and Food Chemistry. 34 (1986) 384–392.

[3] G. McDonnel, A.D. Russell, Antiseptics and disinfectants: Activity, action, and resistance, Clinical Microbiology Reviews 12 (1999) 147–179.

[4] G. McDonnell, Peroxygens and other forms of oxygen: Their use for effective cleaning, disinfection, and sterilization, in: P.C. Zhu (Ed.), New Biocides Development, American Chemical Society, Washington, DC, 2007, pp. 292–308.

[5] G. Cerny, Testing of aseptic machines for efficiency of sterilization of packaging materials by means of hydrogen peroxide, Packaging Technology Science 5 (1992) 77–81.

[6] J. Wang, R. Toledo, Sporicidal properties of mixtures of hydrogen peroxide vapor and hot air, Food Technology 40 (1986) 62–67.

[7] N.A. Klapes, D. Vesley, Vapor-phase hydrogen peroxide as a surface decontaminant and sterilant, Applied Environmental Microbiology 56 (1990) 503–506.

[8] R. Toniolo, P. Geatti, G. Bontempelli, G. Schiavon, Amperometric monitoring of hydrogen peroxide in workplace atmospheres by electrodes supported on ion-exchange membranes, Journal of Electroanalytical Chemistry 514 (2001) 123–128.

[9] R.A. Heckert, M. Best, L.T. Jordan, G.C. Dulac, D.L. Eddington, W.G. Sterritt, Efficacy of vaporized hydrogen peroxide against exotic animal viruses, Applied Environmental Microbiology 63 (1997) 3916–3918.

[10] M. Kokubo, T. Inoue, J. Akers, Resistance of common environmental spores of the genus *Bacillus* to vapor hydrogen peroxide, PDA Journal of Pharmaceutical Science and Technology 5 (1998) 228–231.

[11] Verband Deutscher Maschinen- und Anlagenbau e.V., Code of Practice: Filling Machines of VDMA Hygiene Class V: Testing the effectiveness of packaging sterilization devices, Frankfurt, 2008.

[12] B. Unger-Bimczok, V. Kottke, C. Hertel, J. Rauschnabel, The influence of humidity, hydrogen peroxide concentration, and condensation on the inactivation of *Geobacillus stearothermophilus* spores with hydrogen peroxide vapor, Journal of Pharmaceutical Innovation 3 (2008) 123–133.

[13] S. Reisert, H. Geissler, R. Flörke, N. Näther, P. Wagner, M.J. Schöning, Towards a multi-sensor system for the evaluation of aseptic processes employing hydrogen peroxide vapour ($H_2O_2$), Physica Status Solidi (a) 208 (2011) 1351–1356.

[14] S. Reisert, H. Geissler, R. Flörke, C. Weiler, P. Wagner, M.J. Schöning, Characterization of aseptic sterilization processes using an electronic nose, International Journal of Nanotechnology 10 (2012) 470–484.

[15] P. Kirchner, J. Oberländer, H.-P. Suso, G. Rysstad, M. Keusgen, M.J. Schöning, Monitoring the microbicidal effectiveness of gaseous hydrogen peroxide in sterilisation processes by means of a calorimetric gas sensor, Food Control 31 (2013) 530–538.

[16] C. Forney, R. Rij, R. Denis-Arrue, J. Smilanick, Vapor phase hydrogen peroxide inhibits postharvest decay of table grapes, HortScience: A publication of the American Society for Horticultural Science 1991 (12) 1512–1514.

[17] P. Kirchner, Y.A. Ng, H. Spelthahn, A. Schneider, H. Henkel, P. Friedrich, J. Kolstad, J. Berger, M. Keusgen, M.J. Schöning, Gas sensor investigation based on a catalytically activated thin-film thermopile for $H_2O_2$ detection, Physica Status Solidi (a) 207 (2010) 787–792.

[18] N. Näther, L.M. Juárez, R. Emmerich, J. Berger, P. Friedrich, M.J. Schöning, Detection of hydrogen peroxide ($H_2O_2$) at exposed temperatures for industrial processes, Sensors 6 (2006) 308–317. S.

[19] S. Reisert, H. Geissler, R. Flörke, P. Wagner, T. Wagner, M.J. Schöning, Controlling aseptic sterilization processes by means of a multi-sensor system, Proceedings of the IEEE SSCI (CompSens) (2011) 18–22.

[20] S. Reisert, H. Henkel, A. Schneider, D. Schäfer, P. Friedrich, J. Berger, M.J. Schöning, Development of a handheld sensor system system for the online measurement of hydrogen peroxide in aseptic filling systems, Physica Status Solidi (a) 207 (2010) 913–918.

[21] P. Kirchner, S. Reisert, M. Schöning, Calorimetric gas sensors for hydrogen peroxide monitoring in aseptic food processes, Springer, Heidelberg, *in press*, DOI 10.1007/5346_2013_51.

[22] C.F. Cardoso, J.A.F. Faria, E.H. Miranda Walter, Modeling of sporicidal effect of hydrogen peroxide in the sterilization of low density polyethylene film inoculated with *Bacillus subtilis* spores, Food Control 22 (2011) 1559–1564.

# Chapter 6

## Multi-sensor chip for the investigation of different types of metal oxides for the detection of $H_2O_2$ in the ppm range

Physica Status Solidi (a), 2013, Vol. 210, pp. 898-904

Steffen Reisert[1], Benno Schneider[1], Hanno Geissler[2], Matthias van Gompel[3], Patrick Wagner[3] and Michael J. Schöning[1,4]

1) Institute of Nano and Biotechnologies, FH Aachen, 52428 Jülich, Germany

2) SIG Combibloc Systems GmbH, 52441 Linnich, Germany

3) Institute for Materials Research, Hasselt University, 3590 Diepenbeek, Belgium

4) Peter Grünberg Institute, Research Centre Jülich GmbH, 52425 Jülich, Germany

### 6.1 Abstract

In this work, a multi-sensor chip for the investigation of the sensing properties of different types of metal oxides towards hydrogen peroxide in the ppm range is presented. The fabrication process and physical characterisation of the multi-sensor chip are described. Pure $SnO_2$ and $WO_3$ as well as Pd- and Pt-doped $SnO_2$ films are characterized in terms of their sensitivity to $H_2O_2$. The sensing films have been prepared by drop-coating of water-dispensed nano-powders. A physical characterisation, including SEM and XRD of the deposited metal-oxide films, was performed. From the measurements in hydrogen peroxide atmosphere it could be shown, that all of the tested metal oxide films are suitable for the detection of $H_2O_2$ in the ppm range. The highest sensitivity and reproducibility was achieved using Pt-doped $SnO_2$.

## 6.2 Introduction

Hydrogen peroxide ($H_2O_2$) is a commonly used sterilising agent for carton packages in aseptic food filling processes. Due to its ability to decompose to water and oxygen it is advantageous compared to other chemical sterilisation agents in terms of environmental compatibility [1]. However, in view of its strong oxidising properties, special precautions with regard to the workplace security in the surrounding of sterilisation plants employing $H_2O_2$ as sterilising agent have to be taken into account, especially when applied in vapour phase. Therefore, the American Conference of Governmental Industrial Hygienists (ACGIH) has assigned hydrogen peroxide a threshold limit value (TLV) of 1 ppm. For monitoring the concentration in danger zones and in the workplace environment, electrochemical sensor systems from the German company *Dräger* (Lübeck, Germany) have been established. These monitoring systems typically cover a measuring range either in the lower (0-20 ppm) or in the upper (1000-7000) ppm range, but nothing in between or beyond that, nor are these operable under high flow conditions. With regard to the aseptic filling processes, there is a high demand for monitoring the $H_2O_2$ concentration in the exhaust air of such sterilisation plants, which typically is in the ppm concentration range, not only with respect to the TLV but also in terms of process monitoring.

Previous works have shown that calorimetric-type gas sensors are suitable for monitoring $H_2O_2$ concentrations in the range between 1-8% v/v [2-6]. This is equally true for commercially available metal-oxide semiconductor gas sensors [7]. While the lower limit of detection in case of the calorimetric gas sensors, which determine the exothermic energy due to a catalytic reaction, is in the range of approximately 5000 ppm, it is assumed that metal-oxide gas sensors respond at lower concentrations. Within the frame of this work, different types of metal oxides shall be investigated on their response to $H_2O_2$ in the range between 5 to 1000 ppm. Therefore, a multi-sensor chip, including four individually controllable sensor structures, based on a sapphire substrate with the size of 8 x 8 mm² has been developed. The four sensor structures have been prepared with different types of metal oxides. On one hand, two of the structures were prepared with pure tin oxide ($SnO_2$) and tungsten oxide ($WO_3$) films. On the other hand, two sensor structures have been prepared with

palladium- (Pd) and platinum black- (Pt) doped $SnO_2$, respectively. The doping of metal oxides with catalytically active species is a common strategy to enhance catalytical effects at the sensor surface, in order to increase the sensitivity and selectivity of semiconductor gas sensors for certain gas molecules [8-11]. Typical amounts of such a dopant are in the range between 0.1 to 2% w/w [12, 13].

## 6.3 Experimental

### 6.3.1 Sensor fabrication

The multi-sensor chip fabricated in this work contains four identical sensing structures on a sapphire substrate with a size of 8 x 8 mm². Sapphire was used as substrate due to its thermal properties. It has a lower thermal conductivity (Sapphire: 35 W/m·K @ 300 K) compared to common substrate materials, like silicon (Si: 148 W/m·K @ 300 K), for instance. A low thermal conductivity is beneficial for a thermal insulation between the individual sensing structures on the multi-sensor chip. Furthermore, it offers high chemical stability and good thermal shock properties. Each one of the sensing structure consists of an interdigitated electrode (IDE) and a heating element. The size of the heater is approximately 0.9 x 0.9 mm². A schematic of the sensor chip is shown in Fig. 6.1.

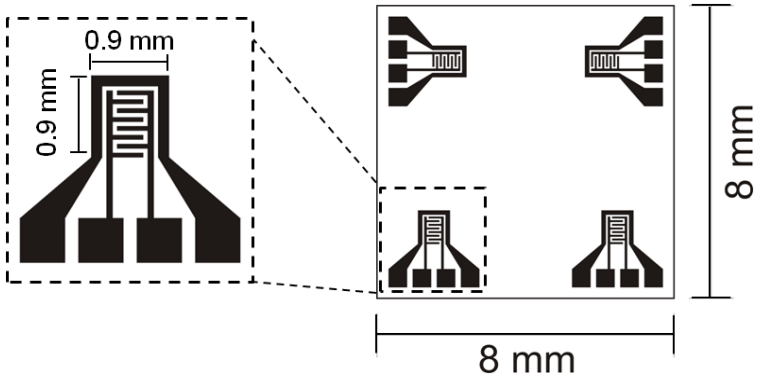


**Figure 6.1:** Schematic of the multi-sensor chip on a sapphire substrate, containing four sensing structures with embedded heater (outer structure) and interdigitated electrodes (inner structure).

The sensor chips were fabricated on a 3" sapphire wafer with a thickness of 430 ± 20 µm. The IDE and heating elements, which consist of 200 nm platinum (Pt) and a 20 nm titanium (Ti) adhesion layer, were deposited by thermal evaporation and patterned by a lift-off process. Subsequently, a 500 nm alumina ($Al_2O_3$) layer was deposited by E-beam evaporation as passivation. As a last step, the $Al_2O_3$ layer was patterned by chemical wet etching (Micropur, BOE 7:1, 9 minutes) [14] in order to uncover the contact pads and IDE.

6.3.2 Sensor preparation

On each of the four structures on the chip a sensitive metal-oxide film has been deposited. As sensitive materials, n-type tin(IV)-oxide ($SnO_2$) and tungsten(IV)-oxide ($WO_3$), respectively, were used. While two of the structures were prepared with pure $SnO_2$ and $WO_3$, the remaining two structures have been prepared with palladium- (Pd) and platinum black- (Pt) doped $SnO_2$, respectively. The metal oxides were available as nano-powder with a particle size smaller than 100 nm (Sigma Aldrich, Germany). 140 mg of the powders were dispersed in 1 ml distilled water [15], while the dispersions for the preparation of the Pd- and Pt-doped films contained 0.5% w/w of platinum black (<20 µm, Sigma Aldrich, Germany) and palladium (<1 µm, Sigma Aldrich, Germany) powder, respectively [16]. The composition of the different dispersions is summarised in Table 6.1.

**Table 6.1:** Composition of the dispersions used for the preparation of the sensing films.

| Spot | Metal oxide | Dopant | Dispensed in |
|---|---|---|---|
| 1 | $SnO_2$ (140 mg) | none | dest. water (1 ml) |
| 2 | $SnO_2$ (140 mg) | Pt (0.5% w/w) | dest. water (1 ml) |
| 3 | $SnO_2$ (140 mg) | Pd (0.5% w/w) | dest. water (1 ml) |
| 4 | $WO_3$ (140 mg) | none | dest. water (1 ml) |

The dispersions were drop-coated onto the sensor surface with a drop volume of 0.5 µl. Afterwards, the chip was heated up to approximately 320 °C in order to evaporate the water and to provide adhesion of the sensing layer. A calcination of the metal-oxide films at higher temperatures than 320 °C had to be avoided

due to the fact that the thin-film resistances suffered changes in their electrical properties, as will be discussed in more detail in **Section 6.3.3.3**. Nevertheless, it was shown in previous studies, that the catalytic activity of the dopants towards $H_2O_2$ is already activated at temperatures below 300 °C [4]. Fig. 6.2 a) provides an image of the sensor chip after the deposition of the semiconductor films. The order of the sensing films as they were deposited onto the substrate is shown in Fig. 6.2 b).

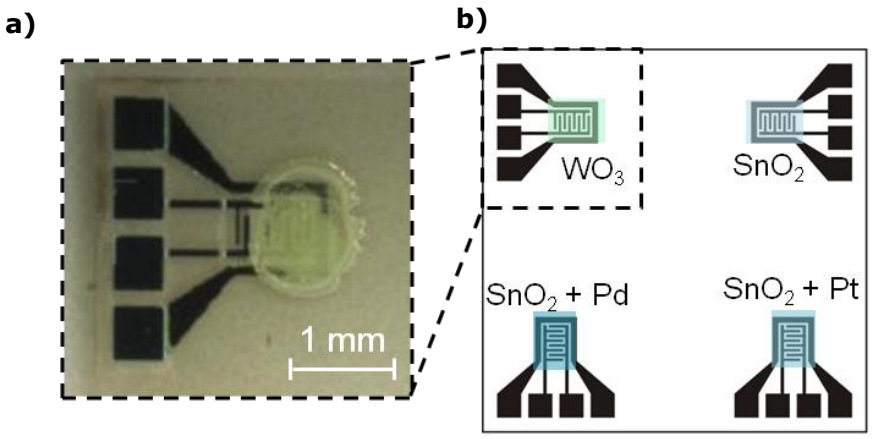


**Figure 6.2:** Microscopic image of the sapphire multi-sensor chip after the deposition of the sensing layers and schematic of the distribution of the sensing films on the chip.

## 6.3.3 Characterisation

### 6.3.3.1 XRD

Prior to the preparation of the sensor chip, the metal-oxide powders, namely $SnO_2$ and $WO_3$, were investigated by x-ray diffraction analysis (XRD). Unlike the final sensor chips, the test samples of the pure metal oxides have been prepared onto a silicon substrate as the sapphire substrates have not been available at the time of material characterisation. To ensure that the results of the test samples are transferrable to the sapphire substrate, the sensitive films have been prepared in an analogous manner (see **Section 6.3.2**). A Siemens D5000 diffractometer with copper $K_\alpha$ radiation ($\lambda$=1.540598 Å) was used to record the spectra. The XRD spectra of $SnO_2$ (Fig. 6.3) and $WO_3$ (Fig. 6.4) were monitored in a two-theta angle range from 20° to 65° and 20° to 37°, respectively.

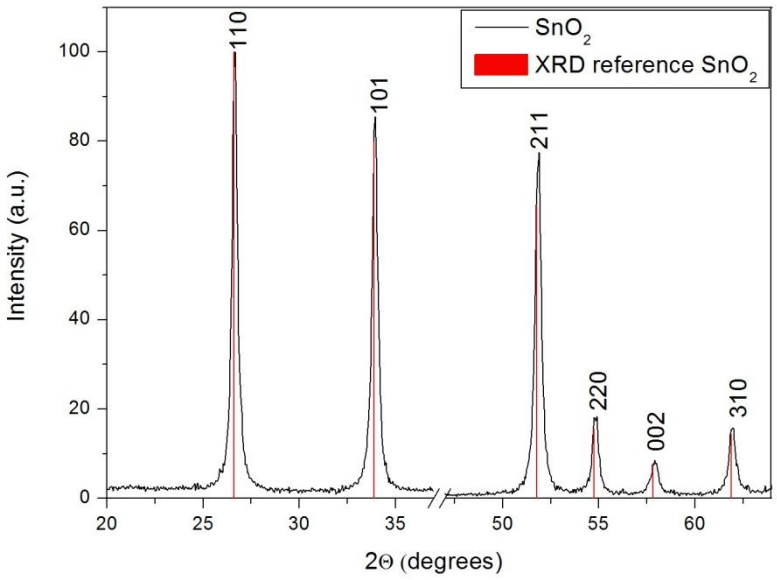


**Figure 6.3:** Indexed XRD spectrum of $SnO_2$ nano-powder prepared on a silicon substrate recorded in a two-theta angle range from 20° to 65°.

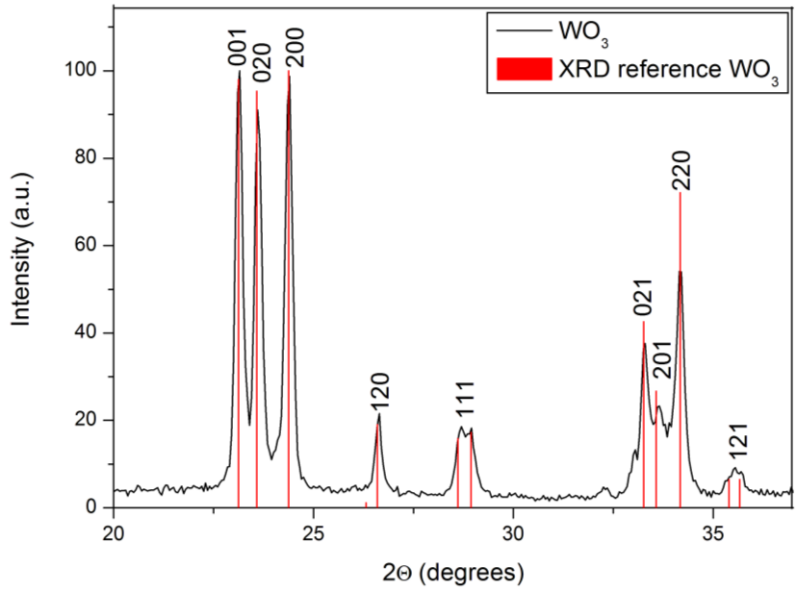


**Figure 6.4:** Indexed XRD spectrum of $WO_3$ nano-powder prepared on a silicon substrate recorded in a two-theta angle range from 20° to 37°.

The diffraction peaks in the XRD pattern can be indexed to the rutile phase $SnO_2$ and orthorhombic crystal structure in case of $WO_3$, respectively, as provided by Urusov and Loopstra [17,18]. No characteristic peaks of impurities, such as pure metals or surfactants, were observed. The average size of the crystallites was deduced from Scherrer's formula for the strongest peaks (110 peak in case of $SnO_2$ and 200 peak in case of the $WO_3$) according to:

$$\tau = \frac{K\lambda}{\beta \cos\theta} \tag{6.1}$$

Here, $\tau$ is the crystallite size in m, $K$ is a dimensionless shape factor close to 1 (admitted 0.94), $\lambda$ is the x-ray wavelength in m, $\beta$ is the full peak width at half maximum in rad and $\theta$ is the Bragg angle. The values for $\tau$ were found to be 14 nm in case of $SnO_2$ and 27 nm in case of $WO_3$. This agrees with the specifications of the data sheets for both materials (particle size <100 nm).

6.3.3.2 SEM

In order to investigate the morphology of the sensing films, the same type of samples as used for XRD have been analysed by scanning electron microscopy (SEM), as the sapphire substrates had not been available at the time of material characterisation. Still, the properties of the sensing films should be comparable to those on sapphire substrate as the method of preparation was exactly the same. Figures 6.5 and 6.6 show the SEM images of the prepared samples with $SnO_2$ (Fig. 6.5) and $WO_3$ (Fig. 6.6) with a magnification of approximately 100k.

Both, the $SnO_2$ and $WO_3$ samples depict a rough and densely covered surface, which is favourable in terms of gas sensing, especially in the lower concentration range. The average size of the crystallites observed in SEM images is consistent with the results obtained from the XRD patterns.

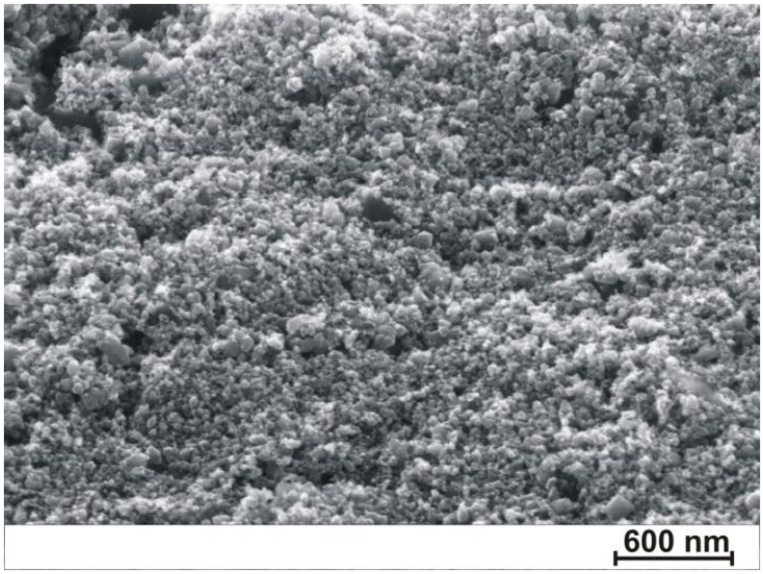


**Figure 6.5:** SEM image of a nanocrystalline $SnO_2$ film prepared on a silicon substrate at a magnification of 100k.

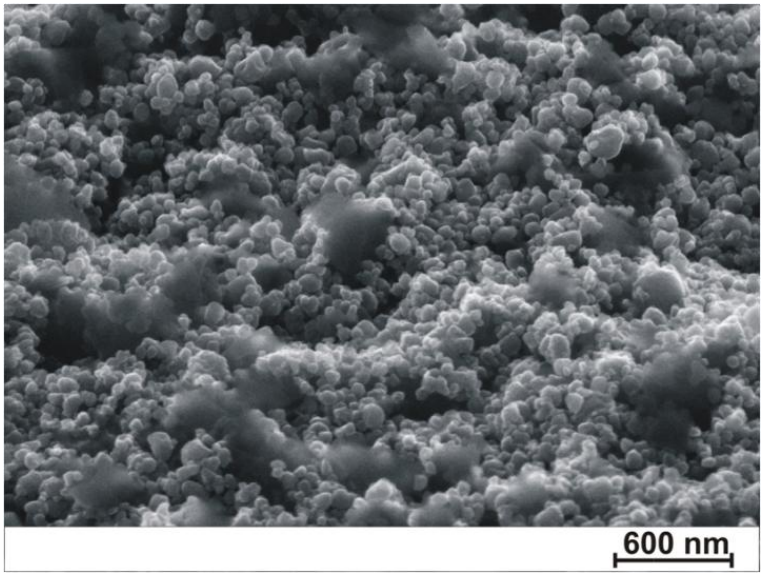


**Figure 6.6:** SEM image of a nanocrystalline $WO_3$ film prepared on a silicon substrate at a magnification of 100k.

6.3.3.3 Thermal characterisation

In order to determine the resistance ($R_0$) and thermal coefficient (α) of the heating elements, a comparison calibration in a defined temperature bath has been done in several steps between 20 °C and 80 °C. From the average of four sensor chips (16 heaters) out of one charge, $R_0$ was found to be 17.41 ±0.64 Ω and $\alpha=3.12*10^{-3} \pm 3.4*10^{-5}$ 1/K. The determined value for α is in accordance with the values obtained for Ti/Pt thin-film resistances by Groenland [19].

The sensor chip was designed in a way that each sensing structure can be heated individually. Nevertheless, for the sensor characterisation the four heaters were operated with a single voltage source in parallel. In order to achieve an operating temperature of 320 ±2 °C in the gas stream (air flow of 70 m³/h, gas temperature of 70 °C), a voltage of 6 V was applied to the heaters, resulting in a current of 688 mA and an overall power consumption of 4.1 W.
In a further experiment, it was found that an excessive heating of the sensor chips caused changes in the electric properties of the heating elements. At chip temperatures >400 °C, the platinum-titanium bilayer thin-film resistances were subject to interlayer diffusion and stress-induced morphological changes, as it was also described in the work of Groenland [19]. This resulted in an >100% increase of the nominal resistance $R_0$ as well as to changes in the thermal coefficient α. In order to avoid changes in the thermal properties of the sensor chip during the film deposition and later on during the measurements, its maximum operating temperature had to be reduced to 320 °C.

6.3.4 Experimental set-up

For the characterisation of the sensing properties, the sensor chip was attached to a printed circuit board (PCB) and contacted via bond wires. The sensor chip was located in the exhaust pipe of an aseptic sterilisation chamber, which is continuously flooded with hydrogen peroxide vapour (see Fig. 6.7). Therefore, a technical grade aqueous hydrogen peroxide solution of 35% w/w is fed to a flow-controlled air stream, which is supplied by compressed air. Subsequently, the gas-liquid mixture is evaporated in a heater. For a detailed description of the $H_2O_2$-vapour generation unit is referred to [4] (see also **Section 1.6.2**). While hydrogen peroxide is vaporised into the chamber at an air flow of 10 m³/h, the exhauster provides a continuously discharge of 70 m³/h. The 60 m³/h lack

between the $H_2O_2$ vapour entry (10 m³/h) and the suction capacity of the exhauster (70 m³/h) is being compensated by aspiration of ambient air via venting slots. As a result, the $H_2O_2$ concentration in the exhausted air is being diluted to 1/7 of its initial concentration in gaseous phase. Since, according to the best of our knowledge, no reference method for the detection of hydrogen peroxide under the given conditions (broad concentration range and high flow) has been available, it was assumed that the dosed amount of hydrogen peroxide fully passes over into the gaseous phase and will be present at the point of measurement. The discharge of 70 m³/h was checked with a flow meter. The diameter of the exhaust pipe is 10 cm. A schematic of the experimental set-up is given below.

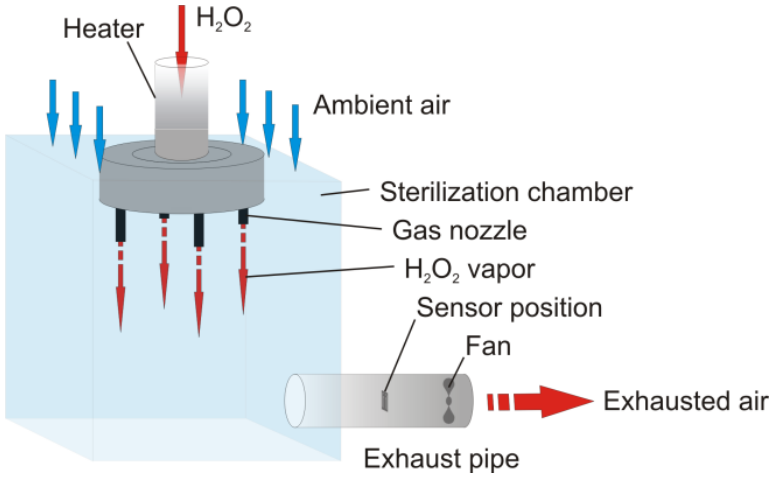


**Figure 6.7:** Schematic of the experimental set-up for the generation of hydrogen-peroxide vapour.

## 6.4 Results and discussion

### 6.4.1 Measurements

For the characterisation of the sensor response to hydrogen peroxide, various concentrations of $H_2O_2$ in the exhaust air stream, ranging from 5 to 1000 ppm, have been provided. The concentration steps in between were 10, 50, 100 and 500 ppm, respectively. After the vaporisation system was heated up to a stable operating temperature, the vaporisation by $H_2O_2$ was started. Initially, a

concentration of 5 ppm $H_2O_2$ was provided for 10 minutes, following a stepwise increase of the $H_2O_2$ concentration up to the maximum concentration of 1000 ppm and in return a stepwise decrease down to 5 ppm. Each concentration step was kept for 10 minutes. The hydrogen peroxide has been vaporised to the sterilisation chamber at a temperature of 270 °C. By dilution with ambient air, the gas stream reaches a temperature of about 70 °C in the exhaust pipe.

### 6.4.2 $H_2O_2$ sensing

The sensor chip with four different types of metal-oxide films was investigated for $H_2O_2$ concentrations between 5 and 1000 ppm. Fig. 6.8 presents the recorded measurement data for the $SnO_2$ as well as Pd- and Pt-doped $SnO_2$ films in one diagram.

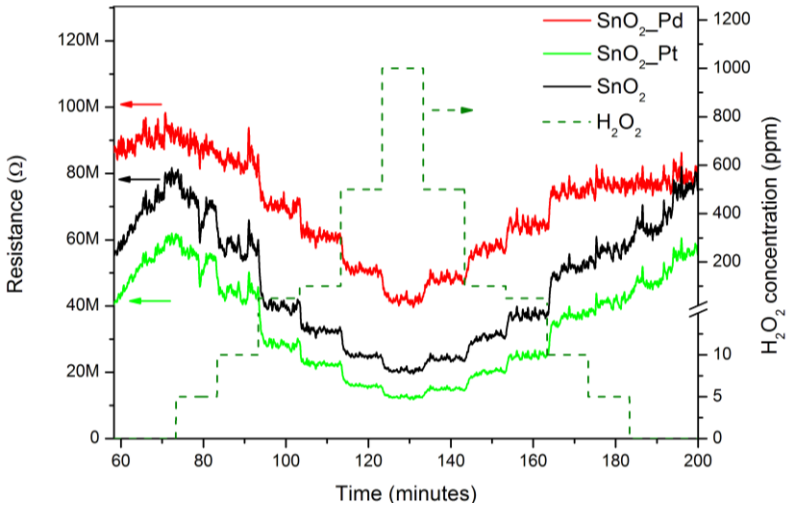


**Figure 6.8:** Resistance data of the undoped, Pt- and Pd-doped $SnO_2$ gas sensors in hydrogen peroxide atmosphere. The concentration profile is given as a dashed line.

Prior to the exposure to $H_2O_2$, the system has to reach steady conditions in terms of flow and temperature in the exhaust pipe (t < 70 minutes). This way, it was also ensured that the operating temperature of the sensor chip is not being influenced by alterations of the temperature in the exhaust air. This condition was assumed to be fulfilled when the relative change in resistance of the sensing films was less than 1% of the absolute resistance value per minute

(t = 70 minutes). At this point, the resistances are in the same order of magnitude between approximately 60 and 90 MΩ. To the exposure of $H_2O_2$ the sensors respond with a decrease in their resistance and with further increase of the $H_2O_2$ concentration, the resistances of the different sensors decrease gradually. After the exposure to the highest concentration of 1000 ppm $H_2O_2$, the resistance values raise again in the direction to lower concentrations. After the exposure to $H_2O_2$ was stopped at t=182 minutes, the resistances of the $SnO_2$ and Pt-doped $SnO_2$ films raise to similar values as prior to the exposure of $H_2O_2$ (t=70 minutes). In case of the Pd-doped sensor, the resistance of the sensing film is somewhat lower compared to its initial value.

The resistance behaviour of the $WO_3$ sensor was recorded in parallel and is shown in Fig. 6.9.

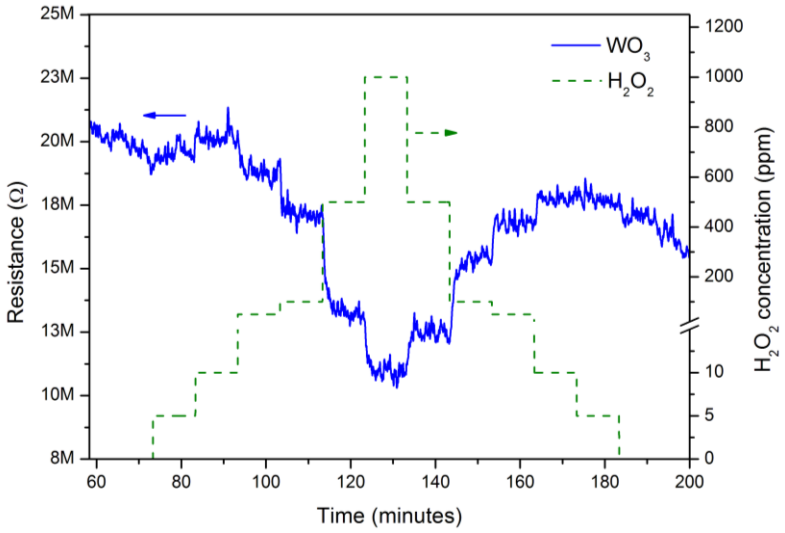


**Figure 6.9:** Resistance data of the $WO_3$ gas sensor in hydrogen peroxide atmosphere. The concentration profile is given as a dashed line.

The initial resistance value of the $WO_3$ film is about 20 MΩ, thus slightly lower as compared to the $SnO_2$ and doped $SnO_2$ films. The response of the $WO_3$ sensor is similar compared to the other sensors, however, it is subject to a higher drift.

In order to characterise the sensor behaviour and to compare the different materials, the relative resistance values of all sensors were plotted in a single diagram. Therefore, the resistance values (R) of the individual sensors at each

concentration step were divided by the initial resistance value ($R_0$) before the exposure to $H_2O_2$ (t=70 minutes). Fig. 6.10 depicts the calibration plots of the four sensors for a logarithmic scale of the $H_2O_2$ concentration. The plotted values correspond to the mean values of the sensor signals for equal concentrations, recorded once towards higher concentrations and towards lower concentrations, respectively. The error bars represent the standard deviation of these values.

All types of sensors exhibit a linear correlation between the change in their relative resistance and the logarithm of the $H_2O_2$ concentration in the range between 5 and 1000 ppm. The lowest sensitivity was observed for the $WO_3$ film, followed by the Pd-doped $SnO_2$ sensor. Also, the reproducibility of the $WO_3$ sensor is lower compared to the other ones (see error bars in Fig. 6.10). The Pt-doped $SnO_2$ offered the highest sensitivity to $H_2O_2$ in the ppm range, whereas it was slightly lower in case of undoped $SnO_2$. The lower limit of detection (LOD) for hydrogen peroxide was found to be 5 ppm in case of the undoped and Pt-doped $SnO_2$, 10 ppm for Pd-doped $SnO_2$ and 50 ppm in case of the $WO_3$ film.

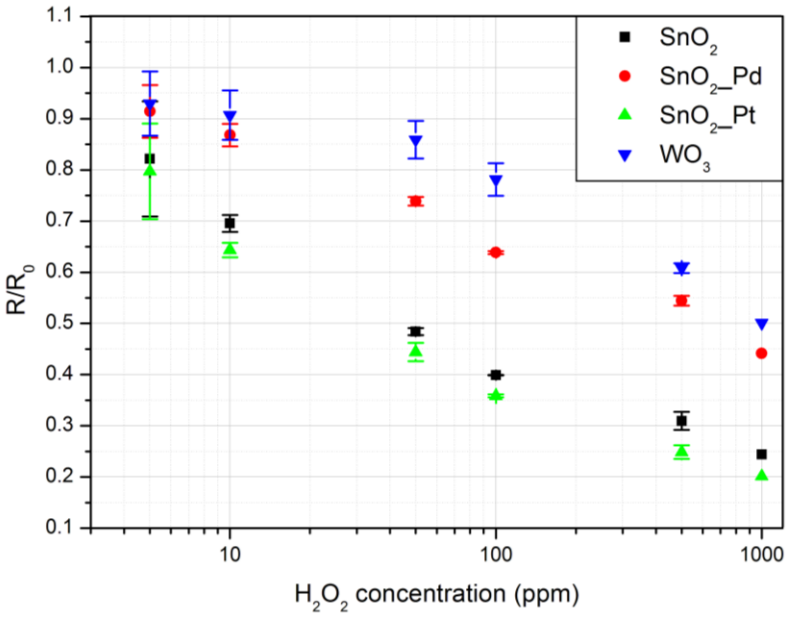


**Figure 6.10:** Calibration plot of a $SnO_2$, $WO_3$, Pt- and Pd-doped $SnO_2$ gas sensor for $H_2O_2$ concentrations in the ppm range.

Considering the relative resistance changes of the sensitive layers, it is found that, for example in case of the undoped $SnO_2$ sensor, the relative change of the resistance ($R/R_0$) upon exposure of hydrogen peroxide is about 1/2.5 per decade. This seems somewhat low compared to the sensitivities that are typically achieved with n-type semiconductor gas sensors when exposed to oxidising or reducing gases. These are typically in the range of 3/1 for oxidising gases such as $O_2$ up to a ratio of 5/1 for reducing gases such as $H_2$ or methane [20]. In an earlier work by the author, similar sensitivities have been observed upon the exposure of commercially available n-type semiconductor gas sensors with $H_2O_2$ in the lower percent range [7] (see Chapter 3).

The fact that the resistivity of the sensors decreases under exposure to $H_2O_2$ seems not to be in accordance with the expected behaviour of n-type metal-oxide semiconductor materials, which exclusively were used in this case, when in contact to oxidising gases, like hydrogen peroxide. It is generally considered that, in case of n-type metal-oxide semiconductor gas sensors, reducing gases react with adsorbed oxygen ions at the metal-oxide surface, so releasing bound electrons which are then free to conduct. As a result, the resistance of the surface layer decreases. For an oxidising gas, the inverse mechanism will operate and the resistance will rise [21].

Though, the same type of behaviour was observed in previous studies for the exposure to $H_2O_2$ in a higher concentration range using commercially available n-type semiconductor gas sensors with not exactly specified composition of the sensing films [7] (see **Chapter 3**). To explain the decrease of the resistance with increasing $H_2O_2$ concentration, one has additionally to take into consideration the mechanism of reaction concerning the decomposition of $H_2O_2$. Although the complete mechanism is not completely uncovered yet, $H_2O_2$ is known to form free hydroxyl radicals ($OH^{\bullet}$) [22] (see Eq. 3.1-3.3 in **Chapter 3**). The occurrence of hydroxyl radicals was proven to have a strong influence on the electrical conductivity of n-type metal oxides as they react with adsorbed oxygen molecules at the metal-oxide surface leading to a decrease in the resistance [23]. As Pd and Pt are known to have a high catalytic activity towards

$H_2O_2$ it was presumed that doping by these two materials may increase the sensitivity due to an enhanced reaction of $H_2O_2$ at the metal-oxide surface [15].

In case of the Pt-doped $SnO_2$ a slightly higher sensitivity compared to the undoped $SnO_2$ was observed, which might be the result of a catalytical reaction of $H_2O_2$ at the Pt particles. In case of the Pd-doped $SnO_2$, which exhibits a lower sensitivity to $H_2O_2$ compared to undoped $SnO_2$, the sensing mechanism seems to be more complex. One proposal could be that the Pd particles catalytically activate the dissociation of molecular oxygen. As a result, atomic oxygen diffuses to the metal oxide increasing both, the quantity of oxygen that will rebind vacancies on the $SnO_2$ surface as well as the rate at which rebinding occurs, resulting in a greater degree of electron withdrawal from the $SnO_2$. This mechanism is well established in literature on catalysis and dates back to the 1960s. In this context Boudart *et al.* coined the term "spillover effect" [24].

The impact of humidity on the sensor response has not been studied in detail yet. Generally, n-type semiconductors as the presented $SnO_2$ and $WO_3$ gas sensors are known to be humidity-sensitive. As for the sensor calibration a 35% w/w aqueous hydrogen peroxide solution was used, the $H_2O_2$ concentrations in gaseous phase have been regulated by adjusting the dosed amount of the aqueous solution. It is therefore generally assumed, that $H_2O_2$ and $H_2O$ will be present in the same mass ratio, regardless of the absolute dosage. This way, similar conditions arise upon the exposure to different concentrations of hydrogen peroxide. Measurements with commercially available sensors of the same type under $H_2O_2$ atmosphere have shown that $H_2O$ shifted the sensor signal of an n-type semiconductor in the same direction such as hydrogen peroxide. However, the response to $H_2O_2$ was about ten times higher [7].

## 6.5 Conclusions

A multi-sensor chip with four individually controllable sensing structures was fabricated and deposited with different types of metal oxides. Both, the $SnO_2$ and $WO_3$ layers seem to be promising candidates for hydrogen peroxide sensing in the ppm concentration range. Regarding the sensing mechanism of the doped

$SnO_2$ films, still some questions remain unanswered. However, it could be shown that doping of $SnO_2$ by platinum black increases the sensitivity towards $H_2O_2$. The lower detection limit was found to be 5 ppm. In this study, $SnO_2$ films showed a higher reproducibility compared to $WO_3$ films.

Even though that the sensor response on $H_2O_2$ is less pronounced as compared to typical target gases such as hydrocarbons, its usability in the illustrated application seems justified, as there are currently no suitable reference methods for the detection of hydrogen peroxide in exhaust systems that cover such a wide measuring range, which potentially spans from the low ppm range up to the percent range. A statement on the lifetime of the multi-sensor, especially in continuous use under exposure to $H_2O_2$, cannot be made at this moment. However, a lifetime of several months would be desirable and seems to be reasonable. Another challenge is yet to detect $H_2O_2$ concentrations below 5 ppm, to make the sensor feasible for workplace monitoring with respect to the threshold limit value (TLV).

### 6.6 Outlook to $H_2O_2$ sensors based on CuO nanofibres

In addition to the sensors with the metal-oxides $SnO_2$ and $WO_3$, measurements were also carried out using a network of electro-spun CuO nanofibres, that were deposited on a sensor substrate. The results of this study were published in a separate article with the participation of the author of this thesis [25]. In contrast to the sensors previously shown in this chapter, the CuO has been deposited on commercially available sensor substrates. Also, the sensing characteristics of this sensor have not been evaluated in the ppm range, but at rather higher concentrations of $H_2O_2$ between 2.3 and 7.4% v/v, similar to the measurements shown in **Chapters 2** and **3**. The operating temperature of the sensor was chosen at 450 °C. The response of the CuO sensor is shown in Fig. 6.11, represented as resistance values normalised to the resistance in absence of $H_2O_2$.

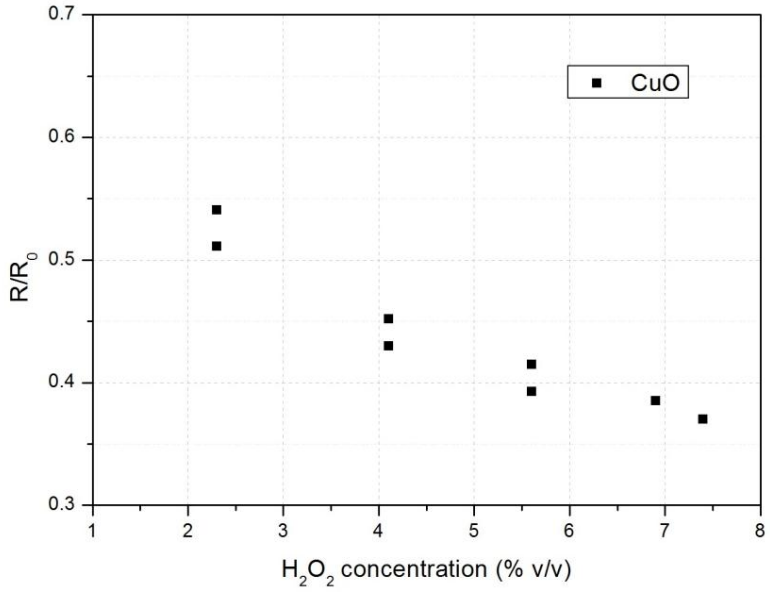


**Figure 6.11:** Calibration plot of the CuO gas sensor for $H_2O_2$ concentrations between 2.3 and 7.4% v/v.

The initial resistance of the sensor, prior to the exposure to $H_2O_2$ was equal to 13.5 MΩ. The sensing behaviour of the CuO sensor is similar to the other sensors already discussed in this thesis. Compared to the commercial sensor TGS 816 presented in **Chapter 3**, the change in the resistance of the CuO sensor is lower by more than one order of magnitude at the highest concentration of 7.4% v/v $H_2O_2$ ($R/R_{OTGS816}\approx0.025$ vs. $R/R_{OCuO}\approx0.33$). This means that the sensitivity of the CuO sensor towards $H_2O_2$ is lower in comparison to the TGS 816. At the same time, a considerable, lower saturation effect at the highest $H_2O_2$ concentration can be observed in case of the CuO sensor. Thus, it can be assumed that the CuO sensor presented here allows an application at even higher $H_2O_2$ concentrations.

More results and details of the CuO sensor and its application in $H_2O_2$ atmosphere can be found in [25]. The aforementioned study also provides data on the $H_2O_2$ sensitivity of the CuO sensor at different operating temperatures. The highest sensitivity was achieved at an operating temperature of 450 °C. The corresponding data is shown in Table 6.2.

**Table 6.2:** Response of the CuO sensor towards $H_2O_2$ at different operating temperatures (adapted from [25]).

| Operating temperature (°C) | $R_0$ prior to $H_2O_2$ exposure (MΩ) | R under $H_2O_2$ exposure (MΩ) | Relative response ($R/R_0$) |
|---|---|---|---|
| 250 | 13 | 5.8 | 0.466 |
| 350 | 15 | 5.6 | 0.373 |
| 450 | 15.50 | 5.5 | 0.355 |

### 6.7 References

[1] S. Reisert, H. Henkel, A. Schneider, D. Schäfer, P. Friedrich, J. Berger, M.J. Schöning, Development of a handheld sensor system system for the online measurement of hydrogen peroxide in aseptic filling systems, Physica Status Solidi (a) 207 (2010) 913–918.

[2] N. Näther, H. Henkel, A. Schneider, M.J. Schöning, Investigation of different catalytically active and passive materials for realising a hydrogen peroxide gas sensor, Physica Status Solidi (a) 206 (2009) 449–454.

[3] N. Näther, L.M. Juárez, R. Emmerich, J. Berger, P. Friedrich, M.J. Schöning, Detection of hydrogen peroxide ($H_2O_2$) at exposed temperatures for industrial processes, Sensors 6 (2006) 308–317.

[4] P. Kirchner, B. Li, H. Spelthahn, H. Henkel, A. Schneider, P. Friedrich, J. Berger, M. Keusgen, M.J. Schöning, Thin-film calorimetric $H_2O_2$ gas sensor for the validation of germicidal effectivity in aseptic filling processes, Sensors and Actuators B: Chemical 154 (2011) 257–263.

[5] P. Kirchner, Y.A. Ng, H. Spelthahn, A. Schneider, H. Henkel, P. Friedrich, J. Berger, M.J. Schöning, Gas sensor investigation based on a catalytically activated thin-film thermopile for $H_2O_2$ detection, Physica Status Solidi (a) 207 (2010) 787–792.

[6] P. Kirchner, J. Oberländer, P. Friedrich, J. Berger, H.-P. Suso, A. Kupyna, M. Keusgen, M.J. Schöning, Optimisation and fabrication of a calorimetric gas sensor built up on a polyimide substrate for $H_2O_2$ monitoring, Physica Status Solidi A 208 (2011) 1235–1240.

[7] S. Reisert, H. Geissler, R. Flörke, N. Näther, P. Wagner, M.J. Schöning, Towards a multi-sensor system for the evaluation of aseptic processes employing hydrogen peroxide vapour ($H_2O_2$), Physica Status Solidi (a) 208 (2011) 1351–1356.

[8] P. Ménini, F. Parret, M. Guerrero, K. Soulantica, L. Erades, A. Maisonnat, B. Chaudret, CO response of a nanostructured $SnO_2$ gas sensor doped with palladium and platinum, Sensors and Actuators B: Chemical 103 (2004) 111–114.

[9] L. Bagal, J. Patil, I. Mulla, S. Suryavanshi, Influence of Pd-loading on gas sensing characteristics of $SnO_2$ thick films, Ceramics International 38 (2012) 4835–4844.

[10] G. Korotcenkov, V. Brinzari, Y. Boris, M. Ivanov, J. Schwank, J. Morante, Influence of surface Pd doping on gas sensing characteristics of $SnO_2$ thin films deposited by spray pirolysis, Thin Solid Films 436 (2003) 119–126.

[11] Y. Lee, H. Huang, O. Tan, M. Tse, Semiconductor gas sensor based on Pd-doped $SnO_2$ nanorod thin films, Sensors and Actuators B: Chemical 132 (2008) 239–242.

[12] V. Mishra, R. Agarwal, Sensitivity, response and recovery time of $SnO_2$ based thick-film sensor array for $H_2$, CO, $CH_4$ and LPG, Microelectronics Journal 29 (1998) 861–874.

[13] J. Srivastava, P. Pandey, V. Mishra, R. Dwivedi, Sensing mechanism of Pd-doped $SnO_2$ sensor for LPG detection, Solid State Sciences 11 (2009) 1602–1605.

[14] K. Williams, K. Gupta, M. Wasilik, Etch rates for micromachining processing-part II, Journal of Microelectromechanical Systems 12 (2003) 761–778.

[15] J.-H. Smått, M. Lindén, T. Wagner, C.-D. Kohl, M. Tiemann, Micrometer-sized nanoporous tin dioxide spheres for gas sensing, Sensors and Actuators B: Chemical 155 (2011) 483–488.

[16] N. Yamazoe, Oxide semiconductor gas sensors, Catalysis Surveys from Asia 7 (2003) 63–75.

[17] V. Urusov, O. Yakubovich, N. Eremin, Dokl. RAN 336, 330 (1994).

[18] B.O. Loopstra, H.M. Rietveld, Further refinement of the structure of $WO_3$, Acta Crystallographica B: Structural Crystallography and Crystal Chemistry 25 (1969) 1420–1421.

[19] A.-W. Groenland, Degradation processes of platinum thin films on a silicon nitride surface, Research report, Transducers Science and Technology Group, (2004).

[20] P. Clifford, D. Tuma, Characteristics of semiconductor gas sensors I. Steady state gas response, Sensors and Actuators 3 (1982) 233–254.

[21] J. Watson, The tin oxide gas sensor and its applications, Sensors and Actuators 5 (1984) 29–42.

[22] A. Hiroki, J.A. LaVerne, Decomposition of hydrogen peroxide at water−ceramic oxide interfaces, Journal of Physical Chemistry B 109 (2005) 3364–3370.

[23] C.M. Lousada, A.J. Johansson, T. Brinck, M. Jonsson, Mechanism of $H_2O_2$ decomposition on transition metal oxide surfaces, Journal of Physical Chemistry 116 (2012) 9533–9543.

[24] M. Boudart, M.A. Vannice, J.E. Benson, Adlineation, Portholes and spillover, Zeitschrift für Physikalische Chemie 64 (1969) 171–177.

[25] J. Hennemann, C.-D. Kohl, S. Reisert, P. Kirchner, M.J. Schöning, Copper oxide nanofibres for detection of hydrogen peroxide vapour at high concentrations, Physica Status Solidi A 210 (2013) 859–863.

# Chapter 7

## Conclusions and outlook

This chapter summarises the main results of this thesis and provides a brief outlook on remaining challenges.

This work aimed at the development of a novel sensor system for the characterisation of aseptic sterilisation processes employing vapour-/gas-phase hydrogen peroxide. In a first step, a prototype of a handheld sensor system for monitoring the $H_2O_2$ concentration was developed (**Chapter 2**). This sensor system fulfils substantial operational requirements for the application in industrial sterilisation processes, as it:

- Is operable under harsh environmental conditions
- Withstands elevated gas temperatures
- Is operable under high gas flows
- Is robust against vibrations
- Offers a high specificity towards $H_2O_2$
- Covers the relevant range of measurement
- Enables online monitoring

This makes it a useful and first of its kind tool for the characterisation of aseptic sterilisation processes, in which the $H_2O_2$ concentration and gas temperature represent important parameters. One further advantage of the presented calorimetric gas sensor is that it could, in principle, be used in sterilisation processes under vacuum conditions, since the catalytic reaction at the sensor, in contrast to e.g., semiconductor gas sensors or conventional catalytic gas sensors, not necessarily presupposes the presence of oxygen. However, the commercial production and distribution of these sensors/systems remain still a challenge.

A main focus of this project was the development of a novel multi-sensor system for monitoring the effectiveness of sterilisation with regard to the microbicidal action of $H_2O_2$ (**Chapters 3-5**). Here, commercially available sensors should be used primarily. In a first work on this topic, two gas sensors, namely a metal-oxide semiconductor gas sensor (MOX) as well as an electrochemical type of sensor have been identified as possible candidates for such sensor systems (**Chapter 3**). A correlation between the sensors' output and the results of microbiological tests in terms of logarithmic cycle reductions (LCR) of *Bacillus*

*atrophaeus* (previously *B. subtilis*) could be established via the $H_2O_2$ concentration.

As the literature suggests that the microbicidal activity of $H_2O_2$ is not only dependent on its concentration, but also on a range of other parameters, such as the temperature and humidity – to name only a few – the microbiological and sensory measurements were extended. In addition, a different strategy was pursued. Thus, the correlation between sensor signals and microbial activity should not be established via the parameters themselves, but by a direct comparison between the LCR and sensor response. Referring thereto, as presented in **Chapter 4**, the list of sensors was extended by three more MOX's and the inactivation kinetics of *B. atrophaeus* by gas-phase $H_2O_2$ have been studied for different conditions in terms of $H_2O_2$ concentration, humidity, gas temperature and gas flow. It could be demonstrated that the sensors in test equally respond to the factors influencing the effectiveness of the sterilisation by gas-phase $H_2O_2$. Additionally, by using image-recognition techniques, the potential of identifying the microbicidal action on the basis of chemical images generated from the sensor responses has been demonstrated. This kind of approach corresponds, in a wider sense, to that of an "electronic nose".

However, for a detailed evaluation of the sensor characteristics and the influencing parameters on the sterilisation, the present data set was still not satisfactory. Thus, the microbiological tests were carried out in an even greater extent in a further set of experiments, which is described in **Chapter 5**. Based on the findings of the previous works, the field of parameter was limited. Therefore, a methodical calibration experiment, in which the parameters $H_2O_2$ concentration, humidity and gas temperature were studied in more detail and with greater statistical significance has been elaborated. The same sensors as in the previous work have been addressed. It was shown that the inactivation of *B. atrophaeus* by gaseous $H_2O_2$ is predominantly dependent on the $H_2O_2$ concentration. This fact is also confirmed by several other, independent studies. Only at lower $H_2O_2$ concentrations, below 2% v/v, the parameters humidity and gas temperature get more weight. For example, the inactivation of spores was increasing progressively with the gas temperature in the lower concentration

range. On the other hand, gas temperatures below the dew point of $H_2O_2$ may favour the microbicidal action due to condensation of the sterilising agent on the spore carrier.

It was further found that high levels of humidity in combination with low $H_2O_2$ concentrations at low gas temperatures likewise affect the sterilisation in a positive way, but higher gas temperatures are rather disadvantageous in this particular combination. It succeeded to establish a correlation between the microbicidal action and the sensor responses. With respect to this, two models were proposed: The first one is related to the calorimetric gas sensor and can be applied at $H_2O_2$ concentrations above 2% v/v, at which the microbicidal effect is primarily dependent on the $H_2O_2$ concentration. For this purpose, an additional compensation model, yielding the equalisation of the temperature influence on the sensor response, has been implemented. In the lower concentration range, a good match between the LCR and the response of two different MOX was found. The second established model also considers the effects of temperature and humidity on the microbicidal activity of gaseous $H_2O_2$. Accordingly, by the combination of these two types of sensors, a sensor system for monitoring the microbicidal effectiveness by means of an online measurement can be realised. The use of several sensors furthermore increases the significance level of the predicted microbicidal action deduced from the sensor responses. In addition, symptoms of failure and malfunctions may be identified by a bilateral comparison of the sensors.

All sensors in test proved high robustness in the harsh conditions of the sterilisation process. Furthermore, the sensors exhibited a good short-term stability. Expressed in numbers, the deviation was lower than 5% for the selected sensors. As in case of the MOX, the relative changes of the resistance are considered as measurement reading, they can be recalibrated in ambient air or in an environment that provides constant conditions by means of a single-point adjustment. This allows a continuous operation of the sensor system in the sterilisation process.

To this day, the validation of aseptic sterilisation processes is regulated by agencies, such as the FDA, which prescribe biological testing with test organisms as a counterpart to potential pathogens. The high temporal and financial efforts related to microbiological testing are evident drawbacks in the practical

application, especially, when an intense testing is required (e.g., for the optimisation of processes or the development of new machinery). In particular for these purposes, the developed sensor system represents a useful tool to considerably save time and costs. In addition, permanently installed in the sterilisation unit of an aseptic plant, it can be used for real-time monitoring of the sterilisation effectiveness.

In a concluding work of this project, the response of metal-oxide semiconductors upon exposure of $H_2O_2$ in the ppm range has been studied (**Chapter 6**). Therefore, two different types of metal-oxide nanoparticles, $SnO_2$ and $WO_3$, have been deposited on a self-developed multi-sensor chip. Additionally, two Pt- and Pd-doped layers have been deposited. This work was essential in order to investigate the sensing mechanism of the metal-oxide semiconductors and the impact of dopants, especially since the exact composition of the commercial sensors is not known in detail.
It was found that the changes in the resistance of the metal oxides upon exposure to $H_2O_2$ are most likely caused by the interaction of electron donors. As such, hydroxyl ions/radicals have been identified. The origin of these hydroxyls, however, could not ultimately be clarified. It seems feasible that these are already present upon arrival at the sensor surface, after they have emerged during the evaporation of the $H_2O_2$, for instance. Or alternatively, they are generated primarily by a reaction at the hot metal-oxide surface. Though, it was demonstrated that the sensing effect can considerably be enhanced by doping the metal oxide with Pt, which represents an excellent catalyst for $H_2O_2$. In any case, the latter finding suggests an at least partly reaction of the $H_2O_2$ at the sensor surface. In the end, it was demonstrated that metal-oxide semiconductor gas sensors are suitable for the detection of $H_2O_2$ at high concentrations in the percentage range as well as at rather low concentrations in the ppm range. Thus, they can be applied for both, the sterilisation process itself (high concentrations) as well as for applications at lower concentrations, e.g., in the exhaust system of such sterilisation devices or for monitoring the ambient $H_2O_2$ concentration in terms of workplace security.

Within the framework of this thesis, a number of important evidences regarding the inactivation kinetics of bacterial spores by $H_2O_2$ are obtained and novel

sensor systems and strategies for the evaluation of sterilisation processes are presented. However, there is still some room for improvements. In particular, the precise mechanisms of microbial inactivation by $H_2O_2$ are still a largely unknown phenomenon, as a view to the literature reveals. A detailed investigation of these mechanisms is therefore, essential to gain a better understanding of the sterilisation process. If the effects of microbial inactivation were better known, it would significantly facilitate the selection of suitable sensors for monitoring sterilisation processes. On the other hand, sensors could also help to reveal those factors that are beneficial for the inactivation.

A not insignificant factor in the inactivation is represented by the condensation of the sterilising agent on the surface. It is in the nature of the sensors presented here that these are either operated at temperatures widely above the dew point of $H_2O_2$, like the MOX and electrochemical sensor, or induce an immediate decomposition of hydrogen peroxide when in contact, in the case of the calorimetric gas sensor. This circumstance thus represents a limiting factor in the validation of sterilisation processes in which condensation plays an important role. Concerning this, a possible alternative is represented, for example, by capacitive humidity sensors on the basis of silica, which in contrast to conventional humidity sensors meet the demands in terms of robustness for the use under harsh environmental conditions, as they arise in aseptic sterilisation processes. These are, in fact, the main reason why only a few types of sensors are qualified to be used under such conditions.

# Appendix 1

## Nomenclature

| | |
|---|---|
| ACGIH | American Conference on Governmental Industrial Hygienists |
| ANN | Artificial neural network |
| *B. atrophaeus* | *Bacillus atrophaeus* |
| *B. subtilis* | *Bacillus subtilis* |
| CCD | Charge-coupled device |
| CFU | Colony forming units |
| CRT | Count-reduction test |
| DAQ | Data acquisition |
| DNA | Deoxyribonucleic acid |
| EPT | End-point test |
| e-sensing | Electronic sensing |
| FDA | Food and Drug Administration |
| FEP | Fluorinated ethylene propylene |
| HPV | Hydrogen peroxide vapour |
| IDE | Interdigitated electrode |
| LCR | Logarithmic cycle reduction |
| LOD | Limit of detection |
| log-rate | Referring to the same as LCR |
| MCM | Multi-component media |
| MOSFET | Metal-oxide semiconductor field-effect transistor |
| MOX | Metal-oxide semiconductor sensor |
| MP | Measuring point |
| MPN | Most probable number |
| PCA | Principal component analysis |
| PCB | Printed circuit board |
| PFA | Perfluoroalkoxy |
| PTFE | Polytetrafluoroethylene |
| RFID | Radio frequency identification |
| ROS | Reactive oxidant species |

| | |
|---|---|
| SAW | Surface acoustic wave |
| SEM | Scanning electron microscopy |
| TLV | Threshold limit value |
| TO | Transistor outline |
| UV | Ultra violet |
| VDMA | Verein Deutscher Maschinen- und Anlagenbau e.V. |
| XRD | X-ray diffraction |

# Appendix 2

## List of publications

**Book chapter**

- P. Kirchner, **S. Reisert**, M.J. Schöning, Calorimetric gas sensor for hydrogen peroxide monitoring in aseptic food processes, Springer series on chemical sensors and biosensors: Gas sensing fundamentals, Springer, Berlin 2013, *in press*, DOI 10.1007/5346_2013_51.

**Peer-reviewed journal articles**

- **S. Reisert**, H. Henkel, A. Schneider, D. Schäfer, P. Friedrich, J. Berger, M.J. Schöning., Development of a handheld sensor system for the online measurement of hydrogen peroxide in aseptic filling systems, Physica Status Solidi (a) 207 (2010) 913–918.
- **S. Reisert**, H. Geissler, R. Flörke, N. Näther, P. Wagner, M.J. Schöning, Towards a multi-sensor system for the evaluation of aseptic processes employing hydrogen peroxide vapour ($H_2O_2$), Physica Status Solidi (a) 208 (2011) 1351–1356.
- P. Kirchner, **S. Reisert**, P. Pütz, M. Keusgen, M.J. Schöning, Characterisation of polymeric materials as passivation layer for calorimetric $H_2O_2$ gas sensors, Physica Status Solidi A 209 (2012) 859–863.
- **S. Reisert**, H. Geissler, R. Flörke, C. Weiler, P. Wagner, M.J. Schöning, Characterisation of aseptic sterilisation processes using an electronic nose, International Journal of Nanotechnology 10 (2013) 470–484.
- J. Hennemann, C.-D. Kohl, **S. Reisert**, P. Kirchner, M.J. Schöning, Copper oxide nanofibres for detection of hydrogen peroxide vapour at high concentrations, Physica Status Solidi (a) 210 (2013) 859–863.

- **S. Reisert**, B. Schneider, H. Geissler, M. van Gompel, P. Wagner, M.J. Schöning, Multi-sensor chip for the investigation of different types of metal oxides for the detection of $H_2O_2$ in the ppm range, Physica Status Solidi (a) 210 (2013) 898–904.
- **S. Reisert**, H. Geissler, C. Weiler, P. Wagner, M.J. Schöning, Multiple sensor-type system for monitoring the microbicidal effectiveness of aseptic sterilization processes, Manuscript under preparation.

**Patent applications**

- **S. Reisert**, N. Näther, M.J. Schöning, R. Flörke, H. Geissler, Method and apparatus for measuring the killing effectiveness of a disinfectant, WO/2011/080135.

**Peer-reviewed conference proceedings**

- **S. Reisert**, H. Henkel, A. Schneider, D. Schäfer, P. Friedrich, J. Berger, M.J. Schöning, Entwicklung eines Handheld-Sensorsystems für die "On-line"-Messung der $H_2O_2$-Konzentration in aseptischen Entkeimungs-prozessen, Dresdner Beiträge zur Sensorik 39 (2009) 285–288.
- **S. Reisert**, H. Geissler, R. Flörke, P. Wagner, T. Wagner, M.J. Schöning, Controlling aseptic sterilization processes by means of a multi-sensor system, Proceedings of the IEEE SSCI (CompSens) (2011) 18–22.

**Oral presentations**

- **S. Reisert**, H. Henkel, A. Schneider, P. Friedrich, M.J. Schöning, Development of a handheld sensor system for the online measurement of hydrogen peroxide in aseptic filling processes, Engineering of Functional Interfaces 2009 (18.-19.06.2009) Hasselt (Belgium).
- **S. Reisert**, H. Henkel, P. Friedrich, H. Geissler, M.J. Schöning, Development of a sensor system for the validation of aseptic processes, 2$^{nd}$ Graduate Symposium (05.11.2009) Aachen (Germany).

- **S. Reisert**, N. Näther, H. Geissler, R. Flörke, P. Wagner, M.J. Schöning, Towards a multi-sensor system for the evaluation of aseptic processes employing hydrogen peroxide vapour ($H_2O_2$), Engineering of Functional Interfaces 2010 (15.-16.06.2010) Marburg (Germany).
- **S. Reisert**, H. Geissler, R. Flörke, P. Wagner, N. Näther and M.J. Schöning, Multi-gas sensor system for electronic nose applications, 3rd Graduate Symposium (04.11.2010) Jülich (Germany).
- **S. Reisert**, H. Geissler, R. Flörke, P. Wagner, T. Wagner, M.J. Schöning, Controlling aseptic sterilization processes by means of a multi-sensor system, IEEE Symposium on Computational Intelligence (11.-15.04.2011) Paris (France).
- **S. Reisert**, B. Schneider, H. Geissler, R. Flörke, P. Wagner, M.J. Schöning, Development of semiconductor gas sensors using micro fabrication techniques, Engineering of Functional Interfaces 2011 (19.-20.07.2011) Linz (Austria).
- **S. Reisert**, H. Geissler, R. Flörke, C. Weiler, P. Wagner, M.J. Schöning, Characterisation of aseptic sterilisation processes using an electronic nose, Humboldt Kolleg (17.-19.03.2012) Hammamet (Tunis).
- **S. Reisert**, B. Schneider, H. Geissler, R. Flörke, P. Wagner, M.J. Schöning, Using an $SnO_2$ gas sensor for the detection of hydrogen peroxide in the ppm range, Engineering of Functional Interfaces 2012 (16.-17.06.2012) Zweibrücken (Germany).
- **S. Reisert**, H. Geissler, R. Flörke, C. Weiler, P. Wagner, M.J. Schöning, Sicher verpackt – Sensoren zur Überwachung von aseptischen Sterilisationsprozessen, 5th Graduate Symposium (15.11.2012) Jülich (Germany).
- **S. Reisert**, H. Geissler, R. Flörke, C. Weiler, P. Wagner, M.J. Schöning, Multiple sensor-type system for real-time analysis of aseptic sterilization processes, Engineering of Functional Interfaces 2013 (08.-09.07.2013) Hasselt (Belgium).

**Poster presentations**

- **S. Reisert**, H. Henkel, A. Schneider, P. Friedrich, M.J. Schöning, Development of a handheld sensor system for the online measurement of hydrogen peroxide in aseptic filling processes, Engineering of Functional Interfaces 2009 (18.-19.06.2009) Hasselt (Belgium).
- **S. Reisert**, H. Henkel, P. Friedrich, H. Geissler, M.J. Schöning, Development of a sensor system for the validation of aseptic processes, 2nd Graduate Symposium (05.11.2009) Aachen (Germany).
- **S. Reisert**, H. Henkel, A. Schneider, P. Friedrich, M.J. Schöning, Entwicklung eines Handheld-Sensorsystems für die "On-line"-Messung der $H_2O_2$-Konzentration in aseptischen Entkeimungsprozessen, 9. Dresdner Sensor Symposium (07.-09.12.2009) Dresden (Germany)
- **S. Reisert**, N. Näther, H. Geissler, R. Flörke, P. Wagner, M.J. Schöning, Towards a multi-sensor system for the evaluation of aseptic processes employing hydrogen peroxide vapour ($H_2O_2$), Engineering of Functional Interfaces 2010 (15.-16.06.2010) Marburg (Germany).
- **S. Reisert**, H. Geissler, R. Flörke, P. Wagner, N. Näther and M.J. Schöning, Multi-gas sensor system for electronic nose applications, 3rd Graduate Symposium (04.11.2010) Jülich (Germany).
- **S. Reisert**, H. Geissler, R. Flörke, C. Weiler, P. Wagner, M.J. Schöning, Smart sensor system for the evaluation of aseptic sterilization processes employing $H_2O_2$ vapor, Annual Meeting of the Institute for thermal processing specialists (IFTPS) (01.-04.03.2011) San Antonio (USA).
- **S. Reisert**, B. Schneider, H. Geissler, R. Flörke, P. Wagner, M.J. Schöning, Entwicklung von Halbleiter-Gassensoren in Chip-Technologie zur Überwachung von aseptischen Sterilisationsprozessen, 7. Deutsches Biosensor Symposium (03.-06.04.2011) Heilbad Heiligenstadt (Germany).
- **S. Reisert**, B. Schneider, H. Geissler, R. Flörke, P. Wagner, M.J. Schöning, Development of semiconductor gas sensors using micro fabrication techniques, Engineering of Functional Interfaces 2011 (19.-20.07.2011) Linz (Austria).

- **S. Reisert**, H. Geissler, R. Flörke, C. Weiler, P. Wagner, M.J. Schöning, Using a multi-sensor system to provide chemical images of sterilisation processes employing $H_2O_2$-vapour, 4$^{th}$ Graduate Symposium (24.11.2011) Aachen (Germany).
- **S. Reisert**, B. Schneider, H. Geissler, R. Flörke, P. Wagner, M.J. Schöning, Using an $SnO_2$ gas sensor for the detection of hydrogen peroxide in the ppm range, Engineering of Functional Interfaces 2012 (16.-17.06.2012) Zweibrücken (Germany).
- **S. Reisert**, B. Schneider, H. Geissler, R. Flörke, P. Wagner, M.J. Schöning, $SnO_2$-Sensor zum Nachweis der $H_2O_2$-Konzentration in der Abluft von aseptischen Sterilisationsprozessen, 8. Deutsches Biosensor Symposium (10.-13.03.2013) Wildau (Germany).
- **S. Reisert**, H. Geissler, R. Flörke, C. Weiler, P. Wagner, M.J. Schöning, Multiple sensor-type system for real-time analysis of aseptic sterilization processes, Engineering of Functional Interfaces 2013 (08.-09.07.2013) Hasselt (Belgium).

# Appendix 3

## List of Figures and Tables

**Chapter 1**



**Chapter 2**

**Chapter 3**



**Chapter 4**



**Chapter 5**

## Appendix 4

## Data flow diagram of the handheld device